

The Theory of Long Distance
Electron Transfer Reactions

Thesis by
David Nathan Beratan

In Partial Fulfillment of the Requirements
for the Degree of
Doctor of Philosophy

California Institute of Technology

1986

(submitted June 11, 1985)

©1985

David Nathan Beratan

All Rights Reserved

Acknowledgments

It is a true pleasure to acknowledge John Hopfield for the patient guidance that he has given me over the past years. John's ability to pose meaningful soluble models for complicated physics is a source of constant inspiration. His generosity in both time and financial support was enormous.

One of the greatest assets of Caltech is the excellent communication between research groups. I have benefited much from discussions with Bob Cave, Rudy Marcus, Dave Blair, Sunney Chan, Walther Ellis, Arnóbio da Gama, and Harry Gray. Special thanks are due Harry and Walther for making the special topics course on electron transfer reactions possible. Thanks are also due Dave Middlemas for discussions of photochemistry and more general aspects of life.

The Hopfield-Dervan group has been a unique place to work. Activities in and out of the "lab" with Alvin Joran, Noam Agmon, José Onuchic, John Reinitz, Burt Leland, and Bo Cartling made life in southern California most pleasant. Noam and José contributed in many basic ways to the work in this thesis and to my education. Thanks also go to due Debbie Chester for typing much of this thesis and many other documents over the years. The research described in this thesis was supported by the National Science Foundation.

I am also indebted to William Luken for encouraging my interest in theoretical chemistry. Finally, special thanks go to my parents who were always low on baking soda and vinegar on my account – and to Kathi who lends a wonderful bit of reality to my life.

Abstract

The rate of electron transport between distant sites was studied. The rate depends crucially on the chemical details of the donor, acceptor, and surrounding medium. These reactions involve electron tunneling through the intervening medium and are, therefore, profoundly influenced by the geometry and energetics of the intervening molecules. The dependence of rate on distance was considered for several rigid donor-acceptor "linkers" of experimental importance. Interpretation of existing experiments and predictions for new experiments were made.

The electronic and nuclear motion in molecules is correlated. A Born-Oppenheimer separation is usually employed in quantum chemistry to separate this motion. Long distance electron transfer rate calculations require the total donor wave function when the electron is very far from its binding nuclei. The Born-Oppenheimer wave functions at large electronic distance are shown to be qualitatively wrong. A model which correctly treats the coupling was proposed. The distance and energy dependence of the electron transfer rate was determined for such a model.

Table of Contents

Acknowledgments	iii
Abstract	iv
List of Figures	vii
Chapter I – Overview	1
I.A. Introduction	2
I.B. General Aspects of the Electron Transfer Problem	4
I.C. References	13
Chapter II. – Tunneling Matrix Elements in Model Systems	16
II.A. Introduction	17
II.B. Tunneling Between Dirac Delta	
Function Potential Wells	18
II.C. Kronig–Penney Models	21
II.D. Edge Effects	33
II.E. References	39
Chapter III – Tunneling Matrix Elements in Systems of	
Experimental Interest	40
III.A. Introduction	41
III.B. “Calculation of Electron Tunneling Matrix Elements in	
Rigid Systems: Mixed-Valence Dithiaspirocyclobutane	
Molecules”, <i>J. Am. Chem. Soc.</i> 106 , 1584(1984)	44
III.C. “Electron Tunneling Through Rigid	
Molecular Bridges: Bicyclo[2.2.2]octane”; to be submitted to <i>J. Am. Chem. Soc.</i>	57

III.D. Further Comments on the Influence of the Bridging Medium on Electron Transfer Rates	86
III.E. References	91
Chapter IV – Calculation of Wave Functions with Correctly Coupled Nuclear and Electronic Motion: Breakdown of the Born-Oppenheimer Approach for the Long Distance Tunneling Problem 93	
IV.A. Introduction	94
IV.B. “Failure of the Born–Oppenheimer and Franck–Condon Approximations for Long Distance Electron Transfer Rate Calculations,” <i>J. Chem. Phys.</i> 81 , 5753(1984)	96
IV.C. Correctly Coupled Wave Functions in Bridged Systems	105
IV.D. References	126

List of Figures

Fig. I.1a, P.8 Born-Oppenheimer surfaces for a non-interacting donor and acceptor.

Fig. I.1b, P.9 Born-Oppenheimer surfaces for the total Hamiltonian.

Fig. I.2, P.10 Electronic energies as a function of nuclear position on the Born-Oppenheimer surfaces.

Fig. II.1, P.19 Electronic potential for tunneling between Dirac delta function potential wells.

Fig. II.2, P.24 Electronic potential for a donor plus periodic bridging medium.

Fig. II.3, P. 26 One orbital per bridging group model.

Fig. II.4, P. 29 Two orbital per bridging group model.

Fig. II.5a, P. 30 $\epsilon + 1/\epsilon$ vs. E for the two orbital per site model.

Fig. II.5b, P. 31 Energetic ordering of linker and trap states.

Fig. II.5c, P. 32 Dependence of ϵ on energy.

Fig. II.6, P. 34 Square well potential model for donor plus bridge of finite length.

Fig. II.7, P. 36 One orbital per site model for a bridge of finite length.

Pgs. 76-84 Figures related to electron propagation in bicyclo[2.2.2]octane (see p. 75 for captions).

Fig. III.1, P. 87 Orbital energy scheme.

Fig. III.2, P. 88 Repeating chains of saturated and unsaturated groups are shown.

Fig. IV.1, P. 108 One orbital per bridge unit model with donor and acceptor interacting adjacent to sites 0 and N .

Fig. IV.2, P.113 $\epsilon - E$ dependence in the one orbital model for several values of the intersite exchange interaction.

Fig. IV.3, P.117 $\epsilon - E$ relations for the one and six orbital per site models of n-alkane.

Fig. IV.4, P.119 Non-linear $\ln k$ vs. distance relation from a non-Born-Oppenheimer calculation.

Fig. IV.5, P. 120 As in Fig. IV.4 for donors and acceptors at various distances from the band of linker states.

Fig. IV.6a, P.121 $\ln k - \Delta E$ dependence for short distance transfer in a non-Born- Oppenheimer model.

Fig. IV.6b, P.122 $\ln k - \Delta E$ dependence for long distance transfer in a non-Born- Oppenheimer model.

Fig. IV.7, P.124 Experimentally measured $\ln k - \Delta G$ plots for short and long distance electron transfer.

Chapter I

Overview

I.A. Introduction

Electron transfer reactions, reactions which involve the exchange of a single electron between a donor and acceptor, are the subject of this thesis. The prototypical reaction is



Electron transfer may occur between atoms or molecules in solids, liquids, gases or heterogeneous media [1]. The reactions discussed in this thesis involve electron exchange when the $D - A$ distance is relatively large ($> 5 \text{ \AA}$). The idealized reaction occurs at *fixed* $D - A$ separation and orientation; no bond breakage or formation accompanies transport. The goal of theory is to calculate k and its dependence on the *chemical* properties of D , A , and the medium between and around D and A . Solvent, temperature, donor-acceptor separation, orientation, energetics, and molecular structure influence the electron transfer rate [2]. This thesis focuses on the dependence of the reaction rates on the donor-acceptor distance and the molecular structure of the bridging medium. Two main topics are considered. First, the electron transfer rate dependence on separation distance, bridge geometry, and energetics is discussed [3]. Long distance electron transfer involves electron tunneling, so the rate is quite sensitive to the molecular structure of the bridge. Second, the complications which arise in the calculation of long distance transfer rates when the electronic and nuclear motions are not separable are considered. Unusual dependence of rate on distance and exothermicity may result because $D^n A^m$ develops some $A^{n+1} D^{m-1}$ character *during* the transfer event [4].

Electron transfer reactions are ubiquitous. The reactions immediately following light absorption by photosynthetic plants and bacteria involve electron

translocation across a membrane. ATP synthesis in animals relies on electron transport reactions in the oxidative phosphorylation cycle [5]. Numerous inorganic, organic, and electrochemical reactions are dominated by an electron transport step [1].

Electron transport rates span a tremendous range. Some light induced photosynthetic electron transfers occur with $k = 10^{12} \text{ sec}^{-1}$ while other biological electron transfer reactions are many orders of magnitude slower [5]. Long distance (5-15 Å) electron transfer reactions are especially important in biological systems. The formal theoretical framework of electron transfer reactions has existed for some time. One of the crucial quantities in the theory is the tunneling matrix element (T_{ab}) or electronic exchange interaction between donor and acceptor [2]. This term differentiates the electron transfer reaction from more typical chemical reactions. In more common reactions the electronic motion follows the nuclear motion smoothly and the rate is determined by the nuclear activation barrier. An electron is classically forbidden to be more than a few Angstroms from its binding nuclei. Long distance thermally stimulated electron transfer involves interactions between non-stationary donor or acceptor localized states which interact via their non-classical exponentially decaying wave function "tails." The general goal of this work was to calculate donor and acceptor wave functions in their asymptotic regions far from the nuclei which bind the electrons. Predictions were made of the dependence of donor-acceptor interaction on distance and on the details of the intervening medium. Because the square of this exponentially decaying interaction energy enters the expression for the transfer rate, it is crucial that the factors influencing it be understood. Prior to this work other groups had estimated the tunneling matrix element in specific sys-

tems [2,3]. Some included molecular details of the reactants and others employed barrier penetration models. Here, more general considerations of the problem are made which allow quantitative predictions of changes in T_{ab} as molecular details of donor, acceptor, and bridge are varied. Section B of this chapter presents the rudiments and vocabulary of electron transfer theory. The second chapter provides some pedagogical examples showing calculations of wave function and tunneling matrix element decay with distance. The calculation of T_{ab} in specific molecules of experimental interest follows in Chapter III. Chapter IV discusses the failure of the Born-Oppenheimer approximation for the calculation of T_{ab} when the donor-acceptor distance is very large. A simple model is exactly solved which illustrates the effect. A more realistic model which uses techniques developed in Chapter III is presented and the circumstances when this effect may become important are discussed.

I.B. General Aspects of the Electron Transfer Problem

Experimental and theoretical interest in electron transfer reactions has blossomed in the last 30 years. Excellent reviews of progress in theoretical and experimental areas are abundant [1]. In this section the quantum mechanical description of distant electron transfer leading to the golden rule formulation for the rate is briefly reviewed. The approximations and variable separations used throughout this thesis are highlighted.

The long distance charge transfer problem is usually modeled as a two-state problem. The electron is localized on the donor (D) prior to transfer and on the acceptor (A) following transfer. Neither of these "states" is an eigenstate of the complete Hamiltonian, so transitions from one state to another occur. In real systems one might, for example, prepare a donor localized state by photon

absorption. The complete Hamiltonian for the problem is [2b,6]:

$$H = H^D + H^A + H^{Br} + V^{D,A,Br} + H^e \quad (I.2a)$$

where

$$H^D = T(Q_D) + T(q_D) + V(q_D, Q_D) \quad (I.2b)$$

$$H^A = T(Q_A) + T(q_A) + V(q_A, Q_A) \quad (I.2c)$$

$$H^{Br} = T(Q_{Br}) + T(q_{Br}) + V(q_{Br}, Q_{Br}) \quad (I.2d)$$

$$V^{D,A,Br} = V(q_D, q_A, q_{Br}, Q_D, Q_A, Q_{Br}) \quad (I.2e)$$

$$H^e = T^e + V^A(e - q_A, Q_A) + V^{Br}(e - q_{Br}, Q_{Br}) + V^D(e, q_D, Q_D). \quad (I.2f)$$

Upper and lower case q's represent the many nuclei and electrons, respectively. $V(,)$ represents all electron-electron, electron-nucleus, and nucleus-nucleus interactions on the site of interest between the quantities in parentheses. $V^{D,A,Br}$ is understood not to repeat interactions included in the previous three equations. "e" corresponds to the transferable electron. The terms donor, acceptor, and bridge mean all species in those regions coupled in any way to the electron transfer event. A dash between elements represents interactions only *between* the two sets of terms in parentheses. This Hamiltonian is obviously rather complicated. Although some calculations do actually include many electron effects directly [3h,i], the usual approach to the electron tunneling problem is to assume that all electrons except one create a pseudo-potential in which the transferring electron and all nuclei move ("one-electron" approximation). The total pseudo-Hamiltonian may then be written

$$H_p = [T^e + V'(e - Q_D) + V'(e - Q_{Br}) + V'(Q_D, Q_A, Q_{Br}) + T(Q_A) + T(Q_{Br}) + T(Q_D)] + V'(e - Q_A) \quad (I.3)$$

where primes represent pseudo rather than true potentials. The total Hamiltonian for the simplified problem is

$$H_P = H'_{D+Br} + V'_A(e - Q_A). \quad (I.4)$$

H'_{D+Br} is the operator enclosed in square brackets in Eq. I.3. In the case of well localized donor and acceptor states, the Hamiltonian for the donor localized (initial) state is

$$H_i = H'_{D+Br}. \quad (I.5)$$

$V'_A(e - Q_A)$ is the perturbation which mixes eigenfunctions of the acceptor localized eigenstate of H_f where

$$H_f = H_i - V'(e - Q_D) + V'(e - Q_A). \quad (I.6)$$

The problem has been reduced to solving the two Schrödinger equations

$$H_i \Psi_i = E_i \Psi_i \quad (I.7a)$$

$$H_f \Psi_f = E_f \Psi_f \quad (I.7b)$$

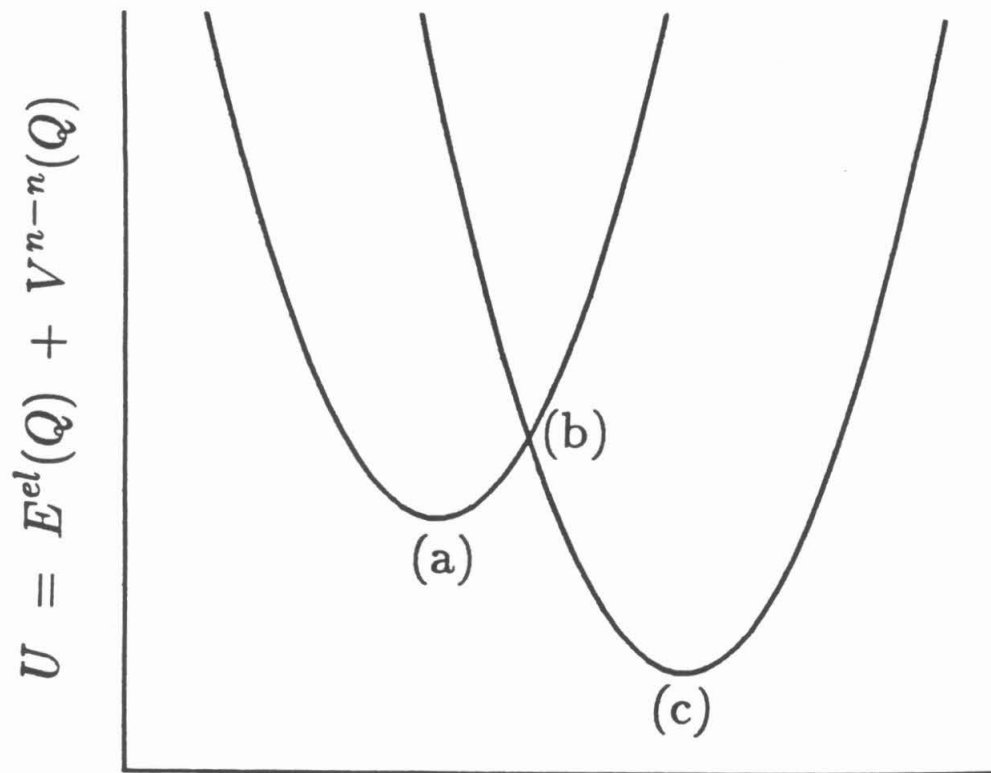
for all initial and final states. To the extent that eigenfunctions of the total pseudo-Hamiltonian (Eq. I.3) can be expanded as a linear combination of the eigenfunctions of Eqs. I.7a and b, the transfer rate is calculable. Since one may, in principle, find all eigenstates of these two equations, including continuum states, an expansion of the form

$$\Psi(e, Q, t) = \sum_i a_i \Psi_i + \sum_f b_f \Psi_f \quad (I.8)$$

describes the time dependent solution of *I.3*. Neglecting the Born-Oppenheimer breakdown operator one arrives at the golden rule expression [7]

$$k = \frac{2\pi}{\hbar} | \langle \Psi_D | V'(e, Q_A) | \Psi_A \rangle |^2 \delta(E_D - E_A). \quad (I.9)$$

This is a first-order perturbation theory result where $\Psi_D = \Psi_i$ and $\Psi_A = \Psi_f$. It assumes only a small depletion of the initially prepared donor state and is valid at short times after preparation of the initial state [7]. In Eq. *I.9* Ψ_D and Ψ_A include both electronic and nuclear coordinates. The golden rule approach requires that Ψ_D and Ψ_A solve zeroth-order Hamiltonians and that V' , the perturbation, induces transitions between zeroth-order states. V' is the difference between the total Hamiltonian and the Hamiltonian of the donor localized state. Equation *I.9* neglects corrections due to the non-orthogonality of the zeroth-order eigenfunctions. These corrections are usually small in the long distance electron transfer problem [6]. The Dirac delta function in *I.9* is understood to be broadened due to coupling of the acceptor to a continuum of medium modes [8]. Two final approximations are commonly applied to Eq. *I.9*, the Born-Oppenheimer separation and the Franck-Condon approximation [9]. The Born-Oppenheimer approximation allows the construction of nuclear potential energy surfaces for the donor and acceptor states before and after transfer. Such a diagram is shown in Fig. *I.1*. All nuclear degrees of freedom except one on each site are often suppressed. The nuclear coordinate might correspond to a solvent or ligand vibrational or rotational mode sensitive to the presence of the electron. If the interaction splitting between donor and acceptor calculated with the total Hamiltonian is $2|T_{ab}(Q)|$, the zeroth-order nuclear potential energy surfaces at the crossing point are distorted by this amount. $2|T_{ab}|$ is the symmetric/anti-symmetric splitting between donor and acceptor at the crossing point of the zeroth-order surface (see Fig. *I.2*)



Q = nuclear (reaction) coordinate

Figure I.1a. A slice through the many-dimensional nuclear potential energy surface is shown. This is the Born-Oppenheimer representation of the problem so $U = E^{el}(Q) + V^{n-n}(Q)$. These surfaces correspond to the *isolated non-interacting* donor and acceptor states. Wave functions calculated on these two surfaces are generally used to calculate the long distance electron transfer rate.

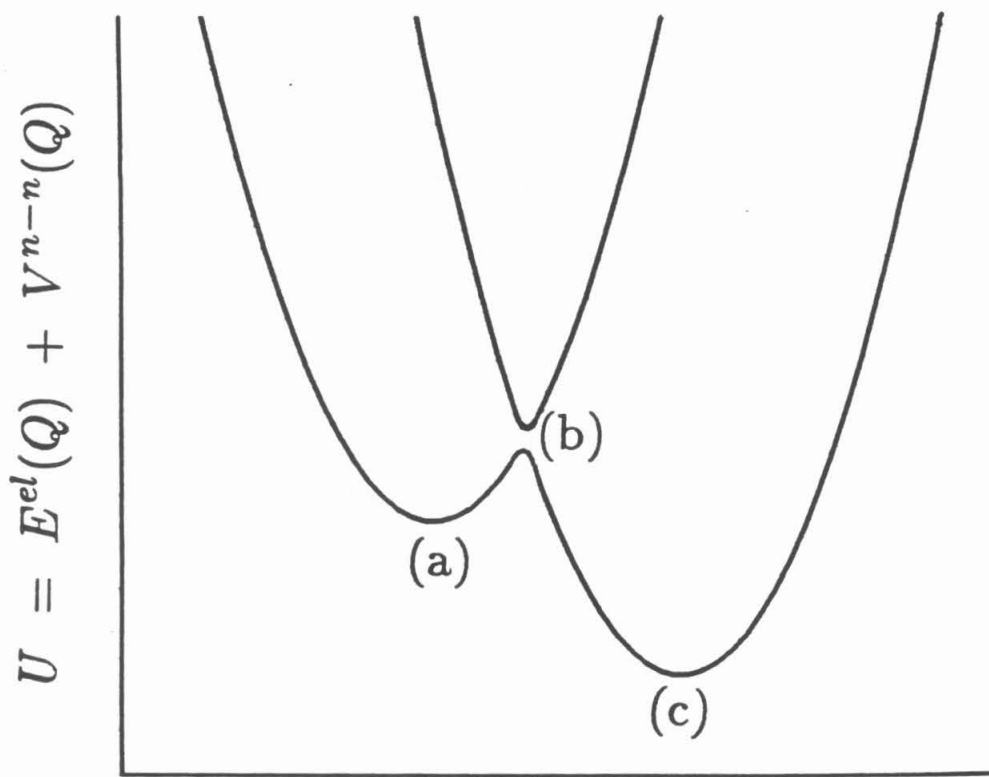


Figure I.1b. When the surfaces are calculated using the *total* Hamiltonian, a splitting occurs at the crossing point (b) of the surfaces for the isolated donor and acceptor molecules.

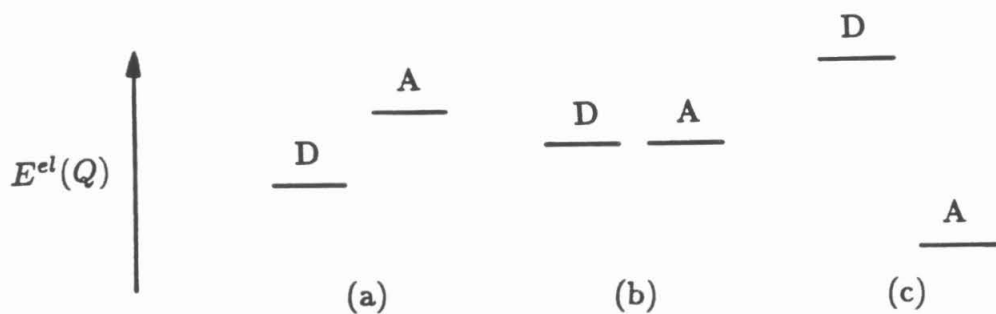


Figure I.2. The *electronic* energies for the non-interacting donor and acceptor molecules at *fixed* nuclear geometries are shown. The horizontal coordinate is the *electronic* position. A small exchange splitting of $2T_{ab}$ occurs in configuration (b).

[3i,10]. The Born-Oppenheimer approximation is generally applied to the donor and acceptor *zeroth-order wave functions* (Fig I.1a, I.2). This approximation presumes that the electronic motion follows the donor (acceptor) nuclei adiabatically in these unmixed states. This separation should be understood as yielding adiabatic motion on the *isolated* donor or acceptor energy surfaces. Motion along the reaction coordinate of the surfaces for the total Hamiltonian (Fig. I.1b) is termed non-adiabatic because electron transfer does not occur each time the nuclei cross (in classical language) the intersection of the reagent and product potential energy surfaces. Non-adiabatic motion *along* the reaction coordinate is the hallmark of long distance electron transfer. The splitting is usually calculated from the integral in I.9 at fixed Q (Franck-Condon approximation).

Instead of measuring a thermally stimulated electron transfer rate one sometimes finds a charge transfer or intervalence optical absorption which promotes an electron from a donor (HOMO) to acceptor (LUMO) at fixed nuclear geometry [1g,11]. The extinction coefficient of this band is proportional to $|T_{ab}|^2$. Since the transition occurs at a different nuclear geometry relative to the thermally stimulated transfer, the optical and thermal tunneling matrix elements may differ.

In summary, many approximations are made to reach a useful theoretical expression for the electron transfer rate. A many-body problem is usually reduced to a one-electron two-state problem. The electron interacts with donor plus bridge or acceptor plus bridge in the zeroth order problems. A first-order perturbation expression is used to find the transition rate between donor and acceptor localized states. The donor-acceptor matrix element can be separated into an electronic tunneling matrix element and a nuclear Franck-Condon factor.

The distance dependence of the electron transfer rate is essentially contained in the electronic tunneling matrix element which is the subject of Chapter II.

I.C. References – Chapter I

- 1a. R.A. Marcus and N. Sutin, *Biochim. Biophys. Acta*, in press.
- 1b. M.D. Newton and N. Sutin, *Ann. Rev. Phys. Chem.* **35**, 437(1984).
- 1c. *Tunneling in Biological Systems*, edited by B. Chance, D.C. DeVault, H. Frauenfelder, R.A. Marcus, J.R. Schrieffer, and N. Sutin (Academic, New York, 1979).
- 1d. R.C. Cannon, *Electron Transfer Reactions* (Butterworths, London, 1980).
- 1e. J. Ulstrup, *Charge Transfer Processes in Condensed Media, Lecture Notes in Chemistry*, No. 10 (Springer-Verlag, New York, 1979).
- 1f. *Discuss. Faraday Society*, **74**(1982).
- 1g. *Prog. Inorg. Chem.*, **30**(1983).
- 1h. D. DeVault, *Q. Rev. Biophys.* **18**, 311(1980).
- 1i. P. Day, *Int. Rev. Phys. Chem.* **1**, 149(1981).
- 1j. L. Eberson, *Adv. Phys. Org. Chem.* **18**, 79(1982).
- 1k. D.E. Richardson and H. Taube, *Coord. Chem. Revs.* **60**, 107(1984).
- 1l. A.J. Bard and L.R. Faulkner, *Electrochemical Methods: Fundamentals and Applications* (Wiley, New York, 1980).
- 1m. J. Jortner, *Biochim. Biophys. Acta* **594**, 193(1980).
- 2a. R.A. Marcus, *Annu. Rev. Phys. Chem.* **15**, 155(1964).
- 2b. N.R. Kestner, J. Logan, and J. Jortner, *J. Phys. Chem.*, **78**, 2148(1974).
- 2c. J.J. Hopfield, *Proc. Natl. Acad. Sci. (USA)*, **71**, 3640(1974).
- 2d. J. Jortner, *J. Chem. Phys.* **64**, 4860(1976).
- 2e. R.A. Marcus, in *Oxidases and Related Redox Systems*, edited by T.E. King, H.S. Mason, and M. Morrison (Pergamon, New York, 1982), p. 3.
- 2f. L.N. Grigorov and D.S. Chernavskii, *Biophysics*, **17**(part 1), 202(1972).

2g. P. Siders, R.J. Cave, and R.A. Marcus, *J. Chem. Phys.* **81**, 5613(1984).

3a. S. Larsson, *J. Am. Chem. Soc.* **103**, 4034(1981).

3b. S. Larsson, *J. Chem. Soc., Faraday Trans. 2*, **79**, 1375(1983).

3c. H. M. McConnell, *J. Chem. Phys.*, **35**, 508(1961).

3d. J. Halpern and L.E. Orgel, *Discuss. Faraday Soc.*, **29**, 32(1960).

3e. A. S. Davydov, *Phys. Stat. Sol. (b)*, **90**, 457(1978).

3f. D.N. Beratan and J.J. Hopfield, *J. Am. Chem. Soc.*, **106**, 1584(1984).

3g. D.N. Beratan, J.N. Onuchic, and J.J. Hopfield, *J. Chem. Phys.*, submitted 1985.

3h. M.D. Newton, *Int. J. Quantum Chem.: Quantum Chem. Symp.*, **14**, 363(1980).

3i. J. Logan and M.D. Newton, *J. Chem. Phys.* **78**, 4086(1983).

3j. A.A.S. da Gama, *Theor. Chim. Acta* 1985, in press.

3k. M.A. Ratner and M.J. Ondrechen, *J. Mol. Phys.* **32**, 1233(1976).

4. D.N. Beratan and J.J. Hopfield, *J. Chem. Phys.* **81**, 5753(1984).

5a. J.L. Dreyer, *Experientia* **40**, 653(1984).

5b. R.K. Clayton and W.R. Sistrom, eds., *The Photosynthetic Bacteria* (Plenum, New York, 1978).

5c. R.A. Holwerda, S. Wherland, and H.B. Gray, *Ann. Rev. of Biophysics and Bioeng.* **5**, 363(1976).

5d. C. Ho, editor, *Electron Transport and Oxygen Utilization* (Elsevier, New York, 1982).

5e. G.R. Moore, *et. al.*, *Faraday Discuss. Chem. Soc.* **74**, 311(1982)

5f. See 1c and 1h also.

5g. K. Sauer, *Bioenergetics of Photosynthesis* (Academic, New York, 1975).

- 5h. H. Gerischer and J.J. Katz, editors, *Light-Induced Charge Separation in Biology and Chemistry-Dahlem Konferenzen* (Verlag Chemie, New York, 1979).
6. P. Siders, Thesis: California Institute of Technology, 1983.
7. E. Mertzbacher, *Quantum Mechanics*, 2nd ed. (Wiley, New York, 1970), Chapter 18.
- 8a. M. Bixon and J. Jortner, *Faraday Discuss. Chem. Soc.* **74**, 17(1982).
- 8b. L.N. Grigorov and D.S. Chernavskii, *Biophysics* **17**, 202(1972).
9. See 1m and 4.
10. See 3i and H. Eyring, J. Walter, and G.E. Kimball, *Quantum Chemistry* (Wiley, New York, 1944), Chapter XI.
- 11a. J.J. Hopfield, *Biophysical J.*, **18**, 311(1977).
- 11b. D.E. Richardson and H. Taube, *J. Am. Chem. Soc.* **105**, 40 (1983).
- 11c. N.S. Hush, *Electrochimica Acta* **13**, 1005(1968).

Chapter II

**Tunneling Matrix Elements
in Model Systems**

II.A. Introduction

The essence of the long distance electron transfer problem is contained in the matrix element $\langle \Psi_D | V_A | \Psi_A \rangle$. The standard variable separations (see Chap. IV) isolate the electronic and nuclear parts of the problem [1]. The *electronic* tunneling matrix element retains a parametric dependence on nuclear configuration related to the vibronic coupling on donor and acceptor.

Calculations of tunneling matrix elements are replete with hidden approximations which are usually manifest in the expansion of a wave function in an incomplete or asymptotically incorrect basis set. Any expansion in a less than complete basis falsifies the wave functions and causes them and the tunneling matrix elements to err in benign or pathological ways. It is especially crucial that the donor state far from the donor nuclei or the symmetric-antisymmetric splitting between donor and acceptor be calculated with great accuracy. The one electron, electronic Hamiltonians of interest (see Chapter I) are:

$$H_D = T^e + V_M + V_D \quad (II.1a)$$

$$H_A = T^e + V_M + V_A \quad (II.1b)$$

$$H^{el} = H_D + V_A = H_A + V_D. \quad (II.1c)$$

For several model potentials T_{ab} is now calculated. The difference between tunneling through a bridge of constant potential as opposed to a bridge of spatially varying potential is discussed. A molecular orbital approach to the problem is introduced in the context of donors and acceptors interacting with an infinite periodic one-dimensional molecular bridge. It is shown that for long-distance transfer the finite nature of the bridge does not substantially alter the nature of the wave functions and matrix elements found for the infinite potentials.

II.B. Tunneling Between Dirac Delta Function Potential Wells

Consider Eq. I.1 when (see Fig. II.1)

$$V_M = 0 \quad (II.2a)$$

$$V_D = -\lambda \delta(x - a) \quad (II.2b)$$

$$V_A = -\lambda \delta(x + a) \quad (II.2c)$$

$$T_{ab} = \langle \Psi_d | V_A | \Psi_A \rangle. \quad (II.3)$$

This problem [2] is chosen to illustrate the fact that in a simple system the tunneling matrix element (or splitting) cannot usually be calculated exactly. It also shows that $\langle \Psi_D | V_A | \Psi_A \rangle$ gives the same value and distance dependence (to first order) for T_{ab} as the value obtained from the calculation of the symmetric-antisymmetric splitting. Since $V = 0$, except at $x = \pm a$, the even (+) and odd (-) wave functions are:

$$\Psi_I = a_{\pm} \exp(-\kappa_{\pm} x) \quad (II.4a)$$

$$\Psi_{II} = b_{\pm} [\exp(-\kappa_{\pm} |x|) \pm \exp(\kappa_{\pm} |x|)] \quad (II.4b)$$

$$\Psi_{III} = \pm a_{\pm} \exp(-\kappa_{\pm} |x|). \quad (II.4c)$$

The unperturbed donor and acceptor states are:

$$\Psi_D = \exp(-\kappa |x - a|) \quad (II.5a)$$

$$\Psi_A = \exp(-\kappa |x + a|) \quad (II.5b)$$

where

$$\kappa = \sqrt{\frac{2m|E|}{\hbar^2}}$$

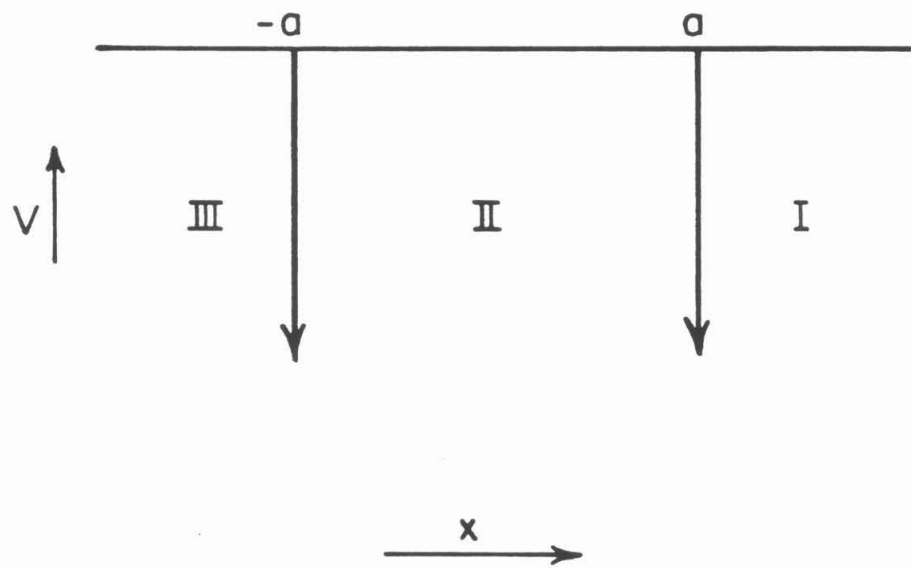


Figure II.1. The electronic potential corresponding to Eq. II.2 is shown.

and $E < 0$. The continuity of the wave function at $x = \pm a$ and the discontinuity of its first derivative gives the transcendental expression for the energies of the two bound states:

$$\kappa_{\pm} = \frac{\lambda m}{\hbar^2} [1 \pm \exp(-2\kappa_{\pm}a)] \quad (II.6)$$

$$\kappa_{\pm} = \sqrt{\frac{-2m|E_{\pm}|}{\hbar^2}}.$$

The eigenvalues are E_+ and E_- . The energy splitting ($\Delta E = E_+ - E_-$) is exactly

$$\Delta E = -\frac{\lambda^2 m}{2\hbar^2} \left\{ 2[\exp(-2\kappa_+a) + \exp(-2\kappa_-a)] + [\exp(-4\kappa_+a) - \exp(-4\kappa_-a)] \right\}. \quad (II.7)$$

Defining an energy E_0 midway between E_+ and E_- , $E_+ = E_0 + \mu$ and $E_- = E_0 - \mu$. μ is small in the problems of interest compared to E_0 . As the separation becomes large, E_0 converges to the binding energy of a single delta well and μ converges to zero. Expanding κ around $\mu = 0$ we find

$$\Delta E \simeq -\frac{\lambda^2 m}{\hbar^2} \exp[-2a\sqrt{-2mE_0/\hbar^2}] \quad (II.8)$$

$$T_{ab} \simeq \Delta E/2. \quad (II.9)$$

The first correction to this expression is of the order

$$\frac{\mu^2}{E_0} \exp[-2a\sqrt{-2mE_0/\hbar^2}]. \quad (II.10)$$

The second order correction is of the order

$$\frac{\mu}{\sqrt{E_0}} \exp[-4a\sqrt{-2mE_0/\hbar^2}]. \quad (II.11)$$

For large $\kappa_{\pm}a$ and small μ^2/E_0 the tunneling matrix element decays exponentially with the distance (2a in this model) to the extent that at large separation

distance the average energy of the symmetric and antisymmetric states is distance independent. At large distance this is indeed the case as the even and odd states converge to the energy of an isolated single well state. E_0 in general is several electron volts and μ is many (> 3) orders of magnitude smaller.

The perturbation matrix element is

$$\langle \Psi_D | V_A | \Psi_A \rangle = -\frac{m\lambda^2}{2\hbar^2} \exp\left(-\frac{2ma\lambda}{\hbar^2}\right) \quad (II.12)$$

since

$$\Psi_D = \sqrt{\frac{\lambda m}{2\hbar^2}} \exp\left[-m\lambda|x|/\hbar^2\right] \quad (II.13)$$

and

$$V_A = -\lambda\delta(x). \quad (II.14)$$

These results are identical if $E_0 = -m\lambda^2/(2\hbar^2)$, the energy of an isolated Dirac well state. When the donor-acceptor interaction is small this is expected to be nearly the case. T_{ab} is calculated well with both methods if distance changes do not affect the energies of the bound states very much (on a percent basis). This result for T_{ab} can also be obtained from the Bardeen transition current between the wells [2b]. Writing $T_{ab} = T_0 \exp(-\alpha R)$, $\alpha = \sqrt{2m|E_0|/\hbar^2}$. This is the dependence of T_{ab} on E expected for one-dimensional tunneling through a square barrier. For thermal electron transfer between two wells of non-zero width, it is not essential that the electronic potentials on the two sites be identical, just that the two isolated sites each support a states with equal electronic energy.

II.C. Kronig-Penney Models

Electron tunneling through a protein or other molecular bridge involves propagation through a spatially varying potential. A model for a bound electron weakly mixed with a bridging medium is now considered. The simplest

such model is the modified Kronig-Penney potential. This is an infinite periodic potential with a single well deeper than all others. Periodic potentials are useful because the wave function decay is purely exponential away from the trap. Tunneling matrix elements calculated for finite bridges do not differ substantially from results for infinite periodic potentials when the transfer distance is large. The decay of the donor localized state in the bridge region can be written, as before, as a function of its energy. The matrix element, and hence the distance dependence of T_{ab} , is known from the decay of Ψ_D .

Delta potentials eigenstates obviously are not useful for modeling details of wave functions near nuclei. However, if the right parameters are chosen, they give the correct asymptotic behavior ($\exp[-\kappa|x|]$) to the states far from the nuclei. Using Dirac potentials may alter the absolute value of T_{ab} compared to its value for a more realistic potential, but does not change its distance dependence if the parameters are chosen appropriately. The wells support only one bound state. When chains of *equally spaced* delta wells are assembled, a single “band” of bound states results. The mixing between donor and acceptor depends on the details of the potential between sites. The splitting calculation tacitly assumes that the change in the average of the donor and acceptor energies with distance is small on the scale of the average energy. The golden rule rate expression includes only first-order perturbation terms. These approximations are certainly valid when the interaction is small but neglect subtle details of the donor-acceptor interaction.

Consider a donor site at $x = 0$ and an infinite periodic one-dimensional chain of Dirac delta function potential wells elsewhere [3]. The potential is

$$V_M = -\lambda \sum_{\substack{n=-\infty \\ n \neq 0}}^{\infty} \delta(x - na) \quad (II.15)$$

on the bridge and

$$V_D = -\Delta\delta(x) \quad (II.16)$$

on the donor. In region I (see Fig. II.2) the wave function is

$$\Psi_I = a \exp(-\kappa x) + b \exp(\kappa x). \quad (II.17)$$

Since the potential away from the donor is periodic [4],

$$\Psi_{II} = \epsilon \Psi_I \quad (II.18)$$

$$\Psi_{III} = \epsilon \Psi_{II} = \epsilon^2 \Psi_I$$

....

The donor eigenstate is symmetric with respect to the origin. The continuity of the wave function and discontinuity of its derivative at each bridging well connects ϵ with E [4]:

$$\epsilon + \frac{1}{\epsilon} = e^{\kappa a} (1 - \lambda) + e^{-\kappa a} (1 + \lambda) \quad (II.19)$$

$$\lambda = \sqrt{\frac{V_b}{|E|}}, \quad V_b = \frac{m\lambda^2}{2\hbar^2}.$$

ϵ may be real or imaginary. It is determined by the boundary and continuity condition of the donor at $x = 0$. If $\Delta = \lambda$ one finds $\epsilon = e^{ikx}$ and $|\epsilon| = 1$. These are the delocalized Bloch states. If $\Delta \gg \lambda$ a single localized state is found in addition to the delocalized states. The energy of the localized state depends principally on the electron trapping site which is weakly perturbed by the chain. The energy of the localized state determines its decay with distance. All excited states are completely delocalized. At higher energy lie the continuum states. In the absence of the bridge ($V_b = 0$) the wave function decay is dictated purely by

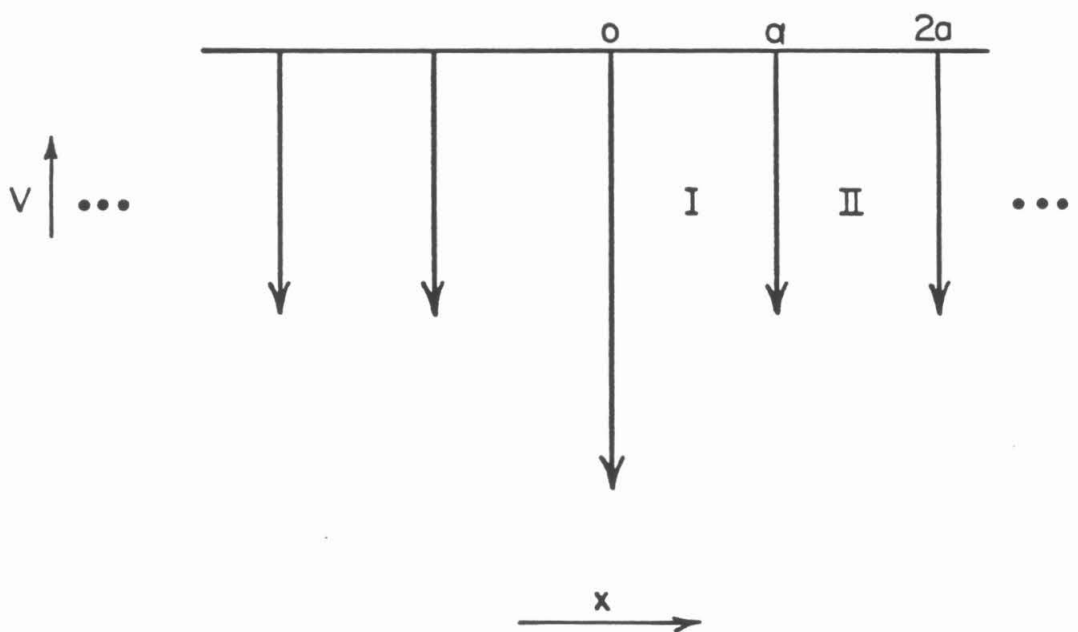


Figure II.2. $V_D + V_M$ is shown for a donor site surrounded by a one-dimensional chain of equally spaced Dirac delta function potential wells.

the binding energy of the electron (energetic proximity of the continuum states). In the presence of a molecular bridge, *both* the energetic distance of the continuum states *and* the unperturbed bridge states influence the electronic tunneling. Proposition 1 and Ref. 5 discuss the circumstances under which one of the two sets of states may dominate the charge mediation process. Decay with distance is exponential, but the energy dependence is rather more complicated than in the case of two delta wells. It appears that, for rigid saturated hydrocarbon bridges, donor interactions with the bridge states enhance the tunneling matrix element considerably more than mixing with the continuum states. Eq. II.19 is exact, including bridge and continuum mediated tunneling as well as non-nearest neighbor bridge unit interactions. Since the donor wave function decays with distance as ϵ^j , the tunneling matrix element when the donor and acceptor are separated by N bridge groups is proportional to ϵ^N . It will next be shown that when bridge mediated transfer dominates, $\alpha \simeq -(1/a) \ln|\beta/E|$ where $T = T_0 \exp(-\alpha R)$. β in this case is the exchange interaction between neighboring delta wells. E is the energy of the electron relative to the energy of the center of the band of unperturbed bridging states. a is the separation between bridging units.

To the extent that bonded interactions dominate, it is useful to study electron transfer with a molecular orbital approach. Consider the molecular orbital analogue of the delta function potential bridge. This is an infinite chain of identical orbitals with one different orbital at $x = 0$ (Fig. II.3). Including only nearest neighbor interactions the Hamiltonian is [6]:

$$H = \alpha \sum_{i \neq 0} a_i^\dagger a_i + \Delta a_0^\dagger a_0 + \beta/2 \sum_i (a_i^\dagger a_{i+1} + a_i^\dagger a_{i-1}) \quad (II.20a)$$

$$\beta = \langle \phi_i | H | \phi_{i \pm 1} \rangle \quad (II.20b)$$

$$\alpha = \langle \phi_i | H | \phi_i \rangle. \quad (II.20c)$$

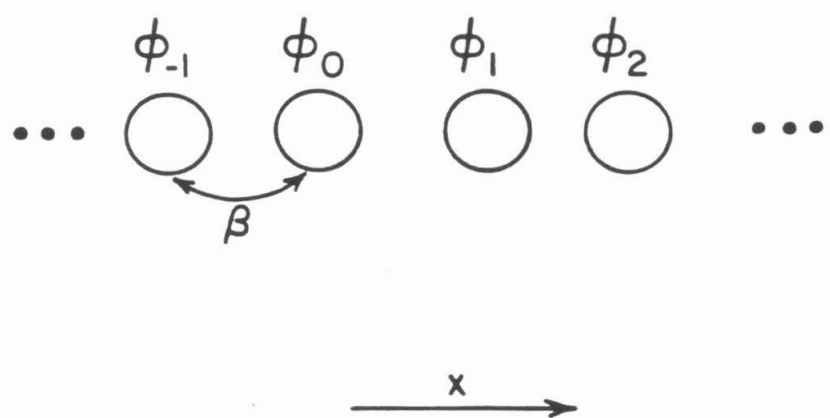


Figure II.3. Each circle represents a basis function on the i^{th} site interacting with a nearest neighbor.

The fermion operator a_i (a_i^\dagger) creates (annihilates) an electron on the i^{th} atomic orbital. Since a chain of identical orbitals was chosen,

$$\Psi = c\chi(\vec{x}) + \sum_j \epsilon^{|j|} \phi_j(\vec{x} - j\vec{a}). \quad (II.21)$$

The wave function is symmetric with respect to the trapping site. Multiplying the Schrödinger equation by the complex conjugate of an orbital with $j > 1$ and integrating one finds [6]

$$\epsilon + \frac{1}{\epsilon} = \frac{E - \alpha}{\beta}. \quad (II.22)$$

For a given E there are two solutions for ϵ . One corresponds to the localized ($|\epsilon| < 1$) state. The perturbation which promotes electron transfer is the additional potential on the acceptor site due to the presence of the acceptor, $\Delta a_N^\dagger a_N$. The wave function decays by the factor $\epsilon \simeq \beta/(E - \alpha)$ per repeating unit (if $\epsilon^2 \ll 1$) so the tunneling matrix element decreases by the factor $\beta/(E - \alpha)$ per unit inserted between donor and acceptor. $(E - \alpha)$ is the energetic distance between the donor state and the *center* of the *single* band of states created by the bridging atoms. In the orbital model the interaction decays with distance as $T_0 \exp(-\alpha R)$ where $\alpha = -(1/a) \ln |\beta/(E - \alpha)|$ and a is the spacing between bridge units. The nearest neighbor approximation is reliable for calculating donor wave function decay to the extent that

$$\sum_{n=2}^N \left(\frac{\beta'_{(n)}}{\epsilon^n} \right) \ll \frac{\beta}{\epsilon}. \quad (II.23)$$

$\beta'_{(n)}$ is the non-nearest neighbor interaction ($\langle \phi_i | H | \phi_{i+n} \rangle$) between bridge sites n units apart and $\beta'_{(n)}$ is on the order of the orbital overlap, $\langle \phi_i | \phi_{i+n} \rangle$.

Two additional aspects of the donor-bridge-acceptor assembly must be considered in order to make quantitative predictions using theoretical $E - \epsilon$ relations.

Realistic systems possess as many bands of states as there are unique basis functions in each repeating chain unit. The multi-band aspect of the problem has been neglected so far. Also, real bridges are of finite length. A more complicated “unit cell” is all that is required to obtain a multi-band problem. Consider, for example, a two orbital per cell model (Fig. II.4) [7]:

$$\langle \phi_i^{(l)} | H | \phi_i^{(r)} \rangle = \gamma \quad (II.24a)$$

$$\langle \phi_i^{(r)} | H | \phi_{i+1}^{(l)} \rangle = \beta = \langle \phi_i^{(l)} | H | \phi_{i-1}^{(r)} \rangle. \quad (II.24b)$$

All other matrix elements are assumed to be zero.

$$H = \alpha \sum_i a_i^\dagger a_i + \beta \sum_i \left[(a_i^{(r)\dagger} a_{i+1}^{(l)} + a_i^{(l)\dagger} a_{i-1}^{(r)}) + c.c. \right] + \gamma \sum_i (a_i^{(r)\dagger} a_i^{(l)} + c.c.) + \Delta a_0^\dagger a_0 \quad (II.25)$$

$$\Psi = \sum_{n \neq o} [\lambda_l \phi_n^{(l)} (\vec{x} - n\vec{a}) + \lambda_r \phi_n^{(r)} (\vec{x} - n\vec{a})] \epsilon^n + c\chi(\vec{x}) \quad (II.26)$$

$$\begin{pmatrix} (E - \alpha) & (\gamma + \beta/\epsilon) \\ (\gamma + \beta\epsilon) & (E - \alpha) \end{pmatrix} \begin{pmatrix} \lambda_l \\ \lambda_r \end{pmatrix} = 0 \quad (II.27)$$

or

$$\epsilon + \frac{1}{\epsilon} = \frac{(E - \alpha)^2}{\beta\gamma} - \frac{\gamma}{\beta} - \frac{\beta}{\gamma}. \quad (II.28)$$

States in the shaded region of Fig. II.5a have $|\epsilon| < 1$ and correspond to decaying wave functions localized on a trap. In the limit of very weak trap-bridge interactions, $E \simeq \Delta$. The two bands of states correspond to bonding (valence) and antibonding (conduction) states of the linker. Proximity of E to either band enhances transfer compared to E midway between the bands. Introduction of more complicated repeating units adds more bands. The donor orbital

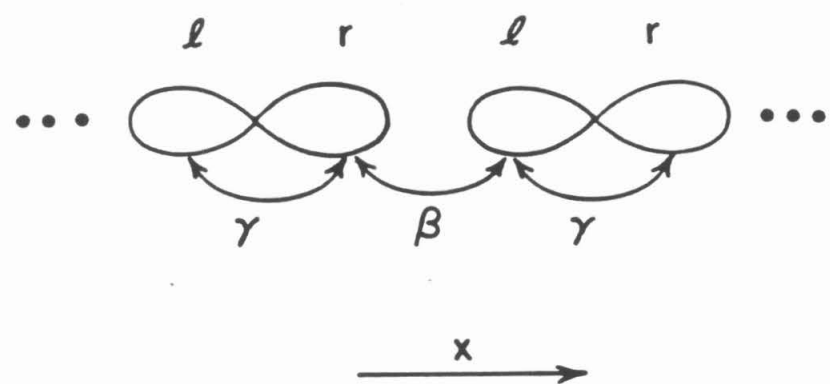


Figure II.4. A two basis function per site (or "unit cell") model is shown.

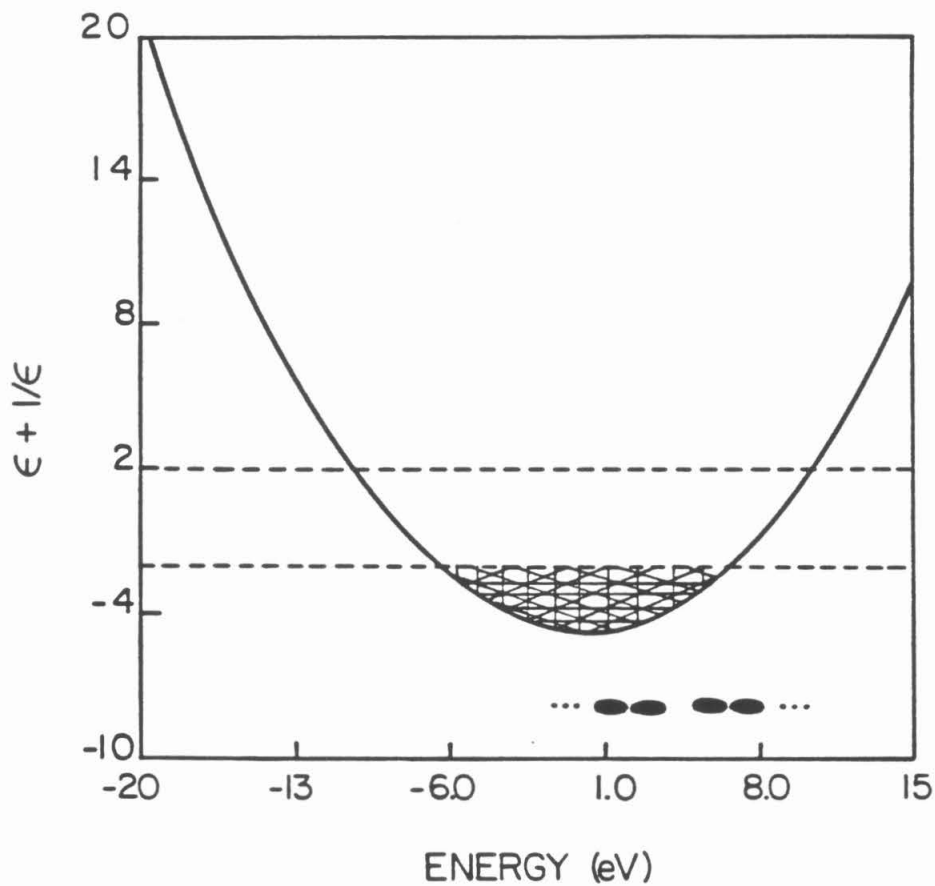


Figure II.5a. With $\beta = -8.47\text{eV}$ and $\gamma = -1.85\text{ eV}$ the two-band model produces this $\epsilon - E$ relation. The band gap is shaded.

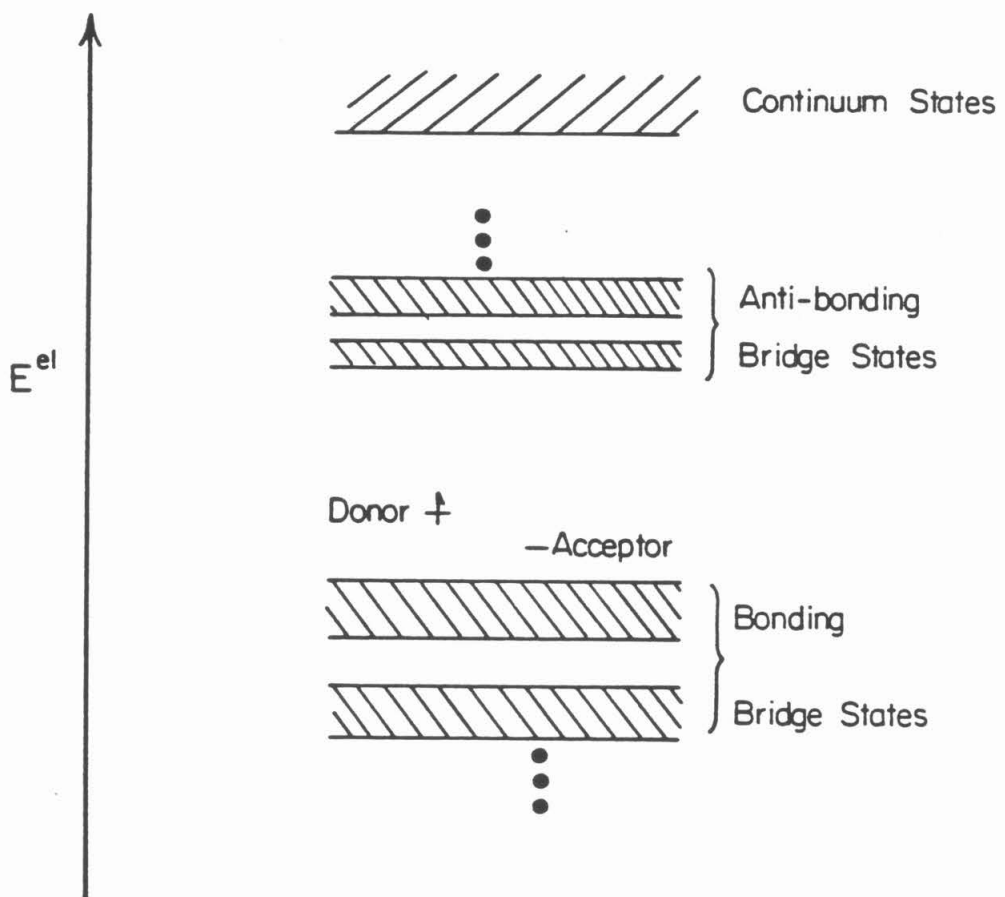


Figure II.5b. The energetic ordering of bridge and trap states is shown.

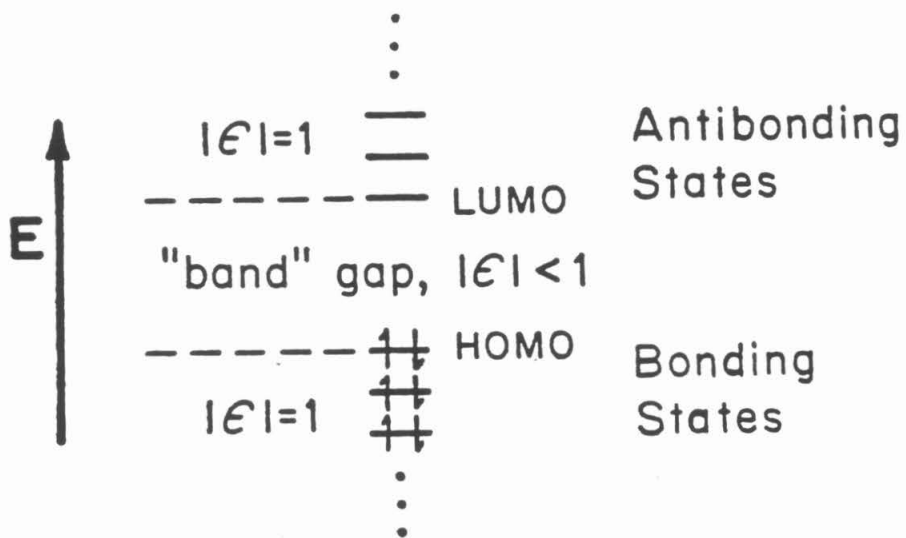


Figure II.5c. $|\epsilon| < 1$ for states with energies in the band gap(s). Other states are delocalized with $|\epsilon| = 1$.

interactions with *all* bands contribute to the bridge assisted exchange interaction. More complicated multi-band $E - \epsilon$ relations can usually be emulated with the two-band approximation if β and γ are chosen appropriately. The additional band gives $\epsilon + 1/\epsilon$ a parabolic shape in the band gap. If $\epsilon^2 \ll 1$, $\epsilon \simeq [(E - \alpha)^2/(\beta\gamma) - (\gamma/\beta) - (\beta/\gamma)]^{-1}$ rather than the one band result $\epsilon \simeq \beta/(E - \alpha)$.

II.D. Edge Effects

Although some crystal potentials can be approximated as being infinite in extent, molecular bridges are characteristically finite. Donor states interacting with *finite* length bridges decay in a somewhat more complicated manner along the bridge, but the general nature of the long distance electron transport problem is unchanged. As in the two delta well example the donor wave function in the intermediate region now may have both growing and decaying parts. Consider the potential (Fig. II.6):

$$V = \begin{cases} -V_0, & \text{if } 0 < x < d \\ 0, & \text{if } d < x < R \\ \infty, & \text{otherwise} \end{cases}. \quad (II.29)$$

The trapping "molecule" is between 0 and d . The bridge is between d and R .

The wave function is

$$\Psi = \begin{cases} \sin kx, & \text{if } 0 < x < d \\ A \exp(-\kappa x) + B \exp(\kappa x), & \text{if } d < x < R \end{cases} \quad (II.30)$$

$$k = \sqrt{\frac{2m(E + V_0)}{\hbar^2}}$$

$$\kappa = \sqrt{\frac{-2mE}{\hbar^2}}.$$

Since $\Psi(R) = 0$,

$$B = -A \exp(-2\kappa R). \quad (II.31)$$

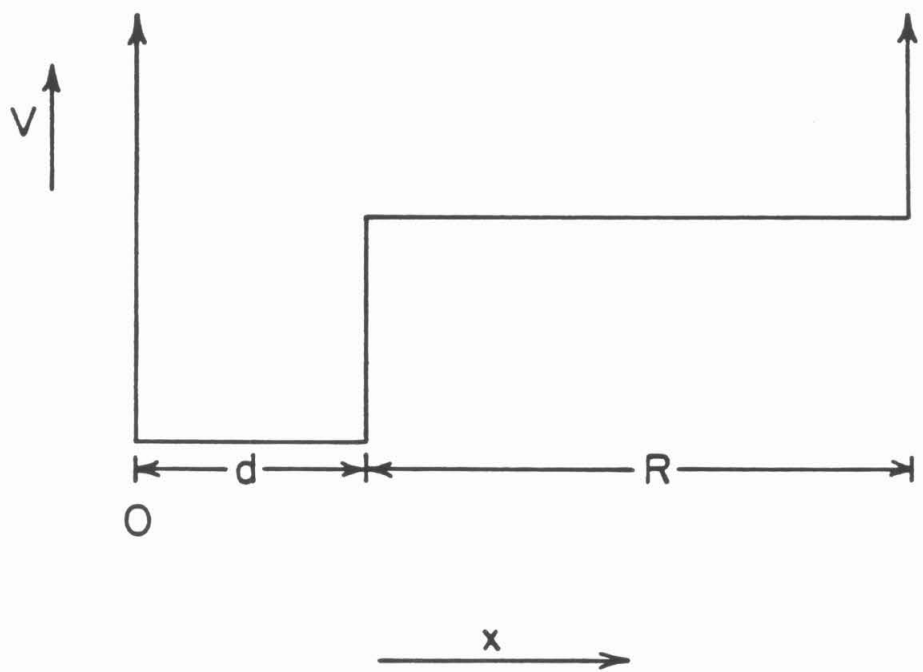


Figure II.6. This is the potential useful as a model for a localized state interacting with a bridge of finite length.

A is determined by normalization and is R independent if $\exp(-2\kappa R) \ll \exp(-2\kappa d)$. The wave function near R (at $x = R - \varsigma$) has the value $Ae^{-\kappa R}(e^{\kappa\varsigma} - e^{-\kappa\varsigma})$. As R increases, $A(e^{\kappa\varsigma} - e^{-\kappa\varsigma})$ is constant to the extent that increasing the bridge size does *not* alter the *energy* of the trap localized state or the relative amount of wave function amplitude in the two regions (see Sect. II.B). For long linkers this approximation is reasonable and can certainly be tested. For distant transfer, the donor wave function amplitude arriving at $R - \varsigma$ decays exponentially with R *even though* the wave function in region II is not a purely decaying exponential. Taking $\langle \Psi_D | V_A | \Psi_A \rangle$ for T_{ab} and V_A well localized in region II near $x = R$, the matrix element decays exponentially with distance even when the bridge is finite, providing it is long compared to the well width.

Consider now the edge effects which arise in the molecular orbital picture for a donor connected to N identical equally spaced orbitals. The orbital coefficient of the donor wave function on the j^{th} bridge site is ($C_j = a\epsilon^j + b\epsilon^{N-j+1}$) since the system may have growing and decaying parts in the linker region. Again, the finite length of the bridge does not alter the *distance* decay of the wave function from its behavior in the infinite constant or periodic bridge case; only a distance independent prefactor enters the wave function. It is necessary that the eigenvalue E change slowly with N , a condition which certainly obtains for large N .

The tunneling matrix element calculated from the molecular orbital picture (Fig. II.7) with both the splitting and the golden rule gives the same ϵ dependence to the matrix element for a finite bridge. Consider again the one orbital per site model with donor atom at $j = 0$ and acceptor at $j = N$. Multiplying the



Figure II.7. The basis functions of a one orbital per site model of finite length are shown.

Schrödinger equation by ϕ_j^* and integrating:

$$<0| : \beta'(a\epsilon + b\epsilon^N) = (E - \Delta) \quad (II.32a)$$

$$<1| : \beta' + (a\epsilon^2 + b\epsilon^{N-1})\beta = E(a\epsilon + b\epsilon^N) \quad (II.32b)$$

$$<2| : \beta(a\epsilon + b\epsilon^N) + \beta(a\epsilon^3 + b\epsilon^{N-2}) = E(a\epsilon^2 + b\epsilon^{N-1}) \quad (II.32c)$$

$$<N| : \beta(a\epsilon^{N-1} + b\epsilon^2) = E(a\epsilon^N + b\epsilon) \quad (II.32d)$$

$$\text{and } \beta' = <\phi_0|H|\phi_1>. \quad (II.32e)$$

Combining (d) with $\epsilon + 1/\epsilon = E/\beta$ (from c):

$$\frac{a}{b} = -\epsilon^{1-N} \left(\frac{\epsilon - E/\beta}{1/\epsilon - E/\beta} \right) = -\epsilon^{-1-N}. \quad (II.33)$$

Since

$$\Psi = \phi_0 + \lambda \sum_j C_j \phi_j \quad (II.34)$$

where $C_j = a\epsilon^j + b\epsilon^{N-j+1}$.

$$C_j = a\epsilon^j - \frac{a\epsilon^{2N+2}}{\epsilon^j}. \quad (II.35)$$

Therefore,

$$C_N = a\epsilon^{N+1}(1/\epsilon - \epsilon) \quad (II.36)$$

$$a = \left(\frac{E - \Delta}{\beta'\epsilon + \beta'\epsilon^{2N-1}} \right) \quad (II.37)$$

and

$$<\Psi_D|V_A|\Psi_A> \propto (1/\epsilon - \epsilon)\epsilon^N \quad (II.38)$$

because the donor occupies the N^{th} site.

The energies of the symmetric and antisymmetric states are (traps at sites 0 and N)

$$(E_{\pm} - \Delta) = \beta'^2 \left[\frac{\epsilon_{\pm} \pm \epsilon_{\pm}^N}{(E_{\pm} - \beta\epsilon)(\epsilon_{\pm} \pm \epsilon_{\pm}^{N+2})} \right]. \quad (II.39)$$

Expansion of this to first order in ϵ^N gives

$$\Delta E \simeq \frac{2\beta'^2}{\beta} \epsilon^N (\epsilon - 1/\epsilon), \quad (II.40)$$

the same ϵ dependence of the tunneling matrix element as in the golden rule expression. When $\epsilon = \exp(-\kappa\zeta)$ the square well result obtains, as expected.

We have seen that: (1) Tunneling matrix elements may be calculated by either an exchange splitting or via first order perturbation theory; (2) Molecular orbital approaches differ from square barrier models in the functional dependence of T_{ab} on the energy of the transferring electron; (3) Edge effects provide very small corrections to the infinite Kronig-Penney models in the long distance transfer problem if $\epsilon^{2N} \ll 1$. When linker length significantly alters the localized state energy, it is unlikely that a golden rule picture for the rate will be relevant.

II.E. References – Chapter 2

- 1a. J. Jortner, *Biochim. Biophys. Acta* **594**, 193(1980).
- 1b. M.D. Newton and N. Sutin *Ann. Rev. Phys. Chem.* **35**, 437, 1984.
- 1c. J.J. Hopfield, *Proc. Nat. Acad. Sci. (USA)* **71** (1974)3640.
- 2a. A.A. Frost, *J. Chem. Phys.* **25**, 1150(1956).
- 2b. M. Redi and J.J. Hopfield, *J. Chem. Phys.* **72**, 6651(1980)
- 2c. P. Siders, R.J. Cave, and R.A. Marcus, *J. Chem. Phys.* **81**, 5613(1984).
- 3a. R. de L. Kronig and W.G. Penney, *Proc. Roy. Soc. (London)* **A130**, 499(1931).
- 3b. D.S. Saxon and R.A. Hunter, *Philips Research Reports* **4**, 81(1949).
- 3c. F. Kuliasko, *Physica* **30**, 2180, 2185(1964).
4. C. Kittel, *Introduction to Solid State Physics*, 5th ed. (Wiley, New York, 1976)
5. D.N. Beratan, J.N. Onuchic and J.J. Hopfield, *J. Chem. Phys.*, submitted 1985.
- 6a. A. S. Davydov, *Phys. Stat. Sol. (b)* **90**, 457(1978)
- 6b. H. M. McConnell, *J. Chem. Phys.* **35**, 508(1961).
- 6c. S. Larsson, *J. Chem. Soc., Faraday Trans.* **2**, **79**, 1375(1983).
- 6d. G.H. Wannier, *Elements of Solid State Theory* (Cambridge University Press, Cambridge, 1959) Chapter 6.
7. L. Salem, *The Molecular Orbital Theory of Conjugated Systems* (Benjamin, New York, 1966), p. 517.

Chapter III

Tunneling Matrix Elements in Systems of Experimental Interest

III.A Introduction

In Chapter II several examples were given of tunneling matrix element calculations for model potentials. The barrier to a quantitative understanding of experimentally measured tunneling matrix elements (understanding means predictive ability too!) is the connection between the simple models and the real systems. Square barrier models do not directly incorporate the symmetry and topological properties of the bridging medium. One electron orbital models can not describe the detailed molecular structure of complicated donors and acceptors. *Ab initio* calculations may be rather basis set dependent and rely on variational techniques which can be insensitive to wave function errors in low amplitude regions. A compromise between these methods must be reached.

Although scarce, experimental measures of the distance dependence of T_{ab} suggest $0.55 < \alpha < 0.75 \text{ \AA}^{-1}$ where $T_{ab} = T_0 \exp(-\alpha R)$. This value suggests an electron energy below the "barrier" between wells of $\sim 1\text{-}2 \text{ eV}$ [1]. This energy is clearly too small to correspond to a true electron binding energy and more likely indicates bond assisted transport. As such, the molecular orbital approach to the problem is justified.

The most useful electron transfer experiments, in light of the theoretical examples presented earlier, are experiments which vary the bridge length, keeping donor-acceptor orientations, energetics, solvent, and temperature constant. It is crucial that the molecules be rigid so that electron transfer, not conformational motion, is rate limiting. Also, bridge interaction must not be too large or the reaction may become adiabatic. Although improvements in experimental design are rapid, only *two* electron transfer systems in the literature fulfill these requirements. One set is the spiroalkane bridged mixed-valence pentaamineruthenium

molecules of Stein, Lewis, Seitz, and Taube [2]. The other set is the one of Joran, Leland, Geller, Hopfield and Dervan consisting of porphyrins and quinones linked with bicyclo[2.2.2] or bisbicyclo[2.2.2]octane [3]. Other experiments carried out in rigid random glasses (e.g., Miller, Beitz and Huddleston [4] and Guarr, McGuire and McLendon [5]) are also of interest but somewhat harder to interpret due to the random nature of the intermolecular interactions. The charge transfer (intervalence) band was observed in the spiroalkane bridged systems. The extinction coefficient and shape of this band allow the calculation of $|T_{ab}(R)|$ [6]. Thermally stimulated transfer from a porphyrin excited state quenches porphyrin fluorescence in the bicyclo[2.2.2]octane bridged systems (see Sect. III.C).

The strategy for calculating the dependence of T_{ab} on the number of linker units in spiroalkane was:

(1) Calculate the $E - \epsilon$ relation for the linker. Since $T_{ab} \propto \epsilon^N$ the band structure provides a quick estimate of the distance dependence of T_{ab} at a given electron tunneling energy. The only necessary assumption, which has not already been discussed, is that the central potential is dominated by the potential of the atoms fixed in that region and is not strongly perturbed by the nearby donor, acceptor, and solvent.

(2) Find the donor and acceptor state Coulomb energies required to place these localized states in the proper positions in the linker band gap. This was accomplished by applying boundary conditions so the energies of the metal-ligand and intervalence bands would be correct. This procedure led to a connection between trap site redox potential and the standard Hückel exchange parameters for hydrocarbons.

(3) Find the wave functions for the two, three, and four ring systems, as-

suming a periodic potential in the linker region. The finite nature of the bridges was included in the calculation.

(4) From the wave functions, find the optical tunneling matrix elements (where $\alpha(Ru^{+2}) \neq \alpha(Ru^{+3})$) and energy splittings ($\alpha(Ru^{+2}) = \alpha(Ru^{+3})$).

III.B "Calculation of Electron Tunneling Matrix Elements
in Rigid Systems:
Mixed-Valence Dithiaspirocyclobutane Molecules"

J. Am. Chem. Soc. **106**, 1584(1984)

Reprinted from the Journal of the American Chemical Society, 1984, 106, 1584.
 Copyright © 1984 by the American Chemical Society and reprinted by permission of the copyright owner.

Calculation of Electron Tunneling Matrix Elements in Rigid Systems: Mixed-Valence Dithiaspirocyclobutane Molecules

David N. Beratan* and J. J. Hopfield†

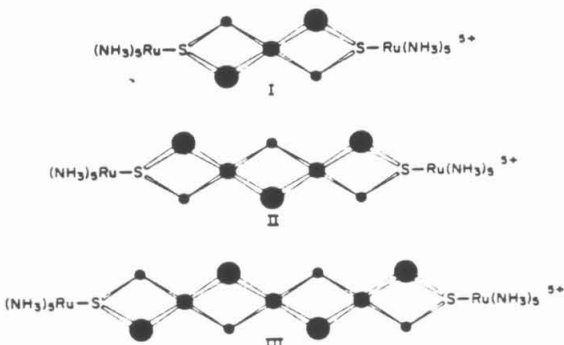
Contribution No. 6850 from the Division of Chemistry and Chemical Engineering, California Institute of Technology, Pasadena, California 91125. Received August 4, 1983

Abstract: A semiempirical model is presented which predicts photoassisted electron-transfer rate dependence on distance for redox groups connected by rigid polymeric linkers. The model approximately reproduces the observed decay of the optical tunneling matrix element with distance found for the rigid ruthenium dithiaspiro mixed-valence complexes of Stein, Lewis, Seitz, and Taube.¹⁻³ The method calculates the through-bond propagation of the wave function tail, by a method which emphasizes obtaining the correct distance dependence of the tunneling matrix element for these weakly interacting donor-acceptor complexes. The method also allows prediction of the magnitude of the matrix element, the importance of hole or electron tunneling in the transport process, the effect of donor and acceptor redox potential on the matrix element, and the thermal tunneling matrix element for these and other compounds.

Introduction

Electron-transfer theory predicts an approximately exponential decrease in electron-transfer rate with distance when the donor and acceptor weakly interact.⁴⁻⁶ Only recently, however, have rigid molecules with weakly interacting electron donor and acceptor groups become available.^{1-3,7,8} Predictions of transfer rates, qualitative in the past, must be refined to treat this new class of compounds. A series of mixed-valence ruthenium molecules (I, II, III) was recently synthesized and studied by Stein, Lewis, Seitz, and Taube.^{2,3}

Interaction between the metal ions is believed to be rather weak and to involve through-bond rather than through-space interactions.^{2,9} If the interaction between donor and acceptor is indeed weak, one may imagine that relaxation of vibrational modes in the molecule and of the solvent around the odd electron (vibronic coupling) stabilizes the localization. This relaxation provides a deeper well for the electron on one side of the molecule compared to the otherwise equivalent site. Hence one finds, for a short time at least, a ground state for the odd electron localized on one relaxed



(1) Taube, H. In "Tunneling in Biological Systems", Chance, B., DeVault, D. C., Frauenfelder, H., Marcus, R. A., Schreifler, J. R., Sutin, N., Eds.; Academic Press: New York, 1979, pp 173-199.

(2) Stein, C. A.; Taube, H. *J. Am. Chem. Soc.* 1981, 103, 693-695.

(3) Stein, C. A.; Lewis, N. A.; Seitz, G. *J. Am. Chem. Soc.* 1982, 104, 2596-2599.

* Also California Institute of Technology, Division of Biology, and Bell Laboratories, Murray Hill, NJ 07974.

metal-ligand group. An unoccupied excited state for an electron localized on the unrelaxed site also exists.¹⁰ Therefore, a charge-transfer optical absorption between these states can be found. For I, II, and III a charge-transfer band was found ($\epsilon = 43, 9, 2.3 \text{ M}^{-1} \text{ cm}^{-1}$, respectively). The extinction coefficient of this band is related to the tunneling matrix element in the Gaussian approximation when the donor and acceptor are identical as shown in eq 1.¹⁰

$$\epsilon(E_0) = \zeta(|T_{ab}|^2/E_0)(a^2/\sigma)G \quad (1)$$

$$\zeta = [2n/(n^2 + 1)](2\pi^2/3)(N_0/2300)(\epsilon^2/\hbar c)(1/2\pi)^{1/2} = 4.60 \times 10^{18} \text{ M}^{-1} \text{ cm}^{-3} \text{ when } n = 1.53$$

$$G = \exp[-(E_0 - \Delta)^2/2\sigma^2]$$

E_0 is the energy of the photon, ϵ is the charge on the electron, a is the donor-acceptor distance, T_{ab} is the optical tunneling matrix element, n is the index of refraction of the sample, N_0 is Avogadro's number, \hbar is Planck's constant/2 π , c is the speed of light, Δ is the reorganizational energy, and σ is the half-width of the charge-transfer band at 0.61 maximum. A first-order perturbation treatment of weakly interacting donor and acceptor groups predicts the electric dipole matrix element of the charge-transfer band is given by¹⁰

$$\langle \psi_g | e\bar{x} | \psi_{ex} \rangle = eaT_{ab}/(E_g - E_{ex}) \quad (2)$$

ψ_g and ψ_{ex} are the ground- and excited-state wave functions, respectively. \bar{x} is the position operator. Equation 1 allows the calculation of $|T_{ab}|$, the optical tunneling matrix element, from the experimentally determined extinction coefficient. $|T_{ab}|$ contains the distance dependence of the electron-transfer rate. Fermi's "golden rule" predicts that the transfer rate depends on the square of $|T_{ab}|$.¹¹ We develop a method of finding the appropriate ground- and excited-state wave functions which allows the independent prediction of T_{ab} . The most important capability of this method is its ability to predict the distance dependence of T_{ab} for donors and acceptors of given redox energy. The relevance of this method to electron transfer in proteins is also considered.

Theoretical Section

The problem of electron exchange between traps at fixed distance has been discussed recently by several authors.¹²⁻¹⁷ Understanding how electron-transfer rates depend on molecular structure is essential for an understanding of biological electron-transfer reactions. This interest in the structure-function relationship forces us to first understand electron-transfer processes in "model compounds". T_{ab} depends critically on the overlap of the two localized wave functions and is difficult to calculate. These matrix elements depend on the details of what is usually an uninteresting chemical aspect of the electronic wave function, its tail. The wave-function tail decay can be significantly altered by changing the atoms between donor and acceptor. The problem of calculating tunneling matrix elements is, as yet, intractable using traditional ab initio methods for molecular structure determination.

The choice of orbital basis set may severely alter the size of T_{ab} . Traditional variational methods, which optimize the energy of a state, are rather insensitive to the form of the small amplitude wave function tail. Variational methods can tolerate errors in the long-range behavior of the function because changes of these tails cause little change in the total energy of the state. We have chosen a semiempirical approach which assures the proper behavior of the wave function in the region between the electron traps where the wave function decay is rapid.

Periodic Approximation. The fundamental assumption which we make is that within the central region of the hydrocarbon linker the potential is periodic; i.e., at corresponding points of different rings the potential is equal. This assumption neglects the perturbing effects of the Coulombic potentials centered on the ruthenium atoms. As the experiments were performed in aqueous DCl, the dielectric screening is expected to shield the central atoms (at least 2.5 Å away) from this potential. The terminal sulfur orbitals perturb the potentials of the neighboring carbon atoms, causing them to differ somewhat from other secondary carbons in the center of the spiro ligand. This effect is expected to be small. Within the standard extended-Hückel theory, our periodic approximation is equivalent to choosing the same orbital exponents for each orbital of the same type.

Let us investigate the form of the wave function for a long chain of spiroalkane rings. Because the potential is periodic along this chain, the translation operator T commutes with the Hamiltonian \mathcal{H} of the system in this region:

$$[\mathcal{H}, T] = 0 \quad (3)$$

The wave function can then be chosen to be an eigenfunction of the translation operator, so:

$$T\psi = (\epsilon)\psi \quad (4)$$

$$T^2\psi = (\epsilon)^2\psi, \dots$$

where ϵ is some number. We may solve the Schrödinger equation to find a relationship between ϵ and the energy of the states.¹⁸ Truncating one end of the chain and adding special end orbitals does not change the energy- ϵ relationship since the potential in the central region is not changed by the truncation. Moreover, one can instead truncate the opposite end, add a different group here, and solve a different single "impurity" problem. Finally, one may truncate these single impurity wave functions and form a linear combination of these two single impurity chains. One is assured (within the LCAO approximation) of having a wave function with the correct behavior in the central region. The energy- ϵ relation true for the infinite spiro chain is also true for the finite molecule. This approach is equivalent to writing the Bloch states for a crystal in terms of some wave vector. Only after the boundary conditions of the crystal are considered, be they cyclic or not, do we obtain explicit values for the wave vector.

The problem of interactions between "special" groups embedded in otherwise normal solvent or crystal pervades chemistry. For example, theories of electronic excitation transfer parallel very closely the central ideas of electron transfer theory.^{4,19,20} Koster and Slater studied the energetics of impurity levels in solids long ago.^{21,22} Semiconductors doped with impurities are known to trap excitons (electron hole pairs) on these impurities or on neighboring impurities. Faulkner and Hopfield developed a theory of the optical properties for a class of these doped semiconductors.^{23,24} These problems are cousins of the photoassisted electron-transfer problem.^{10,25-27} A treatment of wave function propagation similar

(4) Hopfield, J. J. *Proc. Natl. Acad. Sci. U.S.A.* 1974, 71, 3640-3644.
(5) Jortner, J. *J. Chem. Phys.* 1976, 64, 4860-4867.

(6) Eyring, H.; Walter, J.; Kimball, G. E. "Quantum Chemistry"; Wiley: New York, 1944; Chapter XI.

(7) Calcaterra, L. T.; Closs, G. L.; Miller, J. R. *J. Am. Chem. Soc.* 1983, 105, 670-671.

(8) Pasman, P.; Koper, N. W.; Verhoeven, J. W. *Rech. Trav. Chim. Pays-Bas* 1982, 101, 363-364.

(9) Stein, C. A.; Lewis, N. A.; Seitz, G.; Baker, A. D. *Inorg. Chem.* 1983, 22, 1124-1128.

(10) Hopfield, J. J. *Biophys. J.* 1977, 18, 311-321.
(11) Merzbacher, E. "Quantum Mechanics", 2nd ed., Wiley: New York, 1970.

(12) DeVault, D. *Q. Rev. Biophys.* 1980, 13, 387-564.
(13) Jortner, J. *Biochim. Biophys. Acta* 1980, 594, 193-230.

(14) Day, P. *Int. Rev. Phys. Chem.* 1981, 1, 149-193.

(15) Chance, B.; DeVault, D. C.; Frauenfelder, H.; Marcus, R. A.; Schriener, J. R.; Sutin, N., Eds. "Tunneling in Biological Systems"; Academic Press: New York, 1979.

(16) Lippard, S. J., Ed. "Progress in Inorganic Chemistry"; Wiley: New York, 1983; Vol. 30.

(17) Larson, S. J. *J. Am. Chem. Soc.* 1981, 103, 4034-4040.

(18) In the limit of a long chain or orbitals, we discover Bloch's theorem and allowed "bands" of energy eigenvalues for the very large number of eigenstates. See ref 33.

(19) Robinson, G. W.; Frosch, R. P. *J. Chem. Phys.* 1962, 37, 1962-1973.
(20) Robinson, G. W.; Frosch, R. P. *J. Chem. Phys.* 1963, 38, 1187-1203.

(21) Koster, G. F.; Slater, J. C. *Phys. Rev.* 1954, 95, 1167-1176.

(22) Koster, G. F.; Slater, J. C. *Phys. Rev.* 1954, 96, 1208-1223.

(23) Faulkner, R. A. *Phys. Rev.* 1968, 175, 991-1009.

(24) Faulkner, R. A.; Hopfield, J. J. In "Localized Excitations in Solids"; Wallis, R. F., Ed.; Plenum Press: New York, 1968; pp 218-238.

(25) Redi, M.; Hopfield, J. J. *J. Chem. Phys.* 1980, 72, 6651-6660.

(26) Hush, N. S. *Electrochim. Acta* 1968, 13, 1005-1023.

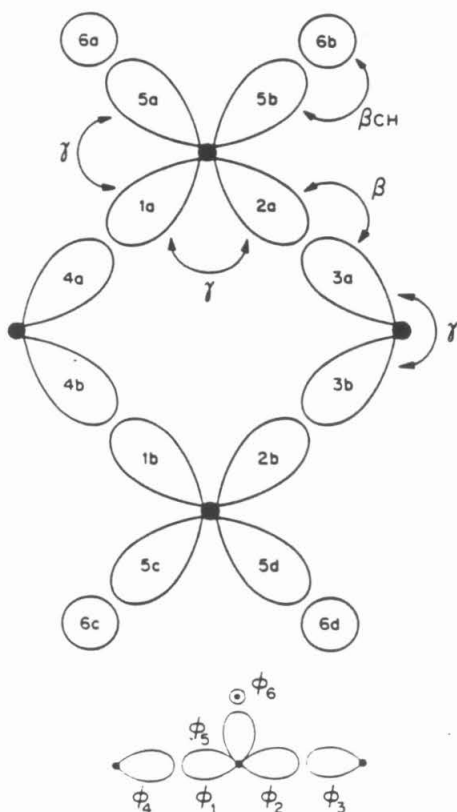


Figure 1. (a) The 16 orbitals of the unit cell are shown. Orbitals with equal integers are combined to form symmetrized orbitals. The orbital interactions are also shown. (b) The six symmetrized basis orbitals that comprise the unit cell are shown.

to ours was used by McConnell to model intramolecular thermally activated charge transfer between aromatic free radicals separated by flexible methylene bridges.²⁸ Morton-Blake recently used a related perturbational method to study defect states in polymers.²⁹ Koiller, Brandi, and Ferreira have studied simple impurity problems using a Green's function formulation.^{30,31} Larsson has compared the distance dependence of σ - and π -mediated transfer rates between metals.³² Most of these methods are adaptations of the tight-binding method of calculating the band structure for crystalline solids.³³ They differ in their description of the "periodic" part and the boundary conditions of the problem.

Because we have already made severe restrictions on the form of the wave-function decay, we choose the most simple model of the Hamiltonian in the central region and of the unit cell. We select the one-electron Hamiltonian

$$\mathcal{H} = \sum_i \alpha_i a_i^* a_i + \sum_{j \neq i} \sum_j \beta_{ij} (a_i^* a_j + a_j^* a_i) + \sum_{k > m} \sum_m \gamma_{km} (a_k^* a_m + a_m^* a_k) \quad (5)$$

where a^* and a are the electron creation and annihilation operators, respectively.³⁴ i sums over all basis functions in the wave

(27) Richardson, D. E.; Taube, H. *J. Am. Chem. Soc.* 1983, 105, 40-51.

(28) McConnell, H. M. *J. Chem. Phys.* 1961, 35, 508-515.

(29) Morton-Blake, D. A. *Theor. Chim. Acta* 1979, 51, 85-95; 1980, 56, 93-112; 1981, 59, 213-227; 1982, 61, 193-202.

(30) Koiller, B.; Brandi, H. S. *Theor. Chim. Acta* 1981, 60, 11-17.

(31) Brandi, H. S.; Koiller, B.; Ferreira, R. *Theor. Chim. Acta* 1981, 60, 89-96.

(32) Larsson, S. *Discuss. Faraday Soc.* 1982, 74, 390-392.

(33) Ashcroft, N. W.; Mermin, N. D. "Solid State Physics"; Saunders: Philadelphia, 1976; Chapters 8, 10, and 28.

(34) Taylor, P. L. "A Quantum Approach to the Solid State"; Prentice Hall: Englewood Cliffs, N.J., 1970; Chapter 2.

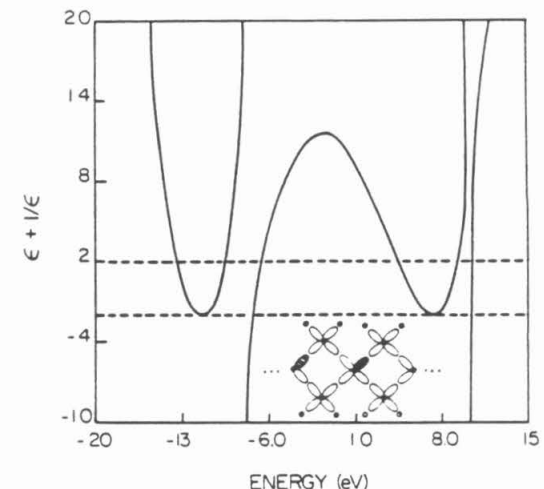


Figure 2. This shows the $(\epsilon + 1/\epsilon)$ dependence on E resulting from eq 7. The band gap falls between -6.6 and +4.2 eV. The eigenstates of the infinite problem fall between the dashed lines.

function. i and j are nearest-neighbor orbitals on adjacent nuclei. k and m are orbitals on the same nucleus. There are 12 sp^3 carbon orbitals and 4 hydrogen orbitals per spiroalkane unit cell. Assuming that the Ru atoms lie on the line of the sulfur atoms and quaternary carbons, the molecule has two mirror planes containing the metal atoms.⁹ This assumption is reasonable if there is π or δ binding between sulfur and ruthenium. Because the effective metal orbitals lie in mirror planes and there must be nonzero orbital coefficients on the intervening atoms to allow electron transfer to occur, the "transferred" electron must occupy an even orbital with respect to these planes. A d_{z^2} like orbital, for example, would suffice. Nonzero coefficients in both planes are required by the form of our Hamiltonian and the assumption of only nearest-neighbor interaction. This restriction causes the following sets of orbitals (shown in Figure 1) to have equal amplitude: $|\phi_{1a}, \phi_{1b}\rangle, |\phi_{2a}, \phi_{2b}\rangle, |\phi_{3a}, \phi_{3b}\rangle, |\phi_{4a}, \phi_{4b}\rangle, |\phi_{5a}, \phi_{5b}, \phi_{5c}, \phi_{5d}\rangle, |\phi_{6a}, \phi_{6b}, \phi_{6c}, \phi_{6d}\rangle$. Because of the symmetry, there are only six unique basis functions per unit cell. The complete 16-orbital and symmetrized 6-orbital unit cells are shown in Figure 1. The wave function is assumed to be of the form (according to the above recipe)

$$\psi = \sum_j [(a\phi_1 + b\phi_2 + c\phi_3 + d\phi_4 + f\phi_5 + g\phi_6)\epsilon^j + W(a\phi_2 + b\phi_1 + c\phi_4 + d\phi_3 + f\phi_5 + g\phi_6)\epsilon^{N-j}] + \lambda\phi_L + \Omega\phi_R \quad (6)$$

where ϕ_1 is the symmetric combination of ϕ_{1a} and ϕ_{1b} , etc. For the central region of the molecule there are three exchange parameters and one Coulomb interaction parameter (α): β , γ , β_{CH} , and α_H . Figure 1a shows the interactions related to these parameters. The carbon sp^3 Coulomb energy is chosen as the energy zero. Zero overlap is assumed between orbitals on neighboring atoms. The special relationship between the energy and the decay constant, ϵ , holds in the infinite spiroalkane as well as in the mixed-valence dithiaphiro complexes. It is determined by integrating the Schrödinger equation for the infinite spiroalkane over the six symmetrized orbitals in the unit cell. Other unit cell choices are possible and should give identical wave functions.

One integrates the Schrödinger equation for the infinite chain ($W = 0$, $\lambda = 0$, $\Omega = 0$ in eq 6) or the finite problem. Assuming zero overlap the matrix equation (eq 7) must hold. The determinant of the matrix must equal zero. This gives the energy- ϵ relationship that is carried into the finite problem due to the

$$\begin{bmatrix} -E & \gamma & 0 & \beta & 2\gamma & 0 \\ \gamma & -E & \beta & 0 & 2\gamma & 0 \\ 0 & \beta & \gamma - E & 2\gamma\epsilon & 0 & 0 \\ \beta & 0 & 2\gamma/\epsilon & \gamma - E & 0 & 0 \\ \gamma & \gamma & 0 & 0 & \gamma - E & \beta_{CH} \\ 0 & 0 & 0 & 0 & \beta_{CH} & \alpha_H - E \end{bmatrix} \begin{bmatrix} a \\ b \\ c \\ d \\ f \\ g \end{bmatrix} = 0 \quad (7)$$

periodic potential in the molecule's central region. Neighboring unit cells only communicate with other cells via orbitals 3 and 4. Therefore, factors of ϵ and $1/\epsilon$ appear in eq 7 only once. It is useful to write this equation in the form $(\epsilon + 1/\epsilon) = x(E)/y(E)$. $x(E)$ is a sixth degree polynomial. $y(E)$ is a second degree polynomial. $x(E)$ arises from the carbon backbone. The C-H bonds split the energies associated with the backbone, giving rise to the second degree $y(E)$. A plot of this equation is shown in Figure 2 for specific choices of the parameters. Points on these curves correspond to eigenstates for molecules containing spiroalkane unit cells. The exact positions of the allowed states for a given problem are determined by the boundary conditions imposed on the linker. ϵ may have real and imaginary parts. Delocalized states (Bloch states) correspond to $\epsilon = \exp(i\vec{k} \cdot \vec{R})$ and $|\epsilon| = 1$.³⁵ These are the states between the dashed lines (± 2) and correspond to allowed energies for the one-dimensional "crystal" comprised of spiroalkane unit cells. Other states ($|\epsilon| < 1$) correspond to localized states.

One must select Coulomb and exchange parameters corresponding to the traditional extended-Hückel parameters. Because we are interested in carbon interactions in periodic networks, we use the tight-binding parameters fit to diamond structure calculations which in turn fit the known band structure and optical properties of diamond.³⁶ We are interested first in getting the $E-\epsilon$ relationship of the system correct rather than calculating experimental energies. Toward this end the diamond parameters are more appropriate than the standard extended Hückel parameters. In this calculation carbon sp^3 hybrid orbitals are chosen as the carbon basis orbitals. It is never necessary to explicitly write these orbitals in terms of Slater or Gaussian functions because the interaction parameters are available from the diamond calculation.³⁷

A form of the extended-Hückel exchange parameter in general use is^{38,39}

$$H_{ab} = K(E_a + E_b)S/2 \quad (8)$$

K is set by the theorist, E_a and E_b are orbital ionization energies, and S is the overlap between atomic orbitals. If E_a and E_b are the orbital ionization energies of sp^3 carbon orbitals (available from tables) and $S \approx 0.65$, then $K = 1.0$ to fit the diamond parameters to eq 8.^{40,41} The orbital ionization energy of hydrogen compared to a carbon 2s orbital is 5.9 eV based on the standard tables.⁴⁰ $\gamma = 1/(\alpha_S - \alpha_P)$. From the diamond calculation, the sp^3 Coulomb energy of carbon is 5.55 eV relative to carbon 2s. The carbon sp^3 Coulomb integral was chosen as the energy zero. Hence, $\alpha_H = 0.35$ eV. A carbon-hydrogen overlap of 0.69, Coulomb energies from the orbital ionization energy tables, and the above K factor gives $\beta_{CH} = -9.14$ eV.^{39,40} These values were used in eq 7 to generate Figure 2. The orbital interactions are summarized in Table I.

Boundary Conditions. Now that the energy-decay constant relationship is determined for the spiroalkane linker, we must find where on Figure 2 the ruthenium localized states appear. The infinite spiroalkane has a band gap from -6.7 to +4.4 eV. Calculations of the solid-state properties of crystalline materials containing impurities suggest that localized states will occur in the gap regions.³⁰⁻³³ Just where these states occur and what their decay constant is depend critically on how we choose the terminal orbitals. We model each metal-pentaammine with a single effective orbital. The important Ru effective orbital must be even with respect to reflection through the two mirror planes which include the metals. Sulfur-ruthenium interactions are probably

(35) \vec{k} is a purely real vector in this case.

(36) Chadi, D. J.; Cohen, M. L. *Phys. Status Solidi. B* 1975, 68, 405-419.

(37) One could also have used the work of footnotes 2 and 13 in Chadi and Cohen's work (ref 36 in this paper).

(38) Daudel, R.; Sandorfy, C. "Semiempirical Wave-mechanical Calculations on Polyatomic Molecules"; Yale University Press: New Haven, 1971.

(39) Yates, K. "Hückel Molecular Orbital Theory"; Academic Press: New York, 1978.

(40) Ballhausen, C. J.; Gray, H. B. "Molecular Orbital Theory"; Benjamin/Cummings: London, 1964; p 122.

(41) Mulliken, R. S. *J. Am. Chem. Soc.* 1950, 72, 4493-4503.

Table I. C and H Parameter Values

parameter	energy (eV)
β	-8.47
γ	-1.85
β_{CH}	-9.14
α_H	0.35
$\alpha_C(sp^3)$	0.00

Table II. Sulfur Parameter Values

parameter	energy (eV)
β_{SC}	-5.11
γ_S	-3.00
α_S	-0.75

mediated by several orbitals.^{9,42-45} It is known that the carbon-sulfur-carbon bond angle in the spiro ring is $\sim 78^\circ$.⁴⁶ Strained bonds such as these prefer an increased p electron content. Yet, for this model we choose to place sp^2 orbitals on the sulfur. This provides ruthenium with an orbital even with respect to the two mirror planes with which to interact. One might have chosen more complex combinations of orbitals. The energy- ϵ relationship shown in Figure 2, however, is independent of these choices. The choice of sulfur orbitals weakly contributes to the position on the plot where the localized states fall. The most critical parameters are the metal Coulomb energies. The sulfur parameters are shown in Table II. They were obtained for sp^2 orbitals using $K = 1.0$, $S_{SC} = 0.37$, and the same orbital ionization energy table.^{40,41}

One now integrates the Schrödinger equation over the six unique boundary orbitals and their nearest neighbors. Simultaneously satisfying these equations (eq 9) and the energy- ϵ equation (eq 7) determines the eigenvalues and eigenfunctions of the system. The first four lines in the determinant result from integrating the Schrödinger equation over the orbitals near Ru(II). The last four lines result from the orbitals near Ru(III). In eq 9 $b' = b/a$ and $f' = f/a$, where b and a represent the coefficients in eq 6. The effective metal-sulfur resonance integrals, β_{3S} and β_{2S} , were calculated by the method of Harrison and Froyen.^{47,48} We find $\beta_{2S} = -2.14$ eV and $\beta_{3S} = -1.57$ eV. The Coulomb energies of the two effective ruthenium orbitals were determined uniquely based on two requirements. First, the energy of the intervalence charge-transfer band must match the experimental energy. Second, the energy of the sulfur to Ru(III) ligand to metal charge-transfer band (LMCT) must match the experimental energy. For the mixed-valence molecules these LMCT energies are 2.74, 2.68, and 2.70 eV for the two-, three-, and four-ring systems. The two "effective" metal pentaammine orbitals each represent 21 atoms by only one orbital. Therefore, the actual Coulomb energy (α_2 or α_3) of this "orbital" is not, of itself, physically meaningful.

With these assumptions the wave functions are uniquely determined for I, II, and III. Computationally, we examined a large number of energies, calculated ϵ from eq 7, and evaluated the determinant in eq 9. For each energy these are two roots of ϵ . By convention we choose the value of ϵ less than 1. The energy of the highest occupied bridge state was determined from an extended-Hückel calculation on the two- and three-ring mixed-valence compounds to be about -7.0 eV. This energy was assumed to remain the same for the four-ring system.

The tunneling matrix element is calculated from the dipole matrix element (eq 2). We calculated the two metal localized wave functions of the system in the band gap and approximated

(42) Kuehn, C. G.; Taube, H. *J. Am. Chem. Soc.* 1976, 98, 689-702.

(43) Stein, C. A.; Taube, H. *J. Am. Chem. Soc.* 1978, 100, 1635-1637.

(44) Stein, C. A.; Taube, H. *Inorg. Chem.* 1979, 18, 1168-1170.

(45) Stein, C. A.; Taube, H. *Inorg. Chem.* 1979, 18, 2212-2216.

(46) Tagaki, W. In "Organic Chemistry of Sulfur"; Oae, S., Ed.; Plenum: New York, 1977; p 247.

(47) Harrison, W. A.; Froyen, S. *Phys. Rev. B* 1980, 21, 3214-3221.

(48) Froyen, S. *Phys. Rev. B* 1980, 22, 3119-3121.

$$\det \begin{bmatrix} \alpha_1 - E & \beta_{1S} & 0 & 0 & 0 & 0 & 0 & 0 \\ \beta_{1S} & \alpha_2 - E & 2\gamma_S & 0 & 0 & 0 & 0 & 0 \\ 0 & \gamma_S & \gamma_S + \alpha_S - E & \beta_{SC}\epsilon & \beta_{SC}\epsilon^N b' & 0 & 0 & 0 \\ 0 & 0 & \beta_{SC} & (2\gamma_f'\epsilon + \gamma b'\epsilon - E\epsilon) & (2\gamma_f'\epsilon^N + \gamma b'\epsilon^N - Eb'\epsilon^N) & 0 & 0 & 0 \\ 0 & 0 & 0 & (2\gamma_f'\epsilon^N + \gamma b'\epsilon^N - Eb'\epsilon^N) & (2\gamma_f'\epsilon + \gamma b'\epsilon - E\epsilon) & \beta_{SC} & 0 & 0 \\ 0 & 0 & 0 & \beta_{SC}\epsilon^N & \beta_{SC}\epsilon^N & \gamma_S - E + \alpha_S & \alpha_S - E & \beta_{1S} \\ 0 & 0 & 0 & 0 & 0 & 2\gamma_S & \beta_{1S} & \alpha_S - E \\ 0 & 0 & 0 & 0 & 0 & 0 & \beta_{1S} & \alpha_S - E \end{bmatrix} \quad (19)$$

the dipole matrix element between these states with the formula

$$\langle \psi_g | e\vec{x} | \psi_{ex} \rangle \simeq e \sum_i C_{gi}^* C_{exi} X_i \quad (10)$$

where C_{gi}^* = coefficient of i th ground-state atomic orbital, C_{exi} = coefficient of i th excited-state atomic orbital, and X_i = X coordinate of i th atom. This formula is reliable to the extent that orbital overlap is small and the x coordinate changes slowly as one moves between metal atoms.⁴⁹⁻⁵² The dipole matrix element involves only the position along the axis joining the metal atoms. The y and z components of the matrix element cancel because of the inversion symmetry of the four-member rings. In eq 1 and 2 a is the through-space distance.

Though semiempirical in approach, this adapted tight-binding method for calculating localized states in mixed-valence molecules offers many benefits. A fairly simple calculation allows the prediction of the rate of decay (ϵ) of a localized wave function with distance as a function of redox energy. The band-structure determination is not complicated. Even simple models of *n*-alkane and spiroalkane produce ϵ - E relationships in the gap region (see Figures 3a and 3b) very similar to the more complex models. We are able to separate the calculation of the tunneling matrix elements into two parts. First the band structure of the rigid bridge is determined. This structure sets limits on the decay of the wave function with distance. Second we impose boundary conditions on the problem dependent on the redox properties of the electron donor and acceptor. Together these properties determine the electronic tunneling matrix element. The band structures for several other unit cell choices are shown in Figures 4a-d. The validity of the form of the wave function in eq 6 was confirmed by finding the eigenvalues and eigenvectors of the full extended-Hückel problem (a 16×16 matrix in the case of the two-ring system). For the two-ring system the wave functions found by the two approaches were consistent.

In the case of long-distance electron transfer between well-localized states, the wave functions may be approximated. For an arbitrary unit cell the two localized wave functions are given approximately by

$$\psi_g \simeq \omega\phi_0 + \epsilon_1\phi_1 + \epsilon_1^2\phi_2 + \dots + \epsilon_1^{N-1}\phi_{N-1} + \epsilon_1^N\phi_N + \zeta\phi_{N+1}$$

$$\text{and}$$

$$\psi_{ex} \simeq \delta\phi_0 + \epsilon_2^N\phi_1 + \epsilon_2^{N-1}\phi_2 + \dots + \epsilon_2^2\phi_{N-1} + \epsilon_2\phi_N + \eta\phi_{N+1}$$

For the optical problem at hand $\epsilon_1 > \epsilon_2$ because the ground state is closer to the bonding states than the excited states (both are very far from the antibonding states); $0 < \epsilon < 1$, $\delta \approx 0$, and $\zeta \approx 0$. The optical tunneling matrix element between the localized states is

$$T_{ab}^{opt} \simeq (\sum_i A_i^* B_i^N) \Delta E / a \simeq (\Delta X / a) (\Delta E) \epsilon_2 \epsilon_1^N \propto \epsilon_2 \epsilon_1^N \quad (11a)$$

N is the number of atoms in the linker backbone, and we have ignored all terms in ϵ_j^N for $j > 1$. A_i and B_i are orbital coefficients. ϵ_1 and ϵ_2 represent the wave-function decay per unit cell but may be converted to the decay per carbon atom. In the thermal electron-transfer reactions, $\epsilon_1 = \epsilon_2$ in the activated complex (by

(49) Robin, M. B.; Day, P. *Adv. Inorg. Chem. Radiochem.* 1967, 10, 247-422.

(50) Mulliken, R. S. *J. Chem. Phys.* 1939, 7, 14-20, 20-34.

(51) Mulliken, R. S.; Person, W. B. "Molecular Complexes"; Wiley: New York, 1969.

(52) Hoijtink, G. J. In "Molecular Orbitals in Chemistry, Physics, and Biology"; Academic Press: New York, 1964.

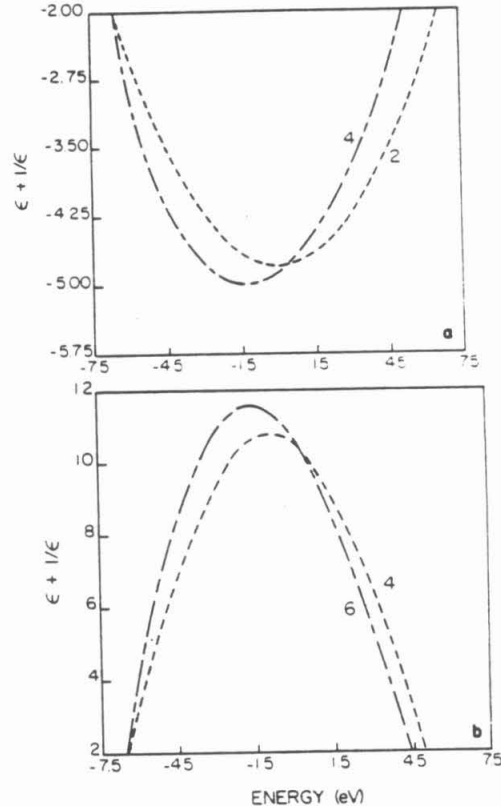


Figure 3. (a) The $\epsilon + 1/\epsilon$ dependence on energy for a two orbital per site *n*-alkane model (marked 2) and the full four-symmetrized orbital per site *n*-alkane (marked 4) is shown. Parameters are taken from Table I. The two orbital per site model makes relatively good predictions of $\epsilon + 1/\epsilon$. (b) As in (a), comparing the full six-symmetrized orbitals per unit cell spiroalkane (marked 6) with the four-symmetrized orbital per unit cell (no C-H bonds) spiroalkane (marked 4). Parameters are taken from Table I.

energy conservation). Rather than relating the thermal matrix element to a splitting between even and odd electronic states (see later section), we may use the above zeroth-order wave functions (when $\delta = \zeta = 0$) to calculate the electronic Hamiltonian matrix element between the states. In the thermal-transfer problem $E_g = E_{ex}$, $\epsilon_1 = \epsilon_2$, $\eta = \omega$, $\zeta = \delta$, and the part of the Hamiltonian omitted in writing ψ_g is $H' = (a_{N+1}^* a_N + a_N^* a_{N+1})\beta'$.

$$\langle \psi_g | H' | \psi_{ex} \rangle = \beta' \eta \epsilon^N \quad (11b)$$

$$T_{ab}^{th} \propto \epsilon^N$$

Thus, addition of an extra unit cell to the linker changes the donor-acceptor matrix element by approximately a factor of ϵ . Tables VI and VII verify that these simple arguments are valid for the spiro molecules. The thermal tunneling matrix element is frequently expressed as

$$T_{ab} \simeq A \exp(-\alpha R) \quad (12)$$

for long-distance charge transfer. ϵ is simply related to α . R is

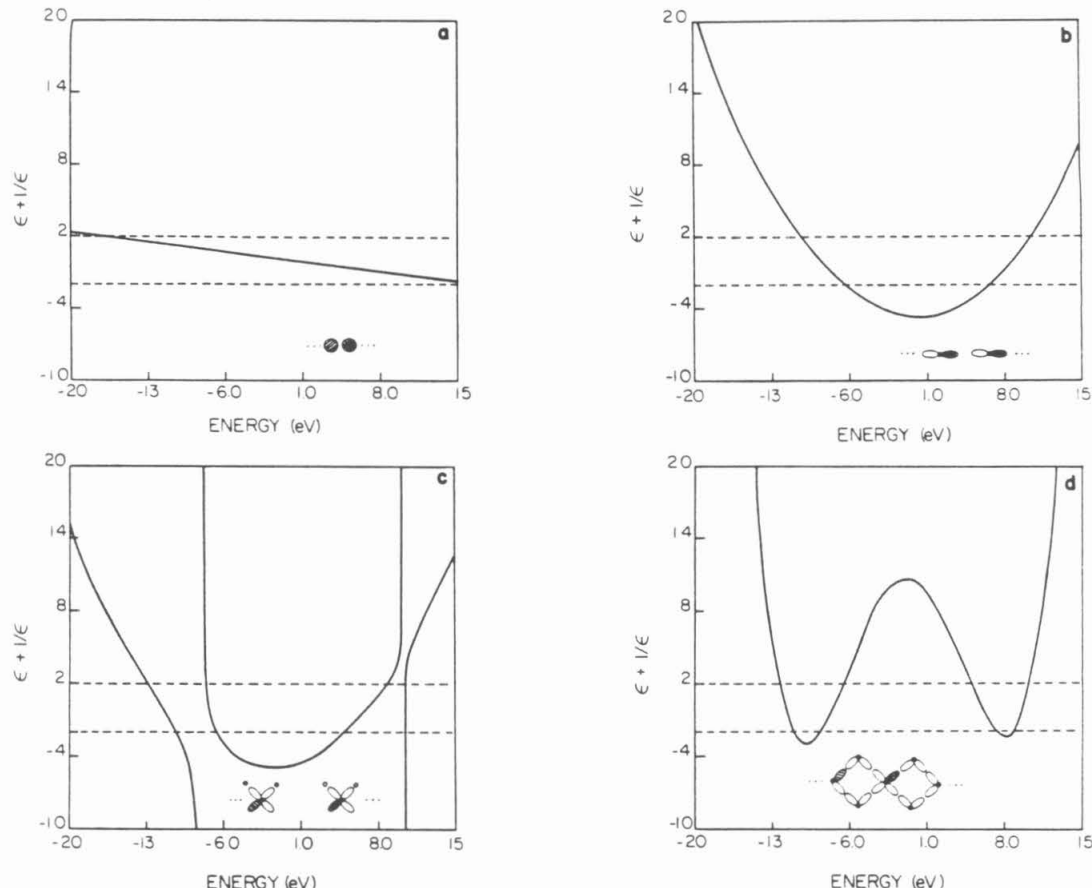


Figure 4. Band structures for several unit cell choices are shown. Interaction parameters are chosen from Table I. $\epsilon + 1/\epsilon = \pm 2$ is marked with dashed lines. (a) The one orbital per site model. (b) The two orbital per site model. (c) The four symmetrized orbital per site *n*-alkane model. (d) The four symmetrized orbital per site model of spiroalkane. Shaded orbitals indicate corresponding orbitals of adjacent unit cells.

Table III. Comparison of Decay Constants ϵ and α

unit cell	distance measured through ^a	carbon atoms traversed	α (\AA^{-1})
<i>n</i> -alkane	bond	1	$-(\ln \epsilon)/1.54$
<i>n</i> -alkane	space	2	$-(\ln \epsilon)/2.4$
spiroalkane	bond	2	$-(\ln \epsilon)/3.08$
spiroalkane	space	2	$-(\ln \epsilon)/2.22$

^a Through-space distance is the shortest distance between ends of a "taut" molecule. All calculations assume bond-mediated transfer. Through-space distances are given for comparison although the transfer is still calculated through bond.

sometimes chosen as a through-bond distance and sometimes as a through-space distance. Table III shows the expressions relating α to ϵ for spiroalkane and *n*-alkane for both through-bond and through-space distance measurements. The actual calculations on the spiroalkanes do not use the approximation of eq 11a and 11b.

Table IV. Calculated Optical Tunneling Matrix Elements^a

no. of rings	α_1	α_3	E_g	ϵ_g	E_{ex}	ϵ_{ex}	$\langle \psi_g \vec{x} \psi_{\text{ex}} \rangle$	T_{ab}
2	-5.4	-4.0	-5.7	0.20	-4.3	0.11	-4.9×10^{-2}	-7.2×10^{-3}
3	-5.6	-4.0	-5.9	0.22	-4.3	0.11	-1.0×10^{-2}	-1.3×10^{-3}
4	-5.9	-4.0	-6.1	0.27	-4.3	0.11	-3.1×10^{-3}	-4.1×10^{-4}
5	-5.9	-4.0	-6.1	0.27	-4.3	0.11	-8.4×10^{-4}	-9.5×10^{-5}
6	-5.9	-4.0	-6.1	0.27	-4.3	0.11	-2.3×10^{-4}	-2.3×10^{-5}

^a Position matrix element in \AA ; all other values are eV.

Comparison with Experiment

Photoassisted Charge Transfer. Varying the end orbital parameters for fixed metal-sulfur interaction parameters we found metal localized states in the band gap region of Figure 2. We varied the Coulomb integrals of Ru(III) and Ru(II) to fit the energy of the intervalence charge-transfer band and the ligand to Ru(III) charge-transfer band. The localized states are very near the valence band. This result suggests that, in these molecules, charge transfer is mediated by hole transfer through the bonding states of the linker. The energies, decay constants, and Coulomb parameters resulting from the fit are given in Table IV. The dipole matrix elements were calculated with eq 2 assuming a distance of 1.11 \AA between all nonmetal nuclei (measured along the metal-metal axis). The metal-sulfur distances were taken from ref 3. The calculation of $|T_{ab}|$ from experiment (ref 3) assumed the appropriate distance to be used in eq 1 was the through-bond distance. In the optical charge-transfer formalism, however, the through-space distance is required when calculating with eq 1 and 2. Corrected values of $|T_{ab}|$ determined from the

Table V. Corrected Experimental T_{ab} 's

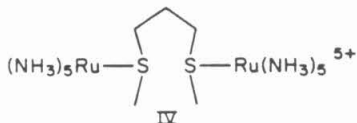
no. of rings	E^{op} (eV)	metal-metal through-space distance (Å)	$ T_{ab} $ (eV)
2	1.36	9.3	2.1×10^{-2}
3	1.54	11.5	8.5×10^{-3}
4	1.80	13.7	4.0×10^{-3}

experiments are given in Table V.

The comproportionation constants for these molecules are not known. Since no separation was observed between the two waves in the cyclic voltammetry experiments, it is reasonable to assume that the metals are oxidized in a statistical fashion with $K_{com} = 4$.²⁷ If the metals were oxidized in a statistical fashion with no regard for the oxidation state of the other end of the molecule, the assumed concentrations of mixed-valence species would be a factor of 2 too large. The calculated values for T_{ab} , in turn, would be too small by the factor $(1/\sqrt{2})$. The experimentally determined $|T_{ab}|$ is roughly $0.62 \exp(-0.37R)$, where R is the through-space metal-metal distance in Å.

Both the magnitude and decay of the calculated T_{ab} fit the experimentally determined values fairly well with respect to decay length and prefactor (eq 12). T_{ab} for the four-ring system is calculated to be 0.31 of the three-ring value. The change corresponds to a through-space α of 0.53 Å⁻¹. The calculated through-space prefactor (A) for the four-ring system is -0.58 eV. The average change of T_{ab} upon addition of a unit cell is a factor of 0.25; thus the average through-space calculated α is found to be ~ 0.63 . This calculation can be performed for an arbitrary number of linkers. T_{ab} is predicted for the five- and six-ring systems (see Table IV).

The value ϵ in spiroalkane is roughly the factor by which the wave function decays upon moving between any two corresponding orbitals in adjacent unit cells. In the case of spiroalkane there are two carbon atoms between the corresponding carbon orbitals on adjacent unit cells. For the purpose of comparing wave-function decays per carbon atom, we define $\epsilon' = \epsilon^{1/2}$. Thus, a mostly localized electron mixing weakly with a spiroalkane chain has an amplitude which decays by a factor of ϵ' per carbon atom in the spiro backbone. Seitz and Taube report an extinction coefficient of $5 \text{ M}^{-1} \text{ cm}^{-1}$ for IV.² This is a nonrigid molecule, but since



the intervalence band extinction coefficient is so small and the Coulombic repulsion between metals favors a large through-space ruthenium distance, it is likely that direct Ru-Ru through-space interactions are small. The extinction coefficient varies as the square of the tunneling matrix element. According to eq 11a $T(\text{alkane})/T(\text{spiro}) \approx (0.25/0.33)(0.33/0.45)^N$. Thus $T^2(\text{alkane})/T^2(\text{spiro}) \approx 0.17$. Hence, the extinction coefficient for IV is expected to be $(0.17)(43)$ or $7.3 \text{ M}^{-1} \text{ cm}^{-1}$, very close to the experimental value. The values of ϵ used here are decay per carbon atom (ϵ') and are taken from Table IV and Figure 5b. N equals 2. Figures 5a and 5b compare *n*-alkane and spiroalkane in the band gap region.

Predictions for Related Experiments. Taube and Stein have prepared the mixed-valence *trans*-isooctaammine complex of the two-ring ligand (isn = isonicotinamide). Little change in extinction coefficient was found. Since there is a fair amount of uncertainty in the choice of the sulfur-metal interactions in our method, we can best compare the *decrease* of T_{ab} with distance for different redox energy electron traps. It is harder to calculate the exact change in rate for a fixed number of rings due to ligand or metal substitution because such changes effect the boundary conditions in subtle ways. The redox potential of $\text{Ru}(\text{NH}_3)_5\text{isn}$ is changed by +0.2 V compared to $\text{Ru}(\text{NH}_3)_5$ in the spiro molecules.² Changing α_3 and α_2 by -0.2 eV from their values in Table IV causes $\langle \psi_g | \vec{r} | \psi_{ex} \rangle$ to change by a factor of 0.23 in going from two

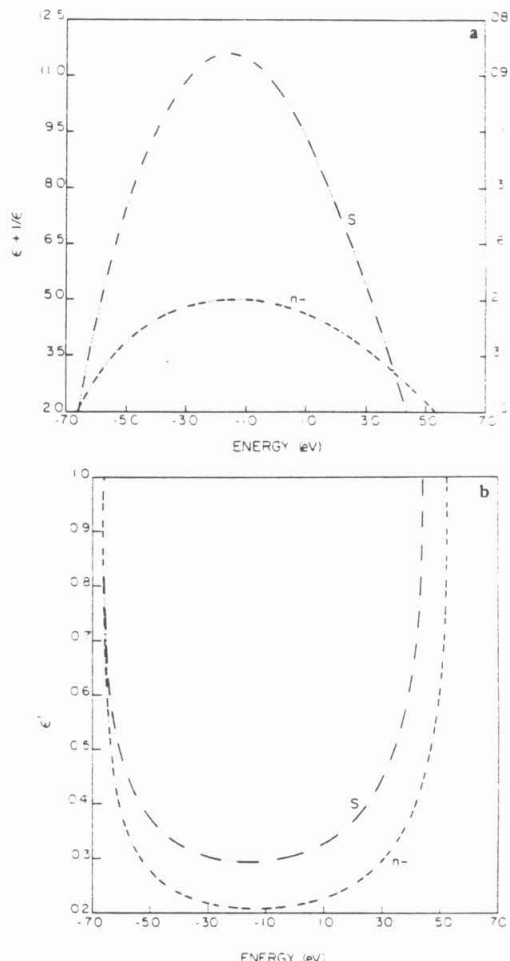


Figure 5. (a) The $\epsilon + 1/\epsilon$ dependence on energy for *n*- and spiroalkanes is shown. The sign of $\epsilon + 1/\epsilon$ for *n*-alkane is reversed from its true value. The horizontal line represents the edge of the band gap. The parameters were chosen from Table I. Figure 6b can be obtained from this by solving a quadratic in ϵ . (b) The ϵ' (decay per carbon atom) dependence on electron energy for spiro- and *n*-alkanes in the band gap. The decay constant for spiro- is everywhere greater than for the *n*-alkane. Parameters are taken from Table I. In both figures "S" marks the spiroalkane curves and "n-" the *n*-alkane curves.

to three rings. T_{ab} according to eq 2, is predicted to change by a factor of 0.21 on going from the two-ring isn to the three-ring isn system. The pentaammine system was calculated to change T_{ab} by a factor of 0.15 on going from the two- to three-ring system. A smaller distance from the valence band was indeed expected to make the isn-localized state wave functions decay more slowly compared to the pentaammine states.

Our method allows the prediction of the effect of altered electron donor and acceptor trap depth (redox energy) on ϵ and hence on T_{ab}^{op} . We give several illustrations for the spiroalkane system where the Coulomb energies of the metals are both changed. Such a change might be induced by ligand or metal substitution, or by a change of solvent. The values of the parameters, energies of the localized states, and the tunneling matrix elements are given in Table VI. Changing the redox levels of the electron traps alters the decay of T_{ab} with distance. This decay constant is, therefore, not a "universal" parameter. Because of uncertainties in $\langle \psi_g | \vec{r} | \psi_{ex} \rangle$ for different redox levels but constant number of rings is discouraged.

Thermally activated electron exchange may also be an im-

Table VI. Optical T_{ab} for Altered Trap Depths^a

no. of rings	α_3	α_1	E_g	ϵ_g	E_{ex}	ϵ_{ex}	$\langle \psi_g \vec{x} \psi_{ex} \rangle$	T_{ab}
2	-4.9	-3.4	-5.3	0.16	-3.8	0.10	-4.4×10^{-2}	-7.1×10^{-3}
3	-4.9	-3.4	-5.3	0.16	-3.8	0.10	-7.4×10^{-3}	-9.7×10^{-4}
4	-4.9	-3.4	-5.3	0.16	-3.8	0.10	-1.2×10^{-3}	-1.3×10^{-4}
2 ^b	-5.6	-4.2	-5.9	0.22	-4.5	0.12	-5.2×10^{-2}	-7.8×10^{-3}
3	-5.8	-4.2	-6.0	0.25	-4.5	0.12	-1.2×10^{-2}	-1.6×10^{-3}
4	-6.1	-4.2	-6.3	0.33	-4.5	0.12	-4.9×10^{-3}	-6.4×10^{-4}
2	-6.3	-4.8	-6.4	0.43	-5.0	0.14	-7.0×10^{-2}	-1.1×10^{-2}
3	-6.3	-4.8	-6.4	0.43	-5.0	0.14	-2.8×10^{-2}	-3.4×10^{-3}
4	-6.3	-4.8	-6.4	0.43	-5.0	0.14	-1.2×10^{-2}	-1.2×10^{-3}
2	-6.5	-5.0	-6.6	0.72	-5.2	0.15	-8.6×10^{-2}	-1.2×10^{-2}
3	-6.5	-5.0	-6.6	0.69	-5.2	0.15	-4.7×10^{-2}	-5.7×10^{-3}
4	-6.5	-5.0	-6.6	0.68	-5.2	0.15	-2.9×10^{-2}	-3.0×10^{-3}

^a $\beta_{2S} = -2.14$, $\beta_{3S} = -1.57$, all energies in eV. ^b The second set of values corresponds roughly to the isn analogues of the pentaammine mixed-valence complexes.

Table VII

no. of rings	$\alpha_3 = \alpha_1$	E_b	ϵ_b	E_a	ϵ_a	T_{ab}
A. Calculated Thermal Tunneling Matrix Elements ^a						
2	-4.7	-5.06	0.14	-5.04	0.14	7.5×10^{-3}
3	-4.8	-5.14	0.15	-5.14	0.15	1.1×10^{-3}
4	-4.95	-5.27	0.15	-5.27	0.15	1.8×10^{-4}
5	-4.95	-5.27	0.15	-5.27	0.15	2.8×10^{-5}
B. Thermal T_{ab} for Altered Trap Depths ^b						
2	-4.2	-4.6	0.12	-4.6	0.12	7.3×10^{-3}
3	-4.2	-4.6	0.12	-4.6	0.12	9.1×10^{-4}
4	-4.2	-4.6	0.12	-4.6	0.12	1.1×10^{-4}
2 ^c	-4.9	-5.2	0.15	-5.2	0.15	7.7×10^{-3}
3	-5.0	-5.3	0.16	-5.3	0.16	1.2×10^{-3}
4	-5.15	-5.4	0.17	-5.4	0.17	2.2×10^{-4}
2	-5.5	-5.8	0.20	-5.7	0.20	9.1×10^{-3}
3	-5.5	-5.7	0.20	-5.7	0.20	1.8×10^{-3}
4	-5.5	-5.7	0.20	-5.7	0.20	3.5×10^{-4}
2	-6.4	-6.5	0.50	-6.5	0.50	1.7×10^{-2}
3	-6.4	-6.5	0.50	-6.5	0.50	7.8×10^{-3}
4	-6.4	-6.5	0.50	-6.5	0.50	3.7×10^{-3}

^a $\beta_{2S} = \beta_{3S} = -1.86$, $T_{ab} = \frac{1}{2}(E_a - E_b)$, all energies in eV.

^b $\beta_{2S} = \beta_{3S} = -1.86$, all energies in eV. ^c The second set of values corresponds roughly to the isn analogues of the pentaammine mixed-valence complexes.

portant process in these mixed-valence molecules. The thermal electron-tunneling matrix element is just half the symmetric antisymmetric splitting when $\alpha_3 = \alpha_2$ and $\beta_{2S} = \beta_{3S}$. Choosing these parameters to be equal to the averages of the parameters used in the optical charge-transfer process yields predictions of the thermal tunneling matrix elements for the pentaammine complexes (Table VIIA).⁵³ We find the distance dependence of T_{ab} to be similar to the distance dependence found for the optical process. Table VIIIB shows the energy splitting for $\alpha_3 = \alpha_2$ and $\beta_{2S} = \beta_{3S} = -1.86$ at several points in the band gap.

For the case corresponding roughly to isn-substituted systems ($\alpha_3 = \alpha_2 = -4.9$ eV, $\beta_{2S} = \beta_{3S} = -1.86$ eV, two rings), $T_{ab} = 7.7 \times 10^{-3}$ eV. For three rings $\alpha_3 = \alpha_2 = -5.0$ eV, $\beta_{2S} = \beta_{3S} = -1.86$ eV, and $T_{ab} = 1.2 \times 10^{-3}$ eV. T_{ab} (thermal) has changed by a factor of only ~ 0.16 . Compare this to the values in Table VA (~ 0.15 per linker cell). More drastic effects will be seen on the thermal matrix element by considerably changing the redox level of the coordinated metals.

General Discussion

Geometric Effects on T_{ab} . The considerable difference in electron mediation properties of *n*-alkane compared to spiroalkane linker arises from the two equivalent electronic pathways in each unit cell of spiroalkane. In the spiro molecules the electrons have twice the number of transfer routes, and the wave function amplitude essentially adds at each quaternary center before decaying into the next ring.

The energy- ϵ relationship for an *n*-alkane where the carbon orbitals are represented by a single orbital and there are two atoms per unit cell is

(53) This argument is justified by electron-hole symmetry.

Table VIII. Comparison of Decay Constants for Spiro- and *n*-Alkane^a

energy, (eV)	alkane		spiroalkane	
	$\epsilon + 1/\epsilon$	$ \epsilon $	$\epsilon + 1/\epsilon$	$ \epsilon $
4.0	-3.0	0.38	2.9	0.40
3.0	-3.7	0.30	5.3	0.20
2.0	-4.2	0.25	7.5	0.14
1.0	-4.6	0.23	9.4	0.11
0.0	-4.9	0.22	10.7	0.09
-1.0	-5.0	0.21	11.5	0.09
-2.0	-5.0	0.21	11.5	0.09
-3.0	-4.8	0.22	10.9	0.09
-4.0	-4.4	0.23	9.4	0.11
-5.0	-3.9	0.28	7.3	0.14
-6.0	-2.9	0.39	4.4	0.24

^a ϵ is the decay per unit cell. $|\epsilon|$ is the decay per carbon atom.

$$(\epsilon + 1/\epsilon) = E^2/\beta^2 - 2$$

For spiroalkane represented with one orbital per carbon atom

$$(\epsilon + 1/\epsilon) = (E^2/2\beta^2) - 2$$

and there are three atoms per unit cell (this equation results from the case even with respect to the mirror planes). Hydrogen atoms were ignored in both cases. We see that the spiro linkage is equivalent to replacing β in the linear problem with $\sqrt{2}\beta$. The thermal matrix element in the one orbital per atom linear problem is proportional to $(\beta/\Delta)^N$, where β is the exchange integral, Δ is energy of the electron traps, and N is the number of unit cells in the bridge.²⁸ Thus, even the most simple model for the spiro unit cell indicates its enhanced electron mediation properties compared to a linear chain.

For long chains, the amplitude of the wave function in the interior of the molecule changes by the factor ϵ on moving one unit cell in the chain. In spiroalkanes there are two carbon atoms between equivalent points in adjacent unit cells. To first order we can calculate the change in optical or thermal matrix element between donor and acceptor wave functions for any groups connected by the linkers using this fact. For example, when $E = -5.0$, the donor-acceptor overlap changes by a factor of about 0.28 upon adding another CH_2 group to the *n*-alkane. At the same energy the overlap between spiro wave functions changes by a factor of 0.14 upon adding an extra spiro unit. This is an average decay factor of only 0.37 per carbon atom for the spiro linker. The significant difference in decay per carbon atom is a unique feature of the spiro linkage and accounts for the "surprisingly rapid" charge transfer observed by Stein, Lewis, Seitz, and Taube. Table VIII highlights this difference for several energies.

We can use this sort of analysis to compare the attenuation of T_{ab} with distance for a specific linker simply by studying the ϵ vs. E plot. Figure 5a compares the band region in the $\epsilon + 1/\epsilon$ plots for *n*-alkane and spiroalkane. ϵ is the decay per unit cell. Figure 5b shows the ϵ vs. E plot for the band gap where ϵ is the decay per carbon atom. Such a divergence from the alkane decay should not occur to such a large degree in the parallel but not frequently intersecting electron-transfer pathways of the steroid derivatives prepared by Calcaterra, Closs, and Miller, for example.⁷

Comparison with Previous Estimates of α . The constant ϵ is related to the decay constant α as shown in Table III. Previous estimations of the energy of the "transferring" electron relative to the medium in which it tunnels have been made. For example, Hopfield estimated $\alpha \approx 0.72 \text{ \AA}^{-1}$ while Jortner suggested $\alpha \approx 1.3 \text{ \AA}^{-1}$ for electron transfer in proteins. It is now clear that this decay depends critically on both the energy of the transferred electron and the detailed structure of the barrier between donor and acceptor. Hopfield's original model assumed a 2-eV barrier height to tunneling. Within our model that means the localized states are 2 eV from either the conduction or valence band (see Figure 5b). In the *n*-alkane model the states 2 eV from the band edges have $\epsilon \sim 0.21-0.23$ or $\alpha = 0.98 \text{ \AA}^{-1}$ (through bond) and $\alpha = 1.3 \text{ \AA}^{-1}$ (through space; notice comment below Table III).

Redi and Hopfield compared the optical and thermal tunneling matrix elements for two model potentials.²⁵ They found $T^o > T^b$, especially at large electron-transfer distances. Their wave functions decay with energy and distance as $\exp(-\sqrt{|E|}R)$. In our calculation ($\epsilon + 1/\epsilon \approx 1/\epsilon$ so $|E| \approx 1/\epsilon$ near the band edges). Thus, from eq 12 and Table III the wave function decays with distance and energy as

$$\exp(-|(\ln E)|R)$$

For given E the wave-function decay is always more rapid in the square well or δ well models of Redi and Hopfield. Also, wave-function decay is more sensitive to energy changes in the Redi and Hopfield model. Because of the different dependence of decay on energy, the vibrational relaxation of the localized state produces a greater change in matrix element in the Redi-Hopfield model than in the current model. This serves to decrease the optical matrix with distance more slowly than the thermal matrix element in their model. In the model described here, the optical and thermal tunneling matrix elements are not very different in magnitude (see Tables IV, VI, and VII).

Quantum Chemical Considerations. Our modified tight binding calculation has predicted that electron transfer between ruthenium ions proceeds via hole transfer through the bonding bridge orbitals. Wave function decay is slow for donor and acceptor eigenstates near the band edges. The two actual exchange mechanisms, double exchange (electron transfer via conduction band) and superexchange (hole transfer through the valence band), involve mixing of trap states with linker states.^{54,55} Since this mixing involves energy denominators (in first-order perturbation theory) of $E(\text{trap}) - E(\text{bridge})$, the strength of the mixing between localized states and linker states is enhanced by their energetic proximity.

An infinite or cyclic chain of spiroalkane orbitals satisfies Bloch's theorem so $\epsilon = \exp(i\vec{k} \cdot \vec{R})$ where \vec{k} is a real reciprocal lattice vector and \vec{R} is a translation vector. In this case $-2 \leq (\epsilon + 1/\epsilon) \leq 2$. We expect (except, perhaps, at points of special symmetry) as many energy roots as basis functions in the unit cell. The six unique orbitals in the spiroalkane give rise to the six bands for $-2 \leq (\epsilon + 1/\epsilon) \leq 2$ in Figure 2. When the linear molecule is truncated, many eigenstates still fall in the range $-2 \leq (\epsilon + 1/\epsilon) \leq 2$ and are well delocalized. Others have ϵ real and correspond to localized states. The singularities in these band-structure plots arise from energy splittings due to orbitals not contributing to C-C bonds.

One could have formulated the boundary conditions of the spiro problem in many other ways. For example, several orbitals on the metals and sulfurs were ignored. Also, a particular geometry was assumed. As long as the position of the sulfur orbitals which participate in the electron transfer do not drastically change in energy, we will be forced to place the localized ruthenium eigenstates very near the valence states and will find similar falloff of T_{ab} with distance. The ability to find this characteristic decay and its dependence on linker geometry is the principal success of this method.

If one believes that the optical absorption reported in the experimental studies promotes an electron between localized states,

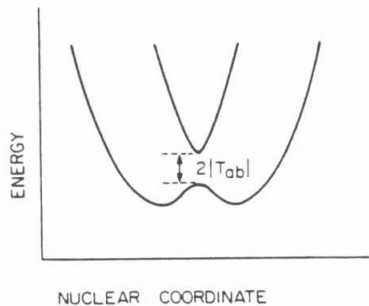


Figure 6. The traditional view of the potential energy surface relevant to electron transfer is shown. The nuclear coordinate represents the metal-ligand and solvent coordinates.

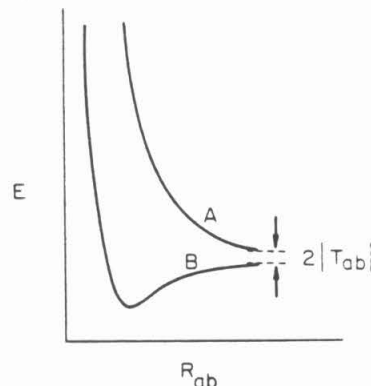


Figure 7. The total energy of the two states, bonding (B) and antibonding (A), formed by a linear combination of two atomic orbitals is shown.

one must build the ability to adopt local character into the wave functions from the very start. The CNDO/2 method that Stein, Lewis, Seitz, and Baker used to analyze only the linker will not predict the exponential dependence of the charge transfer band extinction coefficient on distance found in these molecules.

The thermal tunneling matrix element represents the splitting between nuclear potential energy surfaces at the crossing point between reagents and products (Figure 6).⁵⁶ The nuclear coordinate in this figure symbolically represents the many metal-ligand and metal-solvent coordinates. The size of T_{ab} varies with the metal-metal distance in a fashion shown in Figure 7. We notice from Table VII that the thermal tunneling matrix element decreases with distance but never changes sign. In a two-orbital, one-electron model of electron transfer this energy splitting must not change sign with distance. A sign change implies a crossing of the bonding and antibonding energy surfaces (Figure 7). Such a crossing is forbidden by the nodal theorem.⁵⁷ That is, since the ground state is nodeless and since higher states have nodes, $E_g < E_{ex}$ for any internuclear separation. When intervening orbitals between donor and acceptor are introduced, the sign of T_{ab} may vary with transfer distance. For example, in Figure 4c we see that ϵ for *n*-alkane is negative so the sign of T_{ab} alternates as the number of bridging carbon atoms is increased. However, within our model $|T_{ab}|^2$ is still a monotonically decreasing function of donor-acceptor separation, which may only be changed in integral steps. Newton has calculated the tunneling matrix element for electron exchange between hexaquo Fe(II) and Fe(III) using ab initio quantum mechanical methods.⁵⁸ He finds a node in T_{ab} for an internuclear iron distance of 7.6 Å. Thus, either there is an unusual many-body effect at work or his method incorrectly

(56) Marcus, R. A. *Annu. Rev. Phys. Chem.* 1964, 15, 155-196.

(57) Messiah, A. "Quantum Mechanics"; Wiley: New York, 1958; Vol. 1 pp 109-110.

(58) Newton, M. D. *Int. J. Quantum Chem.: Quantum Chem. Symp.* 1980, 14, 363-391.

(54) Halpern, J.; Orgel, L. *Discuss. Faraday Soc.* 1960, 29, 32-41.

(55) Ratner, M. A.; Ondrechen, M. J. *Mol. Phys.* 1976, 32, 1233-1245.

calculates the long-range wave function decay.

Our method does have severe limitations. It is a one-electron approximation and has the flaws of the standard Hückel techniques.^{39,52,59} Transition and dipole moments calculated from Hückel wave functions are not always reliable. However, to the extent that the "odd" electron in the electron-transfer calculation is in a very different eigenstate compared with the other electrons in the molecule, this approximation may be better than expected. The omnipresent problem of selecting appropriate, consistent parameters is obvious in this calculation. Particularly annoying is the difficulty of treating transition metals within the one-electron approximation.

Biological Applications of This Theory. The techniques described in this paper are applicable to electron-transfer processes where the through-bond rather than through-space electron-transfer pathway dominates. The method requires knowledge of the energy of the "transferred" electron relative to the bridge states. The question of through-bond vs. through-space pathways in metal-labeled proteins is an important one.^{60,61} Our method allows prediction of the changes in electron-transfer rate as a function of redox energy and through-bond distance. To study through-bond effects on long-distance electron transfer in proteins, one would like to roughly fix the through-space distance between donor and acceptor and vary only the number of through-bond links between the centers. Perhaps binding of metals to the surface of a roughly spherical protein with a redox group in its center would be appropriate. Such an experiment would show the importance of through-bond interactions (and the usefulness of this theory) in electron transfer through proteins.

For the mixed-valence spiro molecules the experimental value of ϵ for Ru^{3+} is $\sim 0.4-0.47$ or $\epsilon' \simeq 0.65$ (recall $\epsilon' = \epsilon^{1/2}$). This value of ϵ corresponds to $E = -6.5$ eV. The redox potentials of these molecules are $\sim +0.5$ vs. NHE; however, the redox energy corresponds to thermal charge transfer so we also have ~ 0.75 eV of relaxation energy to include. Using these facts we may correlate the redox potential and decay constant for spiro and other saturated linkers. By changing the sign of the energy scale in Figure 5b, placing the redox energy of $+0.5$ vs. NHE at $-6.5 + 0.75$ eV ($-6.5 + 0.75$) eV on that figure, and converting from ϵ to α we find Figures 8a and 8b. These describe the decay constant as a function of redox energy for the *n*-alkane. Now if we consider the alkane backbone to be a fair model for the protein backbone, we may calculate α for a given number of peptide unit cells.

Electron transfer between native and modified proteins occurs in an activated complex with electronic energy $E^{\text{el}} \simeq (E_d + E_s)/2$ where E^{el} is the energy appropriate for use in Figure 8. E_d and E_s are the redox energies of the separated ligated metals.

Assuming two redox centers are known to be separated by X Å, a "taut" alkane chain between the center and the chain would contain $N = (2X)/(2.4)$ carbon atoms. The tunneling matrix element for this linkage would be

$$\exp[-\alpha(E^{\text{el}})N(1.54)] \quad (13)$$

$\alpha(E^{\text{el}})$ is the through-bond decay constant appropriate to the activated complex (read from Figure 8a). This should be the upper limit of the bond-mediated tunneling matrix element. Calculation of matrix elements through longer chains requires only knowledge of N and E^{el} . For example, in the pentaammine ruthenium(III) (histidine-33)-ferricytochrome prepared by Gray and co-workers, $E^{\text{el}} = 0.21$ V vs. NHE, $X = 15$ Å, $N = 12.5$ so $T_{ab}^{\text{max}} \simeq \exp[-(0.69)(12.5)(1.54)] \simeq 1.7 \times 10^{-6}$ eV. Since the transfer probably does not occur through such a taut structure and T_{ab} decreases by a factor of $\exp[-(0.69)(1.54)(3)] \simeq 0.04$ per amino acid residue, it is unlikely that the dominant pathway in this protein with this choice of metals is a purely bond-mediated one. However, if the more favorable energetic regions (near the

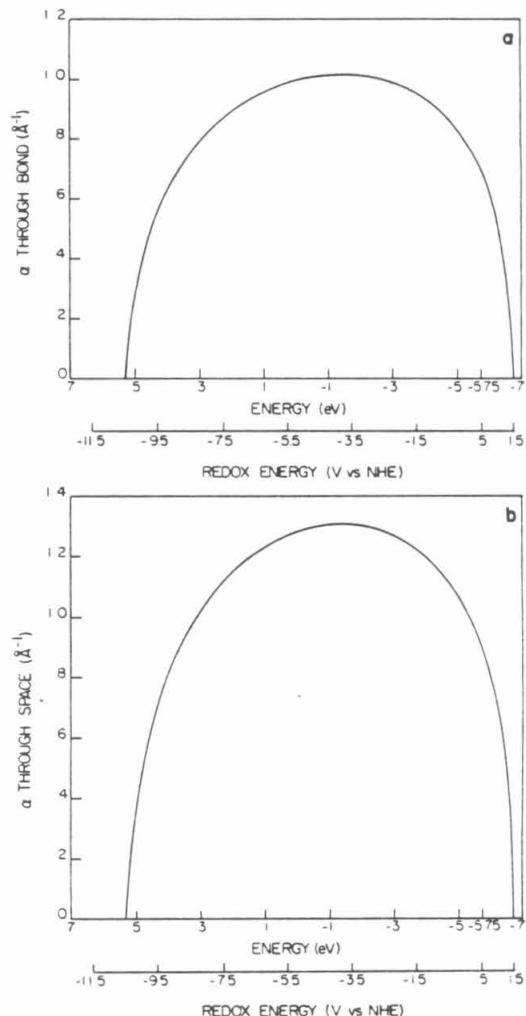


Figure 8. The dependence of thermal matrix element decay constant (α) as a function of the redox energy of the activated complex is shown: (a) when distance is measured through bond for an alkane chain, (b) when distance is measured through space for a "taut" alkane chain.

band edges) are accessible, a through-bond pathway may become more important.

Calculations exploiting the periodic nature of other saturated rigid linkers are now being carried out. Similar calculations on polypeptide backbone are also underway. With this method we hope to achieve a better understanding of the role of bridge geometry and donor/acceptor energetics on the electronic tunneling matrix element.

T_{ab} and "Inverted Behavior". In this paper we have considered only the electronic contribution to the electron-transfer rate. The actual rate is, within the Franck-Condon and Born-Oppenheimer approximations, a product of nuclear and electronic factors. In I-IV the nuclear factors should be approximately equal so a comparison of $|T_{ab}|^2$ may be used to predict ratios of transfer rates.

Both the optical and thermal tunneling matrix elements are quite sensitive to the energies of the donor and acceptor localized states with respect to the bridge states. Therefore, when comparing transfer rate as a function of reaction driving force, one must realize that changing reaction energetics may in fact change the size of T_{ab} (depending on the position of the localized states in the band gap). For this reason, when looking for the "inverted region" in families of molecules, one must also consider the change

(59) Sinanoglu, O.; Wiberg, K. B. "Sigma Molecular Orbital Theory"; Yale University Press: New Haven, 1970.

(60) Margalit, R.; Pecht, I.; Gray, H. B. *J. Am. Chem. Soc.* 1983, 105, 301-302.

(61) Winkler, J. R.; Nocera, D. G.; Yocom, K. M.; Bordignon, E.; Gray, H. B. *J. Am. Chem. Soc.* 1982, 104, 5798-5800.

in the *electronic contribution to the rate with driving force*.^{62,63} Depending on the energy of the localized states, a misinterpretation of the data may result if T_{ab} is assumed constant. Future work will attempt to include a model for nuclear motion.

Conclusions

We have shown that semiempirical quantum chemical techniques predict the dependence of tunneling matrix element on distance and linker geometry. The localized states used in these calculations must have the proper exponential decay in order to calculate meaningful rates. To the extent that the linkers create periodic potentials for the electrons, we are assured of obtaining

proper wave-function decay in these calculations. There are two major qualities of the method that make it especially appealing. It allows direct study of the effect of linker geometry on the electronic tunneling matrix element. The method also allows systematic study of the effect of donor and acceptor redox level on the electronic tunnelling matrix element. It is hoped that the synthesis of other rigidly linked, weakly interacting electron donor-acceptor molecules will provide further tests of this theory.

Acknowledgment. The authors are grateful to Dr. N. Agmon, Dr. R. A. Marcus, Mr. J. N. Onuchic, and Dr. M. A. Ratner for very helpful suggestions with regard to this manuscript. This research was supported in part by NSF Grant No. DMR-8107494.

(62) Marcus, R. A.; Siders, P. *J. Phys. Chem.* 1982, 86, 622-630.

(63) Beitz, J. V.; Miller, J. R. *J. Chem. Phys.* 1979, 71, 4579-4595.

Registry No. I, 76723-23-4; II, 81205-53-0; III, 81205-54-1; IV,

88548-86-1.

This paper has shown that order of magnitude estimates of the tunneling matrix element can be made using a one-electron theory. Since ϵ varies approximately linearly with E near a band edge, errors in the tunneling energy cause errors in ϵ (linear) and in $\alpha = -\ln \epsilon/a$. Using standard parameters we calculated $\alpha = 0.53\text{\AA}^{-1}$ for the mixed valence compounds. Although the experimentally measured matrix element decay is not purely exponential in distance, it can be fit with $0.35 \leq \alpha \leq 0.40 \text{\AA}^{-1}$. Confirmation was given to the idea that $\epsilon^N(E)$ at the appropriate tunneling energy gives an excellent approximation for the decay of T_{ab} with distance. The predictive value of this study comes from the establishment of a connection between ϵ and the experimentally measured redox potentials of the donor and acceptor. Predictions of changes in T_{ab} with distance for electron tunneling through spiroalkane (and other linkers) with different donors and acceptors can now be made. This link is used in the following manuscript to predict the decay of rate with distance in the photosynthetic model compounds [3]. The optical tunneling matrix element was found to be approximately equal to the thermal tunneling matrix element for these compounds. This similarity results from the multi-band nature of the problem as well as the logarithmic rather than square root dependence of α on E . Parameters in a square or delta well model for electron tunneling could be chosen to give similar optical and thermal matrix elements. A previous study predicted a significant difference between the two, in part due to the choice of parameters [6b].

III.C. Electron Tunneling Through Rigid Molecular Bridges:
Bicyclo[2.2.2]octane

David N. Beratan

Contribution from the Division of Chemistry and and Chemical Engineering
California Institute of Technology
Pasadena, California 91125

Abstract

Electron tunneling through polymers of bicyclo[2.2.2]octane is studied. The repeating nature of the linker allows prediction of the dependence of tunneling matrix element on distance and energy by a semi-empirical method exploiting the translational symmetry of the linker. Specific predictions of the dependence of rate on distance are made for recently synthesized photosynthetic model compounds containing porphyrins and quinones linked by this bridge.

INTRODUCTION

Electron transfer reactions between distant weakly interacting sites are of interest in many fields of chemistry [1]. The electronic interaction between donor and acceptor together with the nuclear activation barrier determines the transfer rate. The quantum mechanical expression for the rate when the donor and acceptor weakly interact is [2]

$$k = (2\pi/\hbar) |T_{ab}(E, R)|^2 \text{ (F.C.)} \quad (1)$$

The tunneling matrix element, T_{ab} , is the electronic exchange interaction energy between donor and acceptor in the activated complex. (F.C.) is the thermally weighted Franck-Condon factor discussed elsewhere [2-4]. T_{ab} depends on the distance between donor and acceptor (R) and on the energy (E) of the electron in the activated complex relative to the energy eigenstates of the (unperturbed) intervening material [2-12]. When the donor-acceptor distance is large and the mediating bridge is linear with repeating units, T_{ab} decays approximately exponentially with distance. $T_{ab}(E, R)$ critically depends on the geometry and energetics of the linker [4]. Recent synthesis and measurements of the electron transfer kinetics in **1** and **2** now make theoretical studies of wave function decay in bicyclo[2.2.2]octane linkers ([2.2.2]) timely [13,14].

THEORETICAL SECTION

A. General Aspects

Recently, a method was developed to predict the electronic energy and bridging ligand effects on the distance dependence of non-adiabatic electron transfer reactions [7]. The method guarantees proper wave function tail decay in the linker region, exploiting the fact that within the linker the electron effectively propagates in a one-dimensional periodic potential. A scale linking the redox

potential (E^0) of the transferring electron with the distance decay [3-12] of T_{ab} was established for several bridging groups [7]. This method is now extended to predict the decay of electron transfer rate with distance between π^* orbitals connected by oligomers of the rigid bicyclo[2.2.2]octane unit. The electron mediation properties of this bridge are compared with those of linear and spiro-cyclic alkanes. Predictions are made for the distance dependence of forward and reverse electron transfers in the rigid porphyrin-linker-quinone compounds recently synthesized [13]. The appeal of this method is that a single calculation predicts the decay of T_{ab} with distance for any set of donors and acceptors connected by these linkers.

Neglect of non-nearest neighbor interactions between orbitals and formulation of the problem in a one-electron (extended Hückel or tight binding) framework provides donor and acceptor wave functions. The decay of the donor localized states in the linker is parametric in E . Once found, this wave function decay yields the distance dependence of the electron transfer rate. The analysis of [2.2.2] closely follows the previous study of electron mediation by spiroalkane linkers. The critical assumption is that oligomers of the linker create a periodic potential in which the well-localized electron propagates in its low probability “tail.” One can use a periodic potential representation because the propagation of a wave function in a region does not depend on the potential outside of that region.

The dependence of the tunneling matrix element on distance in thermal electron transport reactions has been found in related systems by calculating the symmetric/antisymmetric splitting of the electronic states at the crossing point of the reagent and product nuclear potential energy surfaces. A golden-

rule/perturbation approach assuming donor interaction with acceptor only via the atomic orbitals in the bridge closest to the acceptor and a periodic linker potential also gives the proper distance dependence of the rate. Indeed for the spiroalkanes the distance dependence of the rate determined by the two methods is nearly identical. The latter formulation is more convenient at present.

B. Formal expresssions for the wave functions and matrix elements

Wave functions in *finite* one-dimensional structures with translational symmetry and unit cells of size $|\vec{a}|$ are of the form

$$\psi_E(x) = \sum_{n=1}^N \{b_E \epsilon(E)^j + c_E \epsilon(E)^{N-j+1}\} \phi_n(\vec{x} - n\vec{a}). \quad (2)$$

The wave function involves growing and decaying contributions for the same reason that the wave function in a constant potential region between two square wells includes growing and decaying parts regardless of the relative depths of the wells. $\epsilon(E)$ may be real or complex depending on the energy of the state. To the extent that electron traps perturb this otherwise periodic system in a localized region and edge effects are not large (valid when $\epsilon^{2N} \ll 1$), the functional form of Ψ (donor+bridge) becomes

$$\Psi^d \simeq \Phi^d + \lambda \sum_{n=1}^N \epsilon(E)^n \phi_n(\vec{x} - n\vec{a}). \quad (3)$$

Corrections to the coefficients due to edge effects are of the order ϵ^{2N} . Edge effects are especially small if the electron has a small probability of residing near the “wrong” trap in the initially prepared state. In any case, the E- ϵ relation true for the infinite one-dimensional chain is valid for the finite system to the extent that the potential in the linker region is not much perturbed by the donor and acceptor. Due to the small value of ϵ for [2.2.2] (see Table 4) this technique is useful even in the one and two linker systems.

At this point a divergence between this method and other perturbational approaches is apparent. Here the requirements of Bloch's theorem are built into the wave functions. Perturbational approaches form the donor wave function from a linear combination of ground and excited bridge states and donor orbital(s) and find the orbital coefficients by energy minimization [9].

The golden rule tunneling matrix element within the Born-Oppenheimer separation is calculated for the electronic states which solve the two Schrödinger equations:

$$H_D^{el}\Psi_D = E_D^{el}\Psi_D; \quad H_D^{el} = T_e + V^{bridge} + V_D \quad (4a)$$

$$H_A^{el}\Psi_A = E_A^{el}\Psi_A; \quad H_A = T_e + V^{bridge} + V_A. \quad (4b)$$

T_e is the electronic kinetic energy operator. Neglecting overlap,

$$T_{ab} \simeq <\Psi_D|V_A|\Psi_A>. \quad (5)$$

$|V_A\Psi_A>$ is localized in the acceptor region and is, to an excellent approximation, transfer distance independent. The distance dependent part of this matrix element is proportional to $\epsilon(E)^N$. N is the number of repeating units in the bridge. In the extended Hückel approach, the perturbation which promotes transfer is $\beta'(a_N^\dagger a_{acceptor} + a_{acceptor}^\dagger a_N)$ and the ϵ^N decay of T_{ab} with distance is nearly exact.

The value of E at the crossing point (E^\ddagger) of the nuclear potential energy surfaces is some value between E_a and E_b , the electronic energies of the unperturbed traps. E^\ddagger is the average of these energies if the vibronic couplings on the donor and acceptor are identical. This is likely a good approximation when the transfer occurs between structurally similar molecules. However, since both inner and outer sphere reorganization energies scale with molecular size, E^\ddagger need

not be proportional to the average of the donor and acceptor redox potentials when the molecules are structurally different [7,12].

C. Wave function symmetry and decay in bicyclo[2.2.2]octane

Following Ref. 7 the dependence of the wave function decay on energy is found for propagation through bicyclo[2.2.2]octane chains. It was shown for linear chain and spiroalkanes that the decay constant may, to an excellent approximation, be found by considering the carbon backbone orbitals only. Within the weak donor-bridge interaction approximation the amplitude of the transferable electron on the bridge is determined by the mixing of the “terminal” donor (atomic) orbital with the neighboring bridging (atomic) orbital and the interactions of the terminal bridging orbital with its neighbors in the bridge. The porphyrin-linker interaction is determined by the π symmetry of the electron donor. There is a symmetry axis joining the two quaternary carbons in each [2.2.2] unit. If the terminal donor orbital were even with respect to rotations about this axis (e.g., s or d_{z^2} atomic orbitals), it would mix directly with the sp^3 carbon orbital of the [2.2.2] bridgehead and electron mediation would proceed with equal amplitude and sign along the three pathways of the linker (see Appendix 3). However the porphyrin excited state is not cylindrically symmetric and mixing of the donor with the three parallel pathways is not equal. In the coordinate system shown in Fig. 1 the donor p orbital may mix only with the two p orbitals at the bridgehead orthogonal to the axis between quaternary carbons. It is simpler to speak of the associated sp^3 hybrid bridge orbitals. These bridge orbitals in turn interact with adjacent sp^3 backbone orbitals. The size of the p_z (donor)– sp^3 (bridge) interaction varies with the angle between the bridgehead orbitals and the donor orbital according to Eq. A1.

Little mixing of the porphyrin excited donor state occurs with the sigma bond joining linker to porphyrin. Hence little direct sigma interaction between bridgeheads occurs. Such a bridgehead to bridgehead pathway may be important with sigma symmetry donors and acceptors joined by similar linkers [12].

The *distance* dependence of the rate is the quantity of interest. The *size* of the donor (and acceptor)-bridge interaction affects the absolute rate but not its distance dependence. This interaction is constant in the family of systems studied and enters the rate of all transfers only as a prefactor. Delocalization of the excited porphyrin electron into the meso phenyl group is also independent of linker length. The appendices show that decay with *distance* is identical in both the staggered and eclipsed chains of [2.2.2].

Analysis of experimentally measured electron transfer rates as a function of distance requires that the data first be corrected for effects due to a change in reaction energetics with distance. Outer sphere reorganization energies and donor-acceptor Coulombic interactions are transfer distance dependent. Direct comparisons of transfer rate measured from the *singlet* excited state may not be immediately compared to a transfer rate from the *triplet* excited state without correcting for the rate difference arising from the different reaction free energies. Using the connection between the Hückel parameters and the redox potentials [7], the donor state wave function decay per linker unit ($\epsilon(E)$) in the activated complex is predicted.

The redox properties of the donors and acceptors have been measured [14]. The outer sphere reorganization energy arising from solvent reorientation near a trap scales with the reciprocal of the trap's radius if Coulombic interactions are neglected. The inner sphere reorganization energy scales as the reciprocal

of the number of bonds over which the electron is delocalized. The smaller the reorganization the closer the energy of transfer will be to the redox potential of that isolated species. Table 1 shows the redox properties of the model compounds in various solvents.

At room temperature the solvent coupling to the charge transfer process can be treated classically. Inner sphere reorganization involves vibrational levels with spacing much larger than $k_b T$. Nuclear tunneling must occur along the inner sphere coordinate even at room temperature. The spectral function for electron removal from the donor in such a two-mode case is

$$D_a(E) \propto (2\pi\sigma^2)^{-1/2} \sum_n [exp(-S)S^n/n!]exp[-(E - E_a + \lambda_a - n\hbar\omega)^2]/(2\sigma^2) \quad (6)$$

where $S = \lambda_{in}/\hbar\omega$. Assuming that the Gaussian and Poisson parts of this function are peaked at approximately the same nuclear position determined by the molecular size ($n\hbar\omega \ll \lambda_a$), the maximum overlap between electron insertion and removal spectral functions occurs at

$$E^\ddagger = \frac{\lambda_a E_d + \lambda_d E_a}{\lambda_a + \lambda_d} \simeq \frac{2}{3} E^0(P^*) + \frac{1}{3} E^0(Q). \quad (7)$$

The Franck-Condon approximation suggests that $\epsilon(E^\ddagger)$ be used in Eq. 3. The first excited singlet porphyrin state is ~ 2.15 eV above the ground state. The lowest triplet state is ~ 1.8 eV above the ground state [13]. The values of E^\ddagger (Eq. 7) and $\epsilon(E)$ (Figs. A4 and A5) for the four solvents, two excited porphyrin states, and forward and reverse electron transfers are shown in Tables 2 and 3. Table 4 shows the corresponding rate predictions.

$\epsilon(E)$ for electron transport from singlet or triplet states of other porphyrins to quinones are readily found. E^\ddagger is first calculated using Eq. 7 and $E_{1/2}(P^*)$ estimated as $E_{1/2}(P) + h\nu$ where $h\nu$ is estimated from the porphyrin optical

absorption spectrum. For the Zn porphyrin, the decay of T_{ab} with distance is not drastically different for the singlet and triplet transfers.

DISCUSSION

Electron tunneling following porphyrin excitation is mediated principally by the bonding states of the linker. This situation results because the porphyrin is excited with a quantum of energy small compared to the HOMO-LUMO energy gap of saturated alkane. In this case, as in the case of the intervalence and thermal transfer between bridged metallic species [16-18], the transfer mechanism is expected to be "hole tunneling" or superexchange via the occupied binding levels of the bridge [19,20]. This prediction can be tested experimentally. Raising the energy of the excited porphyrin moves the energy of the tunneling electron away from the linker bonding states and is expected to cause T_{ab} to decay more *quickly* with distance. The absolute rate, however, may be quite different due to a change in the reaction exothermicity. This prediction runs counter to the notion that the more excited a state is the more "loosely" bound is its electron. Here "looseness" arises only from favorable orbital interaction with the bridge and is *decreased* by an increase in the energy of S_1 . The reverse rate ($Q^{-\cdot}$ to $P^{+\cdot}$) is predicted to decay more slowly with distance than the forward rate for the same reason. An alternative test of hole tunneling would involve initially reducing the quinone and measuring the back transfer from $Q^{-\cdot}$ to P^* by fluorescence or phosphorescence quenching following a light flash.

Only staggered or eclipsed geometries of the π cloud with one of the three electron transfer pathways of the bridge were considered. Decay with distance is identical in each case. Any donor configuration may be decomposed into a linear combination of these geometries. Thus, the decay with distance of the donor

state along the linker obeys the same $E-\epsilon$ relation independent of donor-acceptor orientation. No interference effects occur. Aside from the jumps between bridgehead orbitals, the parallel pathways assist transfer compared to a purely linear network.

A direct comparison with tunneling predictions for spherically symmetric donors is not meaningful because pure p orbitals are introduced to the unit cell and shift the energy of the HOMO-LUMO gap center. Fig. A7 shows a calculation for n-alkane, spiroalkane, and bicyclo[2.2.2]octane linkers where only even symmetry (with respect to all mirror planes) donors and acceptors were considered. Appendix 3 gives the secular equation relating E to ϵ in that case. This is not the case of current interest. A heuristic rule for the relative values of ϵ' (decay per C atom in the unit cell) might have been as shown in Eq.8 based on the topology of the unit cells.

$$\epsilon'(\text{alkane}) = x$$

$$\epsilon'(\text{spiroalkane}) = x\sqrt{2} \quad (8)$$

$$\epsilon'(\text{bicyclo[2.2.2]octane}) = x\sqrt[4]{3}$$

These relationships are true *only* in the center of the band gap for the sigma symmetry donors. However, the *relative* values of ϵ' for spiro and [2.2.2] hold throughout the gap (Fig. A6). Comparison is not made between the even symmetry alkane and spiroalkane chains and the odd symmetry [2.2.2] system because the inter-unit cell interactions are qualitatively different (the band gap edges are shifted). A test of the relative σ mediation by these linkers awaits construction of rigid systems with σ symmetry donors and acceptors.

CONCLUSIONS

Predictions of the decay of the tunneling matrix element with distance for electron mediation by bicyclo[2.2.2]octane have been made assuming that the linker creates a periodic potential between donor and acceptor. Mediation by CH bonds and non-nearest neighbor interactions was neglected. Predictions of the thermal electron transfer rate dependence on the number of bicyclo[2.2.2]octane linkers were made. Hole transfer is predicted to dominate in these systems, suggesting that the reverse transfer will decrease more slowly with distance than the forward transfer. Porphyrins with higher energy excited states are expected to have more rapid wave function decay with distance in the linker. Writing $T_{ab} = T_0 \exp(-\alpha R)$ and distance measured through space, $\alpha^{for} \simeq .9\text{\AA}$ and $\alpha^{rev} \simeq .51\text{\AA}$ for $ZnPL_nQ$ single transfer. No drastic effect of solvent on α is predicted. A slowing of the forward rate from S_1 by a factor of 1500 per [2.2.2] unit is expected. The reverse rate is expected to slow only by a factor of about 60 per linker unit. Preliminary results show a slowing of the forward rate in the two linker system by a factor of 500-1600 compared to the rate in the one linker system.

APPENDIX 1: Interaction of Porphyrin and Quinone with [2.2.2]

Mixing of the porphyrin and quinone states with the bridge is presumed to occur via the adjacent quaternary carbon orbitals. The interaction between the four sp^3 orbitals at the center of a tetrahedron pointed in the (1,1,1), (-1,1,-1), (-1,-1,1), and (1,-1,-1) directions (a, b, c, and d, respectively) with a p orbital (p_{\perp}) at (1,1,1) normal to hybrid a is given by:

$$\langle p_{\perp} | sp^3(a) \rangle = 0$$

$$\langle p_{\perp} | sp^3(b) \rangle = -(2/\sqrt{6}) \sin \theta$$

$$\langle p_{\perp} | sp^3(c) \rangle = -(1/\sqrt{2}) \cos \theta + (1/\sqrt{6}) \sin \theta$$

$$\langle p_{\perp} | sp^3(d) \rangle = (1/\sqrt{2}) \cos \theta + (1/\sqrt{6}) \sin \theta. \quad (A1)$$

θ is the angle between the axes of cylindrical symmetry of the transformed p orbital and one of the p orbitals on the central site normal to the C-C axis. These results were obtained by transforming the hybrid orbitals into s orbitals and p orbitals perpendicular or parallel to the (0,0,0)-(1,1,1) axis. The transformation equations are:

$$\begin{pmatrix} p_x \\ p_y \\ p_z \end{pmatrix} = \begin{pmatrix} 1/\sqrt{3} & 1/\sqrt{2} & 1/\sqrt{6} \\ 1/\sqrt{3} & -1/\sqrt{2} & 1/\sqrt{6} \\ 1/\sqrt{3} & 0 & -2/\sqrt{6} \end{pmatrix} \begin{pmatrix} p_{\sigma} \\ p_{\pi_a} \\ p_{\pi_b} \end{pmatrix}. \quad (A2)$$

APPENDIX 2: Propagation in the Linker

The donor(acceptor) p orbital adjacent to the linker may be converted to a linear combination of p orbitals staggered and eclipsed with the ring. Considering only the two geometries in Fig. A1 the wave function of the donor plus bridge must be odd with respect to the nodal plane of the donor p orbital (see also Eq. A1). Propagation between neighboring [2.2.2] units is identical when the neighboring rings are fully eclipsed or fully staggered (recall that the only bridgehead orbitals contributing to the wave function are the p orbitals perpendicular to the bridgehead axis).

The secular equation in *both* cases which gives the $E - \epsilon$ relation is:

$$\det \begin{pmatrix} -E & \gamma & 0 & 0 & 0 & \beta \\ \gamma & -E & \beta & 0 & 0 & 0 \\ 0 & \beta & -E & \gamma & 0 & 0 \\ 0 & 0 & \gamma & -E & \beta & 0 \\ 0 & 0 & 0 & \beta & -\gamma - E & (\beta' - \beta'')\epsilon \\ \beta & 0 & 0 & 0 & (\beta' - \beta'')/\epsilon & -\gamma - E \end{pmatrix} = 0. \quad (A3)$$

The relation is identical for the even and odd wave functions as can be seen in Fig. A3. Writing the orbitals on the lower half of the unit cell as symmetrized combinations shows this.

From previous calculations [7] the parameters were chosen as:

$$\beta = -8.47 \text{ eV}$$

$$\gamma = -1.85 \text{ eV}$$

$$\beta_{p\pi} = \beta' - \beta'' = -1.325 \text{ eV}.$$

γ is the energy difference between a p and sp^3 orbital.

The $E - \epsilon^{1/4}$ relation corresponding to Eq. A3 is plotted in Fig.A4. The $E - \epsilon^{1/4}$ relation shows the average decay of the donor wave function per carbon

atom in the linker. The result is compared to the spiroalkane and n-alkane results of Ref. 4. Fig. A5 shows an expanded view of the [2.2.2] plot in the region of experimental interest. The corresponding redox scale was determined in [7]. The expanded secular equation relating E to $\epsilon + 1/\epsilon$ (Eq. A3) is:

$$\begin{aligned}
 (\epsilon + 1/\epsilon) \beta^3 \gamma^2 \beta_\pi = & +E^6 + E^5(2\gamma) + E^4(-3\beta^2 - \beta_\pi^2 - \gamma^2 \\
 & + E^3(-4\beta^2\gamma - 4\gamma^3) + E^2(\beta^2\beta_\pi^2 + \beta^2\gamma^2 + 2\beta_\pi^2\gamma^2 + 3\beta^4 - \gamma^4) \\
 & + E(2\beta^2\gamma^3 + 2\beta^4\gamma + 2\gamma^5) - \beta_\pi^2\gamma^4 - \beta^6 + \gamma^6. \tag{A4}
 \end{aligned}$$

The p orbital of the donor (or acceptor) may be decomposed into two p orbitals, one staggered and one eclipsed with respect to the bridge. At fixed donor and acceptor orientations the decay of T_{ab} with linker number is known from Fig. A4. Only the prefactor is orientation dependent.

APPENDIX 3: Sigma symmetry donors

The ϵ -E relation for donors interacting equally with all three bridges is:

$$\det \begin{pmatrix} -E & \gamma & 0 & 0 & 0 & \beta & 0 & 0 \\ \gamma & -E & \beta & 0 & 0 & 0 & 0 & 0 \\ 0 & \beta & -E & \gamma & 0 & 0 & 0 & 0 \\ 0 & 0 & \gamma & -E & \beta & 0 & 0 & 0 \\ 0 & 0 & 0 & \beta & (2\gamma - E) & 0 & 0 & \gamma \\ \beta & 0 & 0 & 0 & 0 & (2\gamma - E) & \gamma & 0 \\ 0 & 0 & 0 & 0 & 3\gamma & -E & \beta/\epsilon & \\ 0 & 0 & 0 & 0 & 3\gamma & 0 & \beta\epsilon & -E \end{pmatrix} = 0. \tag{A5}$$

Fig. A6 shows the corresponding $E - \epsilon^{1/4}$ relation which might be of some use with σ symmetry donors and acceptors linked by [2.2.2]. Fig. A7 compares propagation through such a linker with propagation through other linkers.

REFERENCES FOR III.C

- 1a. L. Eberson, *Adv. Phys. Org. Chem.*, **1982**, *18*, 79-185
- 1b. D. DeVault, *Quantum Mechanical Tunneling in Biological Systems*, *2nd ed.* edition; Cambridge Univ. Press: New York, 1984.
- 1c. Isied, S.S., *Prog. in Inorg. Chem.* **1984**, *32*, 443-517.
- 1d. B. Chance, D.C. DeVault, H. Frauenfelder, R.A. Marcus, J.R. Schrieffer, and N. Sutin, eds., *Tunneling in Biological Systems*, Academic Press: New York, 1979.
- 1e. Winkler, J.R., Nocera, D.G., Yocom, K.M., Bordignon, E., Gray, H.B., *J. Am. Chem. Soc.*, **1982**, *104*, 5798-5800.
2. R.A. Marcus, in *Oxidases and Related Redox Systems*, edited by T.E. King, H.S. Mason, and M. Morrison (Pergamon, New York, 1982), p.3.
3. P. Siders, R.J. Cave, and R.A. Marcus, *J. Chem. Phys.* **1984**, *81*, 5613.
4. J. Jortner, *Biochim. Biophys. Acta* **1980**, *594*, 193-230.
5. J.J. Hopfield, *Proc. Nat. Acad. Sci., U.S.A.* **1974**, *71*, 3640-3644.
6. M. Redi and J.J. Hopfield, *J. Chem. Phys.* **1980**, *72*, 6651-6660.
7. D.N. Beratan and J.J. Hopfield, *J. Am. Chem. Soc.* **1984**, *106*, 1584-1594.
8. S. Larsson, *J. Chem. Soc., Faraday Trans. 2*, **1983**, *29*, 1375-1388.
9. S. Larsson, *J. Am. Chem. Soc.* **1981**, *103*, 4034-4040.
10. A.S. Davydov, *Phys. Stat. Sol (b)* **1978**, *90*, 457-464.
11. A.A.S. da Gama, *Theor. Chim. Acta* **1985**, in press.
12. McConnell, H.M., *J. Chem. Phys.*, **1961**, *35*, 508-515.
13. A.D. Joran, B.A. Leland, G.G. Geller, J.J. Hopfield, and P.B. Dervan, *J. Am. Chem. Soc.* **1984**, *106*, 6090-6092.
14. B.A. Leland, A.D. Joran, Felker, P. , J.J. Hopfield, A.H. Zewail, and P.B.

Dervan, J. Am. Chem. Soc., manuscript in preparation.

15. P.J. Hay, J.C. Thibeault, and R. Hoffmann, J. Am. Chem. Soc. **1975**, *97*, 4884-4899.
16. D.E. Richardson and H. Taube, J. Am. Chem. Soc. **1983**, *105*, 40-51.
17. D.E. Richardson and H. Taube, Coord. Chem. Revs. **1984**, *60*, 107-129.
18. Anderes, B.; Lavallee, D.K. Inorg. Chem., **1983**, *22*, 2665-2666.
19. J. Halpern and L. Orgel, Discuss. Faraday Soc., **1960**, *29*, 32-41.
20. D.N. Beratan, J.N. Onuchic, and J.J. Hopfield, submitted to J. Chem. Phys., **1985**.

Table 1. Redox potentials for model porphyrins and quinones*.

Solvent	$E_{1/2} (Q/Q^{\cdot-})$ NHE ⁺	$E_{1/2} (P/P^{\cdot+})$ NHE ⁺
acetonitrile	-.341V	+.792V
butyronitrile	-.271	+.867
MTHF	-.463	+.906
benzene	-.708	+.842

⁺ Calculated from model porphyrins and quinones measured in these solvents vs. Ag/AgCl(aq) for the first three and vs. Pt⁰ pseudoreference electrode in benzene.

* Data kindly provided by A.D.Joran.

Table 2. Redox potentials for model porphyrins and quinones*.

Solvent	$\Delta G_{\infty}^{for} (S_1)$ eV	$E^{\ddagger} (S_1)$ NHE	$\Delta G_{\infty}^{for} (T_1)$ eV	$E^{\ddagger} (T_1)$ NHE
acetonitrile	-1.02	-1.0V	-.69	-.79 V
butyronitrile	-1.00	-.93	-.67	-.72
MTHF	-.781	-.97	-.45	-.75
benzene	-.528	-1.1	-.20	-.88

* Calculated from Table 1 and Eq. 6. G_{∞} neglects electrostatic interactions between donor and acceptor.

Table 3. Energies of reverse electron transfers.

Solvent	ΔG_{∞}^{rev} eV	E^{\ddagger} NHE
acetonitrile	-1.13	.41V
butyronitrile	-1.14	.48
MTHF	-1.37	.44
benzene	-1.55	.32

Table 4. Decay constants for forward and reverse electron transfers.

Parameter	$(S_1)E_{for}^{\ddagger} = -1.0V$	$(T_1)E_{for}^{\ddagger} = -.78V$	$E_{rev}^{\ddagger} = +.41V$
$\epsilon^{1/4}$.40	.42	.60
$\epsilon^2 = k_{LL}/k_L$	$(1500)^{-1}$	$(1000)^{-1}$	$(59)^{-1}$
$\alpha_{avg.}(\text{\AA}^{-1})$.91	.87	.51

Figure Captions

Figure 1. The carbon backbond orbitals participating in electron transfer are shown.

Figure A1. The view along the donor-linker bond is shown for the staggered and eclipsed linker geometries.

Figure A2. These two geometries of adjacent repeating [2.2.2] units were considered.

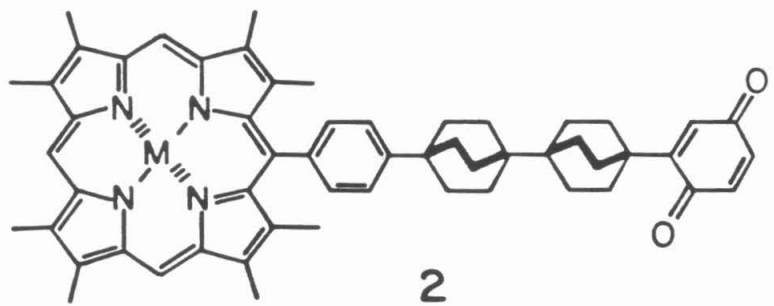
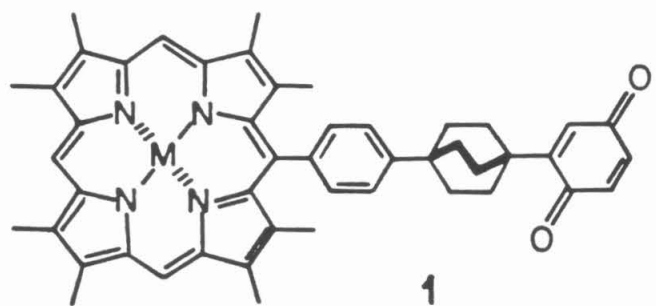
Figure A3. (a) Even symmetry and (b) odd symmetry with respect to a plane containing one of the three parallel pathways of the linker.

Figure A4. ϵ_{alkane} , $\epsilon_{spiro}^{1/2}$, and $\epsilon_{[2.2.2]}^{1/4}$ are shown as a function of energy. The calculation is relevant to odd symmetry donors and acceptors for [2.2.2] but even symmetry donors and acceptors for the other linkers. The center of the band gap for [2.2.2] is different from that of the other linkers.

Figure A5. The $E-\epsilon^{1/4}$ relation for [2.2.2] in the range of experimental interest is shown. The energies of forward transfer from the singlet and triplet P^* states are shown with the energy for Q^- to P^{*+} transfer. $k_{LL}/k_L \propto [\epsilon^{1/4}]^8$.

Figure A6. For even symmetry donors and acceptors the $E-\epsilon$ relation is compared for alkane, spiroalkane, and [2.2.2].

Figure A7. For even symmetry donors the heuristic rule of Eq. 8 is tested.



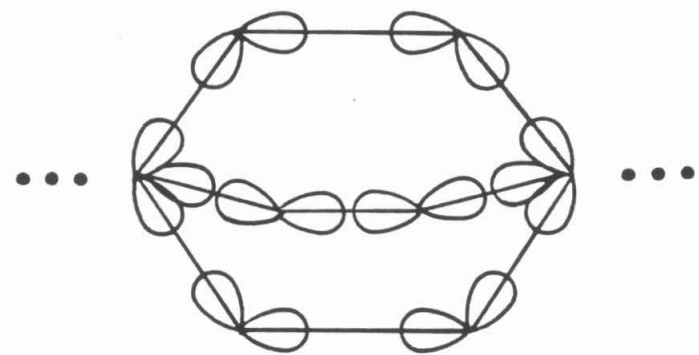


Figure 1.

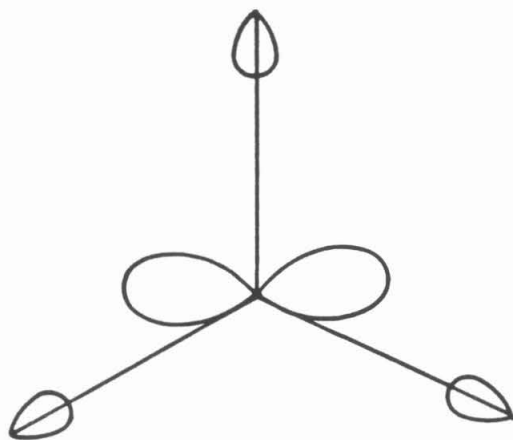
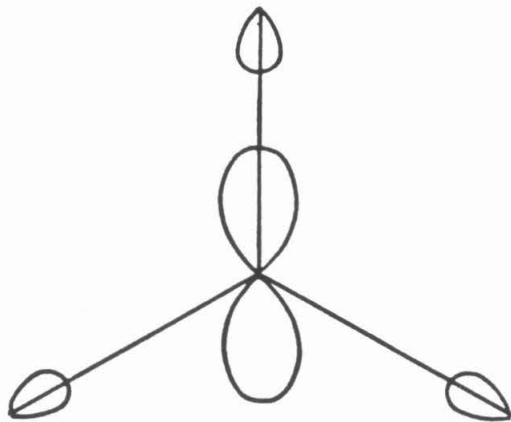
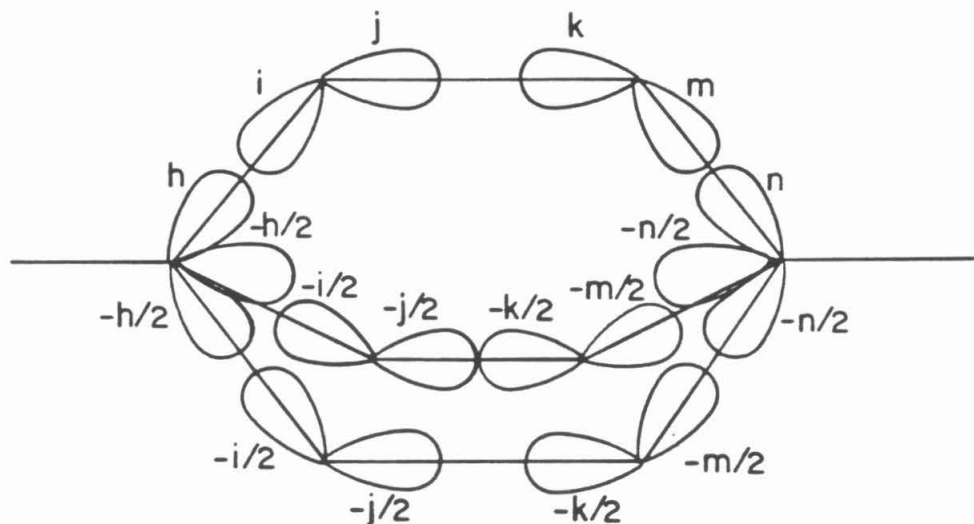


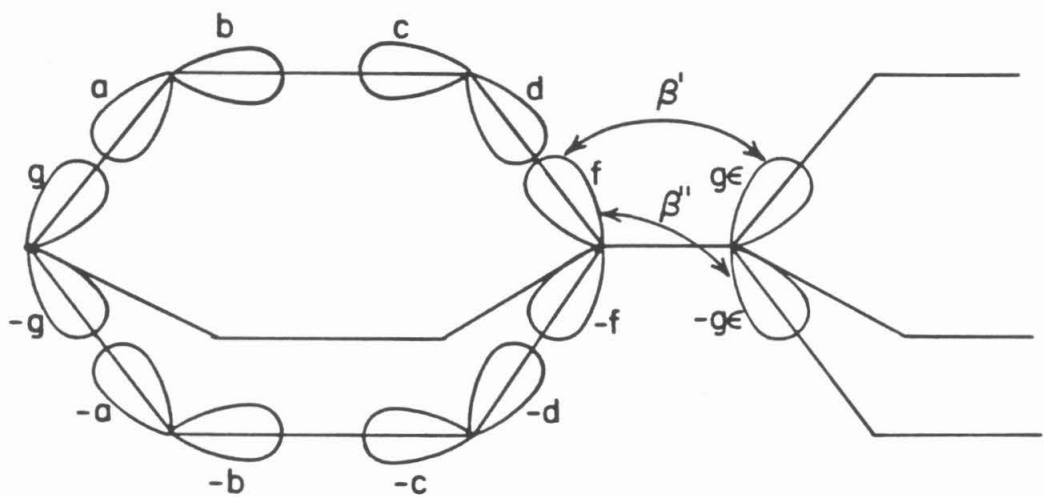
Figure A1.



Figure A2.



(a)



(b)

Figure A3.

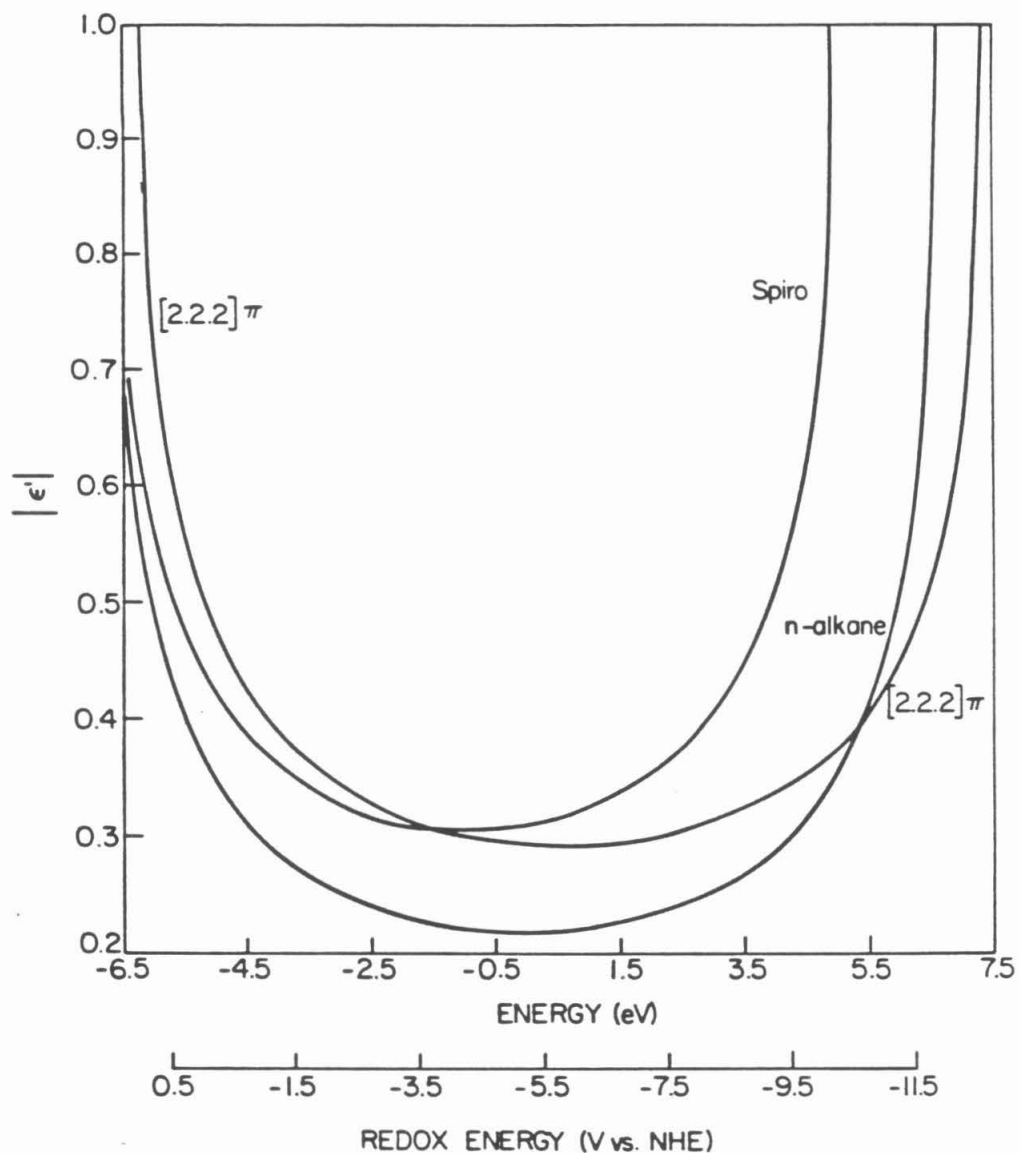


Figure A4.

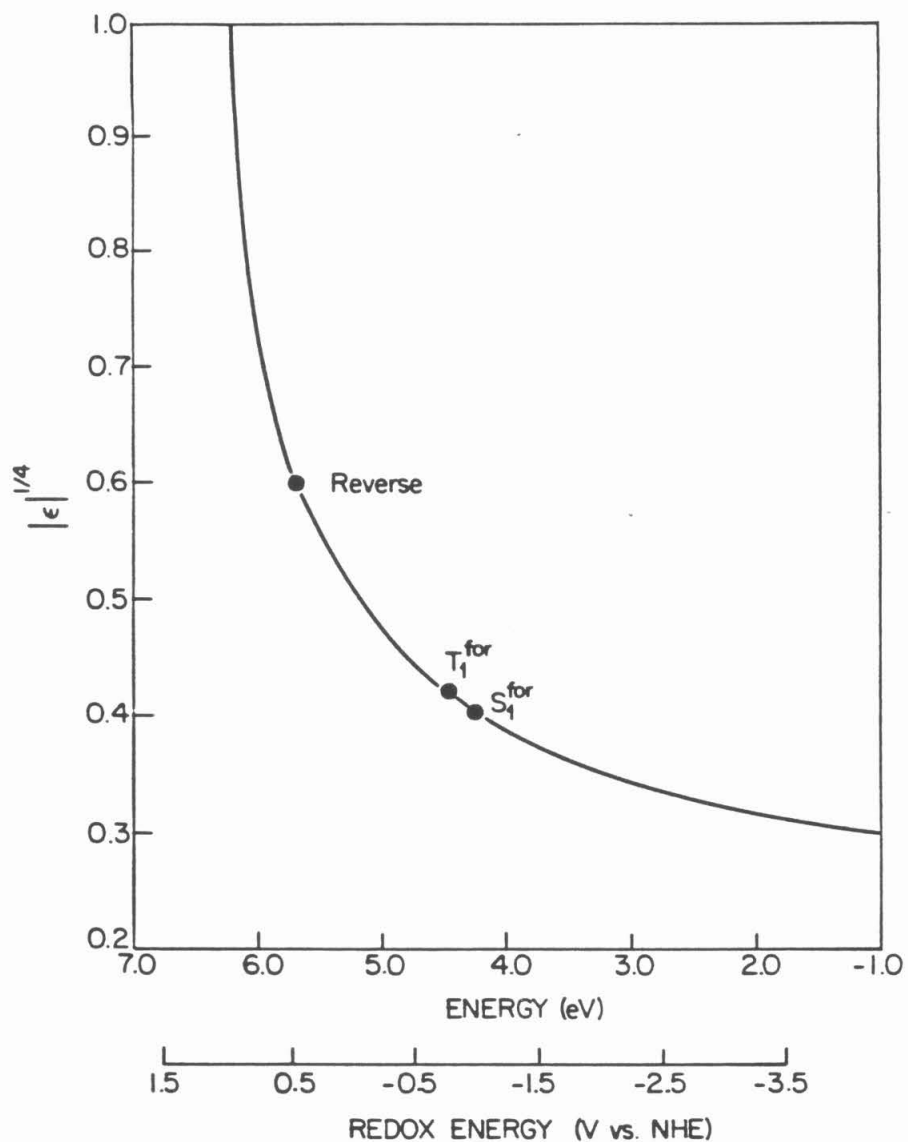


Figure A5.

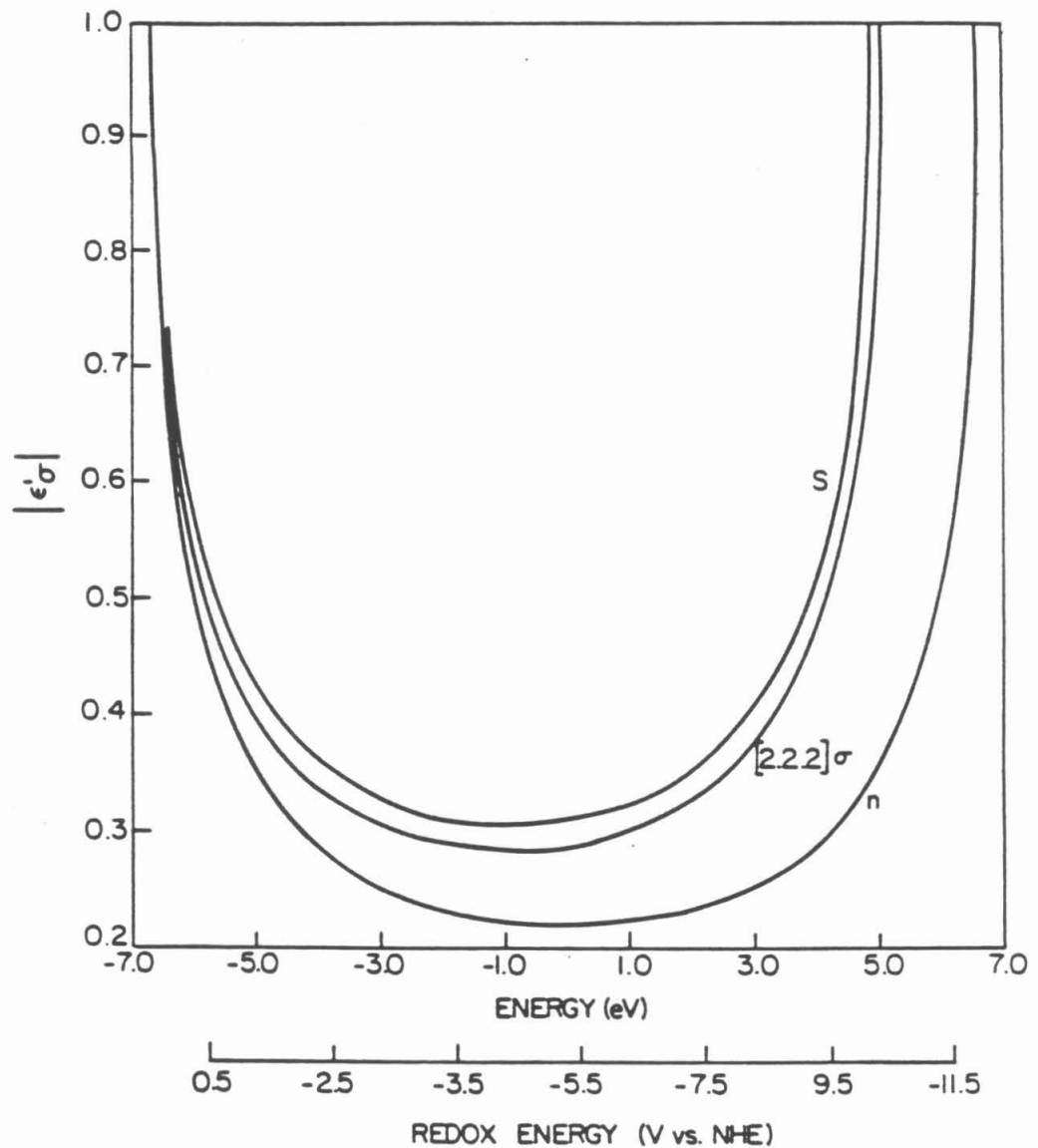


Figure A6.

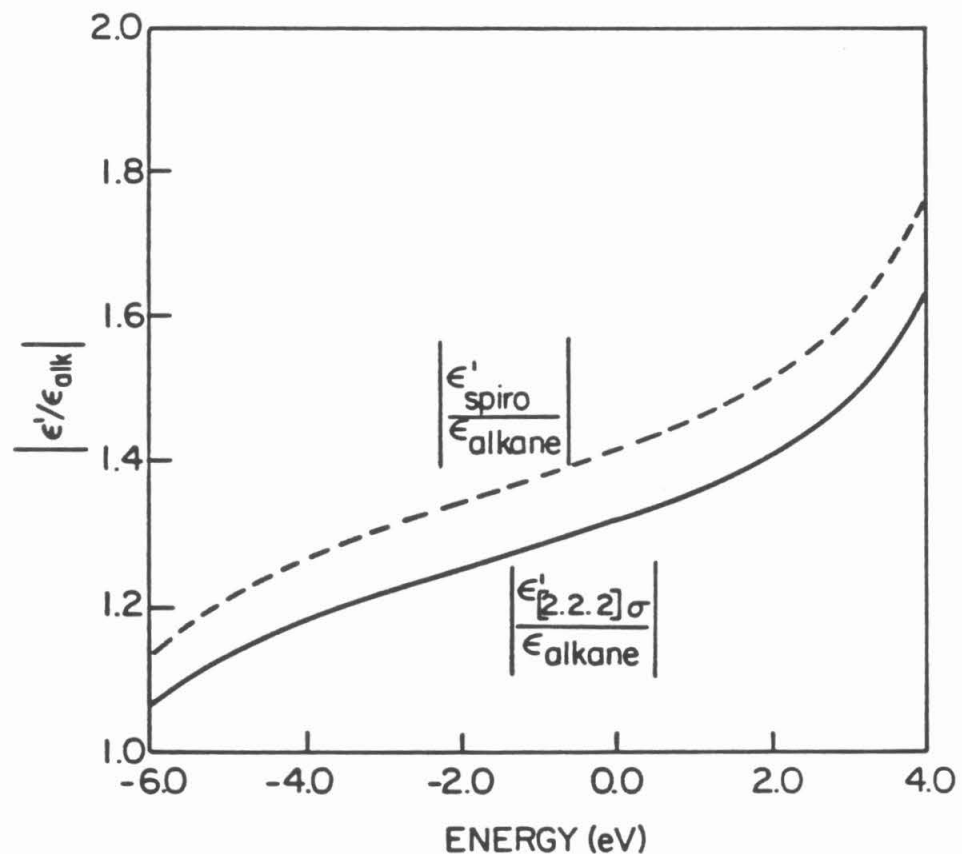


Figure A7.

Acknowledgments

Thanks are due to J.J. Hopfield for discussion of all aspects of this work. I am also grateful to Dr. P.B. Dervan, Mr. A.D. Joran, and Mr. B.A. Leland for making the experimentsl data available prior to publication. This work was supported in part by NSF grant PCM-8406049.

III.D. Further Comments on the Influence of the Bridging Medium on Electron Transfer Rates

Now that the utility of the $E - \epsilon$ relation has been established some general comments regarding electron mediation are in order. Fig. III.1 shows the picture which has been presented. $|\epsilon| = 1$ when the donor state lies in any of the shaded bands. In this multiband picture, of course, the presence of donor and acceptor anywhere but between the HOMO and LUMO would lead to spontaneous oxidation or reduction of the linker. The influence of bridge geometry on ϵ has been discussed. All of the systems considered so far are saturated. This method is also useful for systems with unsaturated substituents. Consider the $E - \epsilon$ relation in systems with some delocalized aromatic repeating units compared to the relation for saturated linkers. This is a topic relevant to charge transport in native and modified protein [7].

For the chains of orbitals shown in Fig. III.2 The corresponding secular equations are:

$$\det \begin{pmatrix} \alpha_p - E & 2\beta & 0 & \gamma/\epsilon \\ \beta & \alpha_p - E & \beta & 0 \\ 0 & \beta & \alpha_p - E & \beta \\ \gamma\epsilon & 0 & 2\beta & \alpha_p - E \end{pmatrix} = 0 \quad (III.1a)$$

and

$$\det \begin{pmatrix} \alpha_{sp^3} - E' & \gamma' + \beta'/\epsilon' \\ \gamma' + \beta'\epsilon' & \alpha_{sp^3} - E' \end{pmatrix} = 0 \quad (III.1b)$$

considering only the states even with respect to the plane containing carbon atoms of adjacent unit cells. The characteristic polynomials are

$$(\epsilon + \frac{1}{\epsilon}) = \frac{1}{2\beta^3\gamma} [E^4 - 5E^2\beta^2 + \gamma^2\beta^2 - E^2\gamma^2 + 4\beta^4]; \quad \alpha_p = 0 \quad (III.2a)$$

and

$$(\epsilon' + \frac{1}{\epsilon'}) = \frac{1}{\beta'\gamma'} [E'^2 - \gamma'^2 - \beta'^2]; \quad \alpha_{sp^3} = 0, \quad (III.2b)$$

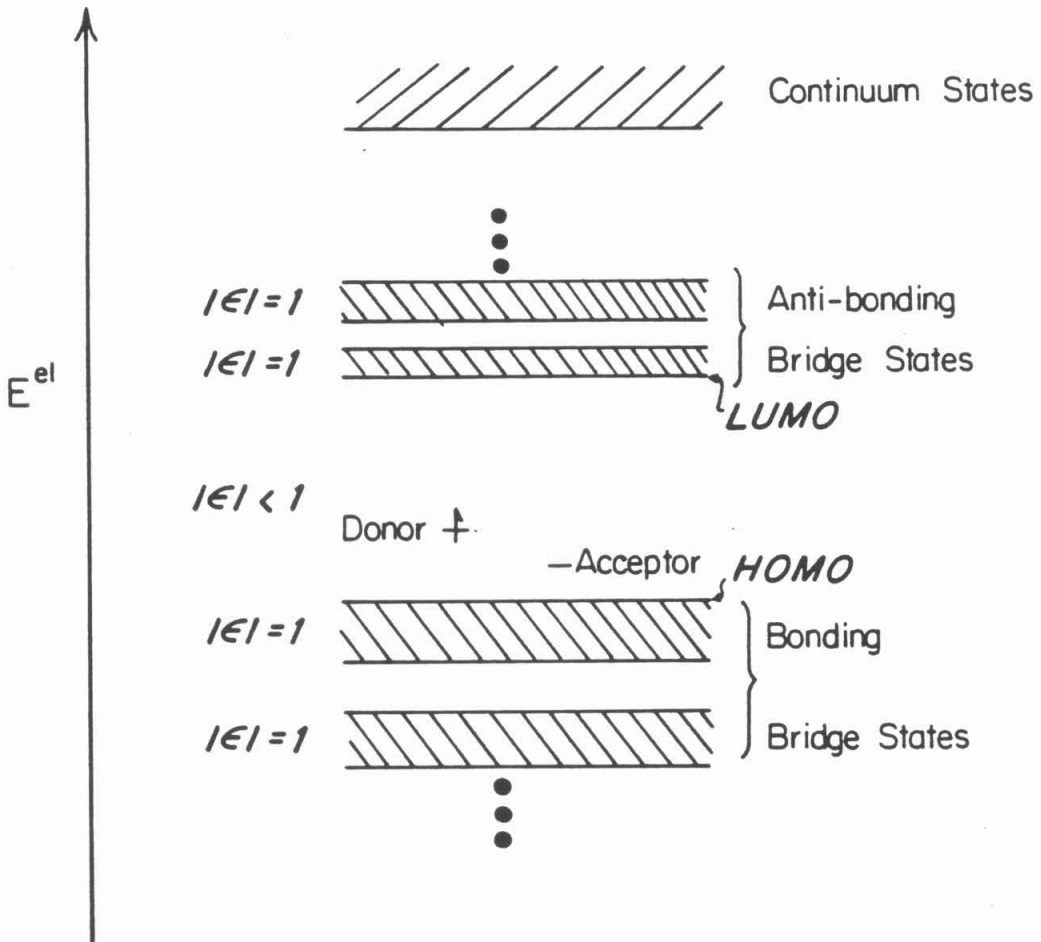


Figure III.1. The shaded bars are bands of linker states with $|\epsilon| = 1$. Localized states can occur if E^{el} falls between bands. In the orbital model, if the intersite interaction goes to zero the tunneling matrix element vanishes. In this case, however, the non-infinite potential between donor and acceptor may allow direct donor-acceptor interaction.

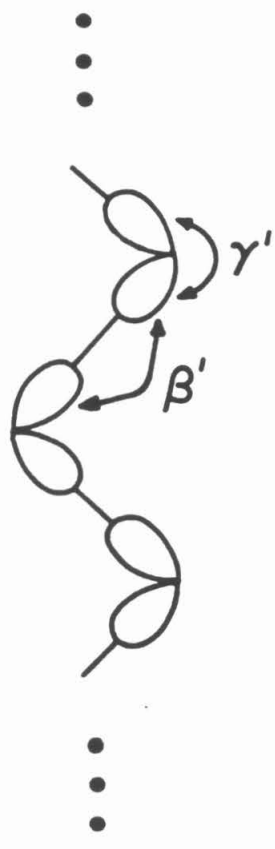
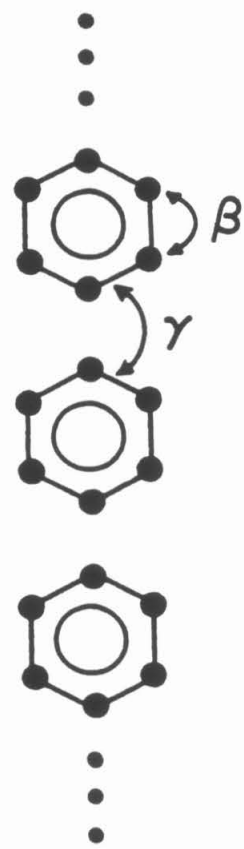


Figure III.2 (a) Repeating chain of phenyl rings. (b) Repeating chain of n-alkane (two-orbital model).

respectively. In most cases $\beta \gg \gamma$ and $\beta' \gg \gamma'$. The smallest values of ϵ and ϵ' occur at $E = 0$ and $E' = 0$. At these points

$$\epsilon + \frac{1}{\epsilon} = \frac{\gamma}{2\beta} + \frac{2\beta}{\gamma}$$

and

$$\epsilon' + \frac{1}{\epsilon'} = \frac{\gamma'}{\beta'} - \frac{\beta'}{\gamma'}. \quad (III.3b)$$

Since $\beta' \gg \gamma'$, $\beta \gg \gamma$, $1/\epsilon \gg \epsilon$ and $1/\epsilon' \gg \epsilon'$:

$$\epsilon_{min} \simeq \gamma/(2\beta) = -.38\gamma \quad (III.4a)$$

$$\epsilon'_{min} \simeq -\gamma'/\beta' = .22 \quad (III.4b)$$

given

$$\beta = -1.3eV$$

$$\beta' = -8.5eV$$

$$\gamma' = -1.9eV.$$

ϵ is the wave function decay associated with traversing a phenyl group and ϵ' is the decay upon traversing a saturated C-C bond. Comparing transfer through ten C-C bonds (for E in the center of the gap) to transfer across three phenyl groups

$$\frac{k_{alkane}}{k_{phenyl}} \leq \frac{(.22)^{20N}}{(.38\gamma)^{6N}} \simeq \left[\frac{3.3 \times 10^{-11}}{\gamma^6} \right]^N. \quad (5)$$

At this tunneling energy the rates are comparable if $\gamma \simeq 0.017$ eV. Three phenyl groups spaced by 3.3 Å span 15 Å. If the interaction between rings is ≥ 0.017 eV, ring-ring interactions can dominate backbone interactions. This approximation is not exact because an electron energy in the center of the gap for

phenyl assisted transfer will be shifted 1-2 eV from the gap center for backbone tunneling. However, since the $E - \epsilon$ curve is rather broad and flat for n-alkane in the gap center, the approximation is probably not too bad. A comparison of rates at *many* tunneling energies is needed and can easily be performed. Since the band structures have different gap energies and origins, the relative importance of phenyl and alkyl mediation will shift with donor and acceptor redox energy in a predictable way. Experimental and theoretical estimates of γ and its distance dependence are needed. Extensions of this particular calculation may be of relevance to electron tunneling in ruthenium modified proteins and other electron transfer model compounds [7]. Calculations exploiting the periodic nature of the protein backbone have been reported by others [8].

III.E. References – Chapter III

1. R.A. Marcus and N. Sutin, *Biochim. Biophys. Acta*, in press.
- 2a. C.A. Stein, N.A. Lewis, G. Seitz, *J. Am. Chem. Soc.* **104**, 2596 (1982).
- 2b. H. Taube in *Tunneling in Biological Systems*, edited by B. Chance, D.C. DeVault, H. Frauenfelder, R.A. Marcus, J.R. Schrieffer, and N. Sutin (Academic, New York, 1979), pp. 173-199.
- 3a. A.D. Joran, B.A. Leland, G.G. Geller, J.J. Hopfield, and P.B. Dervan, *J. Am. Chem. Soc.* **106**, 6090(1984).
- 3b. B.A. Leland, A.D. Joran, P.M. Felker, J.J. Hopfield, A.H. Zewail, and P.B. Dervan, to be submitted to *J. Am. Chem. Soc.*.
- 4a. J.V. Beitz and J.R. Miller, *J. Chem. Phys.* **71**, 4579 (1979).
- 4b. J.R. Miller, J.V. Beitz, and K.R. Huddleston, *J. Am. Chem. Soc.* **106**, 5057 (1984).
- 4c. J.R. Miller and J.V. Beitz, *J. Chem. Phys.* **74**, 6746 (1981).
5. S. Strauch, G. McLendon, M. McGuire, and T. Guarr, *J. Phys. Chem.* **87**, 3579 (1983).
6. J.J. Hopfield, *Biophys. J.* **18**, 311 (1977).
- 7a. S.S. Isied and A. Vassilian, *J. Am. Chem. Soc.* **106**, 1732 (1984).
- 7b. S.S. Isied and A. Vassilian, *J. Am. Chem. Soc.* **106**, 1726 (1984).
- 7c. J.R. Winkler, D.G. Nocera, K.M. Yocom, E. Bordignon, and H.B. Gray, *J. Am. Chem. Soc.* **104**, 5798 (1982).
- 7d. N. Kostić, R. Margalit, C.-M. Che, and H.B. Gray, *J. Am. Chem. Soc.* **105**, 7765 (1983).
- 7e. S.E. Peterson-Kennedy, J.C. McGourty, B.M. Hoffman, *J. Am. Chem. Soc.* **106**, 5010(1984).

8a. M.G. Evans and J. Gergely, *Biochim. Biophys. Acta* **3**, 188(1949).

8b. V.N. Kharkyanen, E.G. Petrov, and I.I. Ukrainskii, *J. Theor. Biol.* **73**, 29(1978).

Chapter IV

**Calculation of Wave Functions with Correctly
Coupled Nuclear and Electronic Motion:
Breakdown of the Born-Oppenheimer Approach
for the Long Distance Tunneling Problem**

IV.A Introduction

Within the golden rule formulation of non-adiabatic electron transfer theory, the quantity of interest is $\langle \Psi_D | V_A | \Psi_A \rangle$ where Ψ_D and Ψ_A represent accessible donor and acceptor states. In the previous sections the electronic and nuclear coordinates in Ψ_D and Ψ_A were separated:

$$\langle \Psi_D(x, y_D, y_A) | V_A | \Psi_A(x, y_D, y_A) \rangle$$

$$\begin{aligned} &\stackrel{B.O.}{\simeq} \langle \Psi_D^{el}(x; y_D, y_A) \phi_i(y_D, y_A) | V_A^{el} | \Psi_A^{el}(x; y_D, y_A) \phi_f(y_D, y_A) \rangle \\ &\stackrel{B.O./F.C.}{\simeq} \langle \Psi_D^{el}(x; \bar{y}_D, \bar{y}_A) | V_A^{el} | \Psi_A^{el}(x; \bar{y}_D, \bar{y}_A) \rangle \langle \phi_i | \phi_f \rangle. \end{aligned} \quad (IV.1)$$

x is the electronic coordinate and y is the donor or acceptor nuclear coordinate. $V_A^{el} | \Psi_A^{el} \rangle$ is, as usual, well localized near the acceptor site. Many nuclear degrees of freedom (e.g., inner sphere ligand vibrations and outer sphere solvent motion) are coupled to the electronic coordinate. Bond lengths and angles are dependent upon whether the electron is present or absent. $\Psi_D(x, y)$ should reflect this coupling because the electronic and nuclear motion is correlated. The Born-Oppenheimer separation limits the functional dependence which the correlation may take. The Franck-Condon approximation requires selection of \bar{y}_D and \bar{y}_A , choices which are not obvious because $\langle \Psi_D^{el}(x; \bar{y}_D, \bar{y}_A) | V_A | \Psi_A^{el}(x; \bar{y}_D, \bar{y}_A) \rangle$ may be *extremely* small at the maximum of $\phi_i^* \phi_f$ and may vary rapidly with both \bar{y} and distance.

Because of these many issues, a model problem was solved exactly. The model allows the nuclei to move smoothly between the equilibrium geometries of D^n and D^{n+1} as the electron is removed. It is this flexibility in Ψ_D which is necessary to estimate the importance of Born-Oppenheimer breakdown in the value of $\langle \Psi_D | V_A | \Psi_A \rangle$.

Another way of stating the problem is to ask to what extent states on more than one nuclear potential energy surface need be added to Ψ_D . These other states may have different equilibrium bond lengths, for example. The difficulty with this approach is that one does not know how many terms to include in the wave function expansion because the wave function decay related to mixing of excited states is *exponentially* larger than decay from the ground states. A perturbational approach to this problem requires careful consideration of the convergence of the result to the analytically correct result. A wave function which gives the correct nuclear geometry for the neutral molecule *and* for the ion ($x \rightarrow \infty$) is necessary.

Many effects of molecular structure on electron transfer rate have been studied using simple electronic potential models with limited numbers (one or two) of nuclear coordinates. Approximately exponential decay of rate with distance and an "inverted" region is predicted from the simplest models as well as from the more complex multi-dimensional ones. Because of this generality and the importance of an analytically correct wave function, a simple model was first chosen to investigate non-Born-Oppenheimer/Franck-Condon effects on the transfer rate.

**IV.B "Failure of the Born-Oppenheimer and
Franck-Condon Approximations for
for Long Distance Electron
Transfer Rate Calculations,"
J. Chem. Phys. **81**, 5753(1984)**

Failure of the Born-Oppenheimer and Franck-Condon approximations for long distance electron transfer rate calculations

David N. Beratan and J. J. Hopfield^{a)}

Division of Chemistry and Chemical Engineering,^{b)} California Institute of Technology, Pasadena, California 91125

(Received 2 August 1984; accepted 14 September 1984)

Quantum mechanical and semiclassical formulations of nonadiabatic electron transfer theory are usually implemented within a Born-Oppenheimer regime. Calculations on real weakly interacting systems are so difficult that this approximation is rarely questioned. The Born-Oppenheimer approximation becomes qualitatively wrong for electron transfers at very large distances. A model vibronic problem is exactly solved and compared with the Born-Oppenheimer result. Rate expressions are derived from the wave functions using the "golden rule" approximation. Electron propagation is intimately correlated with nuclear motion so that the vibrational energy left on the donor critically affects the electronic decay length. Several deviations from the usual predictions appear for transfers over very large distances.

I. INTRODUCTION

Many aspects of the long distance nonadiabatic electron transfer reaction distinguish it from other (adiabatic) chemical reactions.¹⁻⁴ Biologically important electron transport occurs over large distances, typically $\sim 5-15 \text{ \AA}$.⁴ Because these distances are so large the electron donor nuclei coupled to the transfer event may react to the absence of the electron even before it has been trapped by the acceptor. If so, wave functions which explicitly and correctly couple the electronic and nuclear motion must be found. The need to properly treat coupling in the wave functions and rate calculation when the transfer distance is large leads one to question the utility of the most common quantum chemical approximations, the Born-Oppenheimer (BO) and Franck-Condon (FC) approximations.

Ionizing H_2 to H_2^+ causes a bond length change of 0.31 \AA . It is apparent that the electronic and nuclear motion is coupled. Yet, a typical bound state BO wave function for H_2 is found for a single nuclear geometry and does not suggest that the nuclear wave function should change as an electron wanders far from the bond. Using bound state theory one usually solves the equilibrium geometry H_2 and H_2^+ problems separately and there is no natural way of passing to a limit in the H_2 problem and obtaining the H_2^+ states (or vice versa). Yet, this intermediate region where the molecule is not quite an ion and not quite a neutral is the region important to long distance electron transfer reactions. The detailed answer to the question "What are the nuclei doing when the electron is far from but still bound to the donor?" is the one relevant to electron transfer theory. Three limiting situations exist for a molecule with electronic-nuclear coupling: (1) The electron is mostly near its bond and the sluggish nuclei populate a Boltzmann average of the nuclear states available to the neutral molecule. In this limit the BO approximation is probably quite reliable. (2) The electron donor molecule is ionized and the formerly bound electron is very far away. The nuclei populate a Boltzmann average of the ion's final nuclear states which are different from the

neutral's. The equilibrium displacement and force constant of the bond may be different from the neutral. (3) The electron is far from the donor which is neither neutral nor fully ionized. The details of the electronic-nuclear coupling strongly influence the molecular behavior in this region. The nuclei may be in some linear combination of neutral and ionic molecular vibrational states. The spatial extent of this region depends on the strength of the coupling.

A model "molecule" which has both nuclear and electronic coordinates (and coupling between the two) but which can be solved with no assumptions concerning the separability of motion is developed. Electron transfer rates between two such sites are calculated. The BO solution of the problem is also found. In a second paper this model will be extended to include a more realistic treatment of the donor-acceptor bridging medium. In some cases this model which correctly treats the long distance behavior of the wave functions better explains the distance dependence of experimental electron transfer rates. Several predictions, at odds with standard electron transfer theory, will also be presented there.⁵ Explicit numerical comparison with experiment is avoided here because only a model problem for which it is not easy to choose meaningful parameters is solved. The aim of this paper is to clarify the influence of the vibronic interaction on the long distance behavior of a wave function by studying a simple example.

II. MODEL FOR A BOUND ELECTRON COUPLED TO A MOLECULAR VIBRATION

The many assumptions and limitations of the usual nonadiabatic electron transfer theories are discussed in several excellent recent reviews.^{1,3,6} Recently Hopfield, Sarai and DeVault, and Day raised serious questions concerning the separability of nuclear and electronic motion in the wave functions used to calculate long distance electron transfer rates.⁷⁻⁹ Lee and de Pristo recently studied the H_2-H_2^+ system within the BO regime and evaluated the quality of the FC approximation.¹⁰ It will be shown that the electronic-nuclear interaction couples the amount of vibrational energy left on the electron donor molecule after the transfer with the ability of the electron to tunnel between donor and acceptor.

^{a)} Also California Institute of Technology, Division of Biology, and AT&T Bell Laboratories, Murray Hill, NJ 07974.

^{b)} Contribution No. 7041.

This behavior appears because the coupling introduces terms related to nuclear motion to what in the uncoupled problem was a purely electronic long distance decay constant. The electronic decay with distance is no longer just related to a static electronic potential barrier between donor and acceptor, but is also influenced by details of the nuclear motion.

The simplest two molecule system involving electron exchange between the interacting molecules is H_2-H_2^+ . Each molecular wave function should be found without any assumptions about the separability of the motions of the particles. Analytical solutions (wave functions), however, do not exist even for these simple molecules.^{10,11} It is more instructive to set up a simpler one electron problem in which an electron in a contrived potential well is coupled to one nuclear degree of freedom. Such a system is the "small polaron," ubiquitous in electron transfer theory though often not identified by name.^{12,13} This model establishes an electronic potential well and simple harmonic oscillator at a site with linear (usually) coupling between the electron and vibration. The role of the coupling is to shift the equilibrium position of the oscillator, our bond, when the electron is between the nuclei comprising the bond. A similarly coupled acceptor without an electron is then added. Since distant electron transport is being investigated the Hamiltonian matrix element between these sites required for the Golden Rule calculation of the transfer rate will be found. The functional forms of the initial and final states Ψ_i and Ψ_f critically influence the calculated rate. The Golden Rule expression for the rate is

$$k = (2\pi/\hbar) \sum_{i,f} B_i |\langle \Psi_i | H' | \Psi_f \rangle|^2 \rho_f(E_i). \quad (1)$$

B_i is the Boltzmann population of the initial state i . $\rho_f(E_i)$ is the density of final states at energy E_i . H' is the perturbation which couples the donor and acceptor. The matrix elements between BO states will be found using the FC approximation. For the exact wave functions no assumptions about the separability of the matrix elements will be made.

The electron donor (small polaron) Hamiltonian H_d is

$$H_d = H^{\text{el}} + H^{\text{nuc}} + H^c, \quad (2)$$

$$H^{\text{el}} = -(\hbar^2/2m_e)\partial^2/\partial x^2 - \mu\delta(x), \quad (3)$$

$$H^{\text{nuc}} = (b^\dagger b + 1/2)\hbar\omega, \quad (4)$$

$$H^c = +\lambda\delta(x)(b^\dagger + b). \quad (5)$$

b and b^\dagger are the Boson annihilation and creation operators, respectively.¹² A Dirac delta function potential $-\mu\delta(x)$ binds the electron ($\mu > 0$).¹⁵ More complicated electronic potential models are also soluble. One such model will be described in a second paper. The coupling term is positive ($\lambda > 0$) so that the equilibrium nuclear displacement is decreased when the electron is between the nuclei. The nuclei are treated as a single reduced mass. $(b^\dagger + b)$ is proportional to y , the nuclear coordinate, so H^c produces an energy shift and equilibrium displacement for the oscillator when $x = 0$. Only local modes are coupled to the transfer. No donor-acceptor vibrational coordinate is presumed to be coupled to the transfer event.¹⁴

Exact solution

Any function of two variables may be written

$$\Psi(x,y) = \sum_{i,j} c_{ij} X_j(x) Y_i(y) = \sum_i f_i X_i(x) Y_i(y). \quad (6)$$

No assumptions about the separability of the function have been made. The $X_j(x)$ and $Y_i(y)$ form complete orthonormal sets. The actual basis functions ($X_i \propto \sum_j c_{ij} X_j$) are not orthogonal. Surprisingly, this simplifies the calculation. Since the harmonic oscillator eigenstates span a complete set each nuclear basis function may be expanded as a linear combination of these eigenstates (ϕ_n) centered at $y = 0$:

$$Y_i(y) = \sum_j d_{ij} \phi_j(y). \quad (7)$$

The oscillator states chosen are the vibrational eigenstates of the uncoupled ionized molecule. Substituting Eq. (7) into Eq. (6):

$$\Psi(x,y) = \sum_i g_i X_i(x) \phi_i(y). \quad (8)$$

For the range $x \neq 0$ the Schrödinger equation for the donor is

$$[-(\hbar^2/2m_e)\partial^2/\partial x^2 + H^{\text{nuc}}] \Psi(x,y) = E^{\text{Total}} \Psi(x,y) \quad (9)$$

but

$$H^{\text{nuc}} \phi_n(y) = (n + 1/2)\hbar\omega \phi_n(y) = E_n \phi_n(y). \quad (10)$$

Thus

$$-(\hbar^2/2m_e)\partial^2/\partial x^2 \Psi(x,y)$$

$$= \sum_i (E^{\text{Total}} - E_i) g_i X_i(x) \phi_i(y), \quad x \neq 0. \quad (11)$$

Multiplying the Schrödinger equation by ϕ_m^* and integrating over the nuclear coordinate gives

$$-(\hbar^2/2m_e)\partial^2/\partial x^2 X_m(x) = (E^{\text{Total}} - E_m) X_m(x) \quad (12)$$

or

$$X_m(x) = \exp[-\kappa_m |x|],$$

$$\kappa_m^2 = (2m_e/\hbar^2) [-E^{\text{Total}} + (m + 1/2)\hbar\omega], \quad m = 0, 1, 2, \dots. \quad (13)$$

E^{Total} is the total energy of the coupled state. The decay length of the electron is intimately coupled to the nuclear motion by the $(m + 1/2)\hbar\omega$ term in κ_m . The probability of finding an electron far from the donor bond (large x) is coupled to the vibrational state of the developing ion.

As in the standard one dimensional Dirac delta well problem the Schrödinger equation is integrated across the electronic origin to find the eigenvalues¹⁵

$$\begin{aligned} \lim_{\epsilon \rightarrow 0} \left\{ \int_{-\epsilon}^{+\epsilon} [-(\hbar^2/2m_e)\partial^2/\partial x^2 - \mu\delta(x) \right. \\ \left. + (b^\dagger b + 1/2)\hbar\omega + \lambda(b^\dagger + b)\delta(x)] \right. \\ \times \sum_n g_n \exp(-\kappa_n |x|) \phi_n(y) dx \\ = E^{\text{Total}} \int_{-\epsilon}^{+\epsilon} \sum_n g_n \exp(-\kappa_n |x|) \phi_n(y) dx \right\}. \quad (14) \end{aligned}$$

Integration over the electronic coordinate followed by multiplication by $\phi_n^*(y)$ and integration over the nuclear coordinate gives the recursion relation

$$g_{j+1} = - [1/(\lambda \sqrt{j+1})] [(\hbar^2/m_e)\kappa_j - \mu] g_j - \sqrt{j/(j+1)} g_{j-1}, \quad (15)$$

$$j = 0, 1, \dots, \quad g_{-1} = 0.$$

The normalized coupled wave function is

$$\Psi = N \sum_n g_n \exp(-\kappa_n |x|) \phi_n(y), \quad (16)$$

where

$$1/N^2 = \sum_n g_n^2 / \kappa_n.$$

Equation (15) is a recursion expression connecting the wave function mixing amplitudes with the energy eigenvalues. Any energy determines a set of g_i 's and, potentially, a wave function. Wave functions must be square integrable so the g_i 's must remain finite for any i . This occurs only when the g_i 's are evaluated for an energy "guess" which is in fact an eigenvalue of the problem. The simplest way to find the eigenvalues is to guess a range of energies, calculate a large number (~ 20) of the g_i 's for each guess and watch for sign changes in g_i for large i . The g_i 's diverge with different signs on the opposite sides of the eigenvalue. The energy eigenvalues may be approximated by solving the electronic delta well and nuclear oscillator problems separately (ignoring H^c) and then treating H^c as a perturbation [the second order term must be considered, see Eq. (29)].

One way to see the correlation aspects of the wave function is to calculate the probability of simultaneously finding an electron at $x = R$ and nuclear motion corresponding to the n th vibrational state. This quantity is the square of the coefficients of ϕ_n in Eq. (16) evaluated at $x = R$. This scales with distance and number of vibrations left on the donor as

$$g_n^2 \exp[-\sqrt{(2m_e/\hbar^2)}(|E^{\text{Total}}| + (n + 1/2)\hbar\omega) |R|], \quad (17)$$

since $E^{\text{Total}} < 0$. The electron propagates away from its bond with the slowest falloff with distance when it leaves no vibrational excitation behind.

These correct donor states behave properly in all three of the distance domains. For the small $|x|$ the exponential terms are approximately one and do not depend strongly on n . If $|x|$ were always equal to zero the problem would be separable and the g_i^2 would reduce to the overlap functions known for shifted harmonic oscillators.^{3,16} For the ground state wave function the $\{g_i^2\}$ would reduce to a Poisson distribution in i . An excellent approximation is apparent because the $\{g_i\}$ are distance independent. It is shown in the Appendix that to first order in the energy of the vibrations left behind plus the coupling energy, the g_i^2 are Poisson distributed in the ground state coupled wave function. Exact calculations show that this approximation is quite reliable. Because many terms contribute to the wave function sum for small $|x|$ the oscillator is in a mixture of the unshifted (ion) vibrational states. For large $|x|$, however, the exponential terms are quite small and only terms with small values of n contribute to the wave function. Therefore, the more energy the electron is able to carry away the further it can tunnel. The nuclei are preferentially left in the lower vibrational states of the unshifted oscillator when the electron is far from the donor. That the electron tunnels best when little vibra-

tional energy is left behind is reasonable since particles tunnel better at higher energies.¹⁷

Product wave functions and the BO solution to the coupled Schrödinger equation

The simplest approximate solution to a coupled Schrödinger equation is derived using the "crude adiabatic approximation".^{2(a)} The solution is a product wave function where the electronic state is determined using the BO approximation but the parametric nuclear dependence of the electronic state is removed by fixing the nuclei at the equilibrium position of the total nuclear potential energy surface y_0 . Even the parametric dependence on the nuclear coordinate, which is not itself adequate, is removed from the electronic state. These wave functions are of the form

$$\Psi_n(x, y) = \psi^e(x, y_0) Y_n^{\text{nuc}}(y). \quad (18)$$

$\psi^e(x, y_0)$ in our problem is a Dirac well electronic wave function. The coupling is reintroduced to the problem by assuming a different nuclear geometry for the ion and independently solving the corresponding eigenvalue problem. Most approximations of the tunneling matrix element tacitly assume that the "crude adiabatic" approximation is adequate.^{18,19}

A correct adiabatic BO solution to the Schrödinger equation is obtained in the usual manner: (1) freeze the nuclei and solve the electronic problem parametrically in the nuclear position and (2) solve the nuclear problem. This method neglects the "adiabatic" matrix elements of the nuclear kinetic energy operator with the electronic wave functions and is questionable when the electronic states are closely spaced.^{2(a)} The electronic Schrödinger equation is

$$H^e \psi^e(x, y) = E^e \psi^e(x, y), \quad (19)$$

where

$$H^e = -(\hbar^2/2m_e)(\partial^2/\partial x^2) + (-\mu + \lambda A) \delta(x) \quad (20)$$

and the A is a given nuclear position (times a constant). The electronic solution is analogous to the purely electronic Dirac delta well eigenvalue problem with an altered strength parameter¹⁵:

$$\psi^e(x, y) = \sqrt{m_e \zeta / \hbar^2} \exp(-m_e \zeta |x| / \hbar^2), \quad (21)$$

where $\zeta = (-\lambda A + \mu)$ and $E^e = -\zeta^2 m_e / (2\hbar^2)$. The nuclear Schrödinger equation is $H^{\text{nuc}} \Phi = E^{\text{nuc}} \Phi$, where

$$H^{\text{nuc}} = (b^+ b + 1/2)\hbar\omega - [\mu - \lambda(b^+ + b)]^2 m_e / (2\hbar^2). \quad (22)$$

This Hamiltonian is more easily interpreted in the coordinate representation. Recall that

$$(b^+ + b) = \sqrt{2M\omega/\hbar} y. \quad (23)$$

Define $\lambda' = \lambda \sqrt{2M\omega/\hbar}$. The force constant for the oscillator of the ionized molecule is $k = M\omega^2$. Defining

$$k' = k - \lambda'^2 m_e / \hbar^2,$$

$$\epsilon = \mu \lambda' m_e / (2\hbar^2),$$

$$\Delta = \mu^2 m_e / (2\hbar^2),$$

and completing a square in the Hamiltonian gives

$$H^{\text{nuc}} = -(\hbar^2/2M) \partial^2 / \partial y^2 + (1/2)k'(y + \epsilon/k')^2 - \Delta - \epsilon^2 / (2k'). \quad (24)$$

The nuclear eigenfunctions $\Phi_n(y - y_0)$ are harmonic eigenstates with shifted origin and frequency compared to the uncoupled (or ion) problem. The BO states are thus

$$\Psi_n(x; y) = N(y) \exp[-(m_e/\hbar^2)(\mu - \lambda'y)|x|] \Phi_n(y + y_0). \quad (25)$$

The electronic wave function depends parametrically on the nuclear position. The vibronic coupling (H') shifted the frequency of the oscillator and shortened its equilibrium displacement compared to the ion. The nuclear wave function is sensitive to the presence of the "transferable" electron in an average sense when the electron is nearby. The nuclear wave functions are products of the form

$$\exp[-(M\omega/2\hbar)(y + y_0)^2] H_n[\sqrt{M\omega/\hbar}(y + y_0)],$$

where H_n is a Hermite polynomial. The term $\exp(m_e\lambda'y|x|/\hbar)$ in the electronic wave function may be combined with the Gaussian part of the nuclear wave function. This term shifts the Gaussian envelope of the oscillator by an amount proportional to the electron's distance from the bond! This shift corresponds to a bond length increasing in proportion to the distance of the electron from the bond. Such behavior is reasonable to the extent that the bond length increases as the molecule becomes ionized. However, the coupling increases the bond length without limit in an amount proportional to the electronic position. The bond expansion is not "turned off" at the length appropriate to the ion. The electronic wave function itself decays incorrectly with distance. Setting $\hbar = m_e = \mu = \lambda' = 1$:

$$\psi_e(x; y) \sim \exp(y|x|) \times \exp(-|x|). \quad (26)$$

Large bond lengthenings beyond the equilibrium separation for the ion increase the long distance electron amplitude in conflict with the exact result which showed that stretching the nuclei too far past the equilibrium separation for the ion (large n) decreases the ability of the electron to surmount its barrier.

The nonadiabatic correction to the energy of a BO wave function is often used as a measure of the quality of that state. This quantity is proportional to matrix elements of the nuclear kinetic energy operator with the BO states. The energy is usually trivially small compared to the binding energy of the electron but is not indicative of the kind of wave function errors which seriously affect electron transfer rate calculations. The BO states fail in the low probability regions of the wave functions which do not contribute much to the state's energy but critically affect the calculated long distance electron transfer rate.

The total nuclear potential energy is defined as $U(y) = E^{\text{el}}(y) + (1/2)ky^2$. $U(y)$ has zero derivative at $y = \lambda'/\mu/(k - \lambda'^2)$ (atomic units). This point is the minimum of a parabolic energy curve if $k > \lambda'^2$. However if $k < \lambda'^2$ no energy minimum exists and the linear coupling model itself is inadequate.

III. RATE CALCULATIONS

Although by no means the only (or necessarily best) way to calculate electron transfer rates, the Golden Rule formulation is the most often chosen for problems of weak interaction. A small perturbation is assumed to mix the donor and

acceptor states. The nature of this perturbation is model dependent. The assumption of weak interaction is probably reasonable for long distance transfers. Marcus, Siders, and Cave verified the validity of some aspects of the Golden Rule approximation for distant electron transfer.^{20,21} For the model problem at hand two sticky questions remain. What "perturbation" allows the electron transport? How can we conserve energy during a transfer process if the donor and acceptor have anything but identical energy level spacing?

This donor-acceptor problem is solved in three steps. The coupled donor (here the "left" molecule) is solved and a simple harmonic oscillator (without electron) on the acceptor (the right "molecule") is the initial state. The vibronic coupling on the acceptor $\lambda_R \delta(x - R_{ab})(b_R^\dagger + b_R)$ has no significant effect on the initial state i assuming weak overlap. R_{ab} is the donor-acceptor separation and is held fixed during the transfer event. The initial wave function is

$$\Psi_i(x; y_L, y_R) = \psi_L^{\text{coupled}}(x; y_L) \times \phi_R(y_R). \quad (27)$$

The coupled acceptor (right) problem is solved similarly assuming a simple harmonic oscillator (without electron) on the left. This gives the final wave function

$$\Psi_f(x; y_L, y_R) = \phi_L(y_L) \times \psi_R^{\text{coupled}}(x; y_R). \quad (28)$$

The part of the total Hamiltonian omitted when solving the Schrödinger equation for the initial state is $H' = -\mu_R \delta(x - R_{ab})$.

Before calculating transfer rates, Eq. (1) must be examined in more detail. Electron transfer reactions must conserve energy. By solving a "molecular" eigenvalue problem only discrete energies were found. Real donors and acceptors are not necessarily identical and may have properties corresponding to unequal values of μ , λ , and $\hbar\omega$. Treating the coupling [Eq. (5)] as a perturbation on the electronic and nuclear Hamiltonians the donor energy to second order is

$$E_L \approx -m_e\mu_L^2/(2\hbar^2) + (n + 1/2)\hbar\omega_L - [(m_e/\hbar^2)\mu_L\lambda_L]^2/\hbar\omega_L. \quad (29)$$

This estimate of the donor energy shows that if the acceptor has a slightly different electronic well depth, vibronic coupling, or vibrational frequency the donor and acceptor will have only accidentally aligned energy levels, if any. Alignment is required for strict energy conservation if the initial and final states are infinitely narrow. The standard escape from this predicament follows from the realization that the density of states is not a sum of delta functions but should be broadened. The finite lifetimes (homogeneous broadening) of the acceptor states or coupling the acceptor to a continuum of medium modes may provide this broadening.^{22,23} A Lorentzian function is usually chosen for the density of states:

$$\rho_f(E_f) = \Gamma / [(E_f - E_f)^2 + \Gamma^2/4]. \quad (30)$$

When the energy mismatch is much less than Γ the calculations are insensitive to the degree of broadening (Γ). This is the limit in which we are working. Now

$$k = (2\pi/\hbar) \sum_{i,f} B_i |\langle \Psi_i | H' | \Psi_f \rangle|^2 \times \Gamma / [(E_i - E_f)^2 + \Gamma^2/4]. \quad (31)$$

The exact matrix elements in Eq. (31) will be found for the exact eigenfunctions. The matrix elements between the BO states will be found using the FC separation. Finally, the matrix elements between the crude adiabatic wave functions will be calculated. The multiplicative constants (μ_R and normalization constants) which should appear in the matrix elements are omitted. In all cases zero temperature is assumed. Generalizations to higher temperatures are simple but need not be considered at this time.

1. Exact wave functions

The initial and final states are

$$\Psi_i = \left[N_L \sum_j g_j \chi_j^L(x) \phi_j^L(y^L) \right] \times [\phi_0^R(y^R)], \quad (32)$$

$$\chi_j^L(x) = \exp(-\kappa_j |x|),$$

$$\Psi_{f_k} = [\phi_{k'}^L(y^L)] \times \left[N_R \sum_k h_k \chi_k^R(x - R_{ab}) \phi_k^R(y^R) \right]. \quad (33)$$

The g 's (h 's) are the mixing constants for the donor (acceptor). For allowed k' (energy "conserving"):

$$\langle \Psi_i | H' | \Psi_{f_k} \rangle_{x, y_R, y_L} \propto \sum_k g_k^0 \exp(-\kappa_k^L R) \times \sum_k h_k^0. \quad (34)$$

The upper index on g (h) is the quantum number of the coupled initial (final) state. The lower index on g (h) identifies the term's origin in the wave function expansion. This index on g is the number of vibrational quanta left on the electron donor after the transfer event. $i \approx \Delta E / \hbar\omega - k'$ (assuming $\hbar\omega_L = \hbar\omega_R$). Since zero temperature was assumed only one initial state contributes to the sum. All final states, however, must be included in Eq. (34). Some of the experiments which will ultimately be analyzed were performed at low temperature so these matrix elements are indeed useful. Approximate values for the g 's and h 's are found in the Appendix, but they are also readily found numerically. The rate decays with distance as the square of a linear combination of terms each proportional to $\exp(-\kappa_n R_{ab})$ where

$$\kappa_n^2 = [\text{const.} + (n + 1/2)\hbar\omega] (2m_e/\hbar^2). \quad (35)$$

n is the number of vibrations left on the donor after transfer. Terms in the sum which correspond to leaving few vibrational quanta on the donor are exponentially emphasized in long distance transfers. At short transfer distances all terms in the matrix element sum contribute to the rate. This suggests that $k(R)$, the distance dependent rate of electron transfer, does not decay in a simple exponential manner. If one could study nonadiabatic electron transfer in the same class of molecules over a range of distances one would expect a rapid falloff of the rate with distance at short distance and a somewhat slower drop of rate with distance at longer distance. Decay of rate with distance should become exponential with distance at large distance as only a single exponential dominates the sum. It is sometimes useful to formulate electron transfer theory in terms of spectral functions for electron removal and insertion.²⁴ In this case the spectral functions for electron removal are transfer distance dependent and become narrower as the transfer distance increases (see Fig. 1).

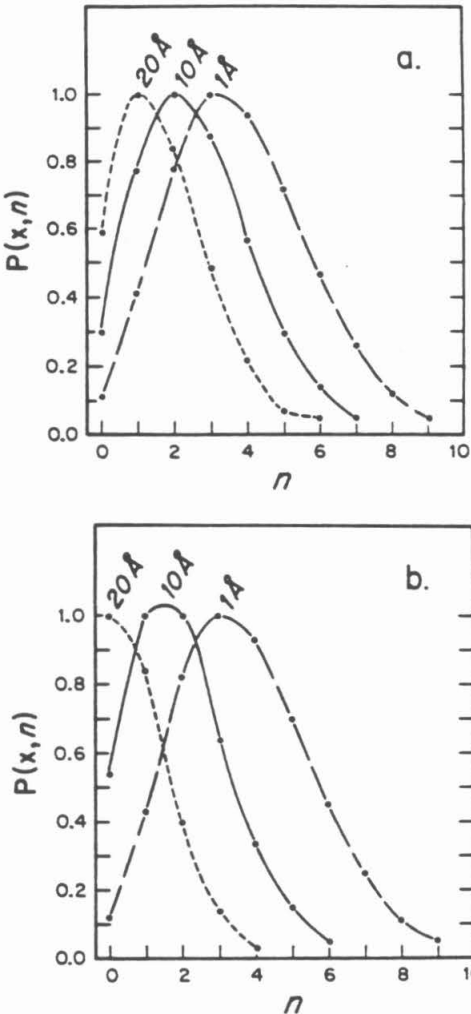


FIG. 1. Probability of finding electrons at x Å and the nuclei in the n th vibrational state of the ion. $P(x, n) = \exp(-2\kappa_n |x|) \exp(-x|x|/n!)$. (a) Energy = -5.0 eV (E_{Total}), coupling energy = 0.8 eV [$|m, \lambda, \mu/\hbar^2|^2/\hbar\omega$], and $\hbar\omega = 0.2$ eV. The probability values are not normalized but the curves are scaled by factors of $1, 1.8 \times 10^9$, and 2.5×10^{19} for the electron fixed at $1, 10$, and 20 Å, respectively. (b) Energy = -1.5 eV, other parameters the same as (a). Since the states are closer to the continuum ($E = 0$) the electronic effects are more important. The tendency to leave fewer vibrations behind is stronger here than in (a) despite the equally unfavorable $\exp(-x|x|/n!)$ factor. The curves are scaled by factors of $1, 4.0 \times 10^5$, and 2.3×10^{11} .

2. BO wave functions

The BO donor states show slower decay of electronic amplitude with distance when the donor bond is stretched (ion like), but the propagation incorrectly increases without bound as y increases. This result conflicts with the exact model. The failure of the BO model is not surprising in light of the notion that neutral and ionic potential surfaces (BO surfaces) for the same molecular skeleton should be calculated independently. The natural approximation for simplifying

ing matrix elements between separable wave functions, the FC approximation, will be used. The perturbing matrix element is simplified by choosing a constant nuclear position in $\psi^e(x, y)$ before integrating over electronic and nuclear coordinates. A single value for y must be chosen for substitution in the electronic wave function [Eq. (21)]. The choice of this parameter is not obvious but a first guess might be the value of y at the crossing point of the nuclear potential energy surfaces (e.g., $-y_0/2$ for thermoneutral reactions).³ Calling this point \bar{y} :

$$H_f \propto \langle \psi_L^e(x; \bar{y}_L) | \delta(x - R_{ab}) | \psi_R^e(x; \bar{y}_R) \rangle \langle \Phi_L \Phi_R | \phi_L \Phi_R \rangle, \quad (36)$$

The Φ refer to shifted oscillators and the ϕ to unshifted oscillators. The BO-FC matrix element is of the form

$$\exp(-\text{const.} \times R_{ab}) \times \exp(\bar{y}_L \times R_{ab}) / |\text{FC}_L| |\text{FC}_R|. \quad (37)$$

There is now no special contribution to the matrix element related to the fact that the acceptor site nuclear and electronic motions were coupled except through the somewhat arbitrary and incorrectly signed (for large nuclear displacement) \bar{y}_L . The rate decays exponentially with donor-acceptor separation for any given \bar{y}_L .

3. Product wave functions

The crude adiabatic wave function for the donor is $\psi_n^{\text{donor}}(x, y) = \psi^e(x, y_0) \phi_n(y)$. Exact matrix elements of the perturbing operator have the same functional form as those in the BO-FC treatment of the coupled problem when $\bar{y}_L = y_0$ [Eq. (37)]. The matrix element is exactly separable into nuclear and electronic parts. The electronic part decays exponentially with distance. The nuclear part of the donor wave function is a harmonic oscillator eigenstate. In this approximation the three curves in Fig. 1(a) or 1(b) superimpose.

IV. DISCUSSION

The quality of a bound state wave function is usually judged by comparing its calculated energy to an experimental energy or reference calculation. Long distance electron transfer occurs between bound states but the molecular interactions which promote electron exchange occur between the minuscule wave function "tails". For this reason wave functions which produce quite acceptable eigenvalues must be carefully considered before use in an electron transfer rate calculation. One also makes assumptions about the relative time scales of motions (e.g., the FC approximation) based on intuition gained from bound state problems or optical processes. The answer to the question "How far can an electron stray before the nuclei react to the fact that the molecule is becoming an ion?" is not obvious without fully examining the range of coupling parameters which determine the long distance wave function behavior. The transfer distance and the nature of the coupling determine which motions (electronic or nuclear) should be treated as slow. If the nuclei really adjust their displacements on the time scale of the electron transfer it is conceivable that some electron transfers may be nonadiabatic in the electronic rather than the nuclear motion. Sethna has addressed related solid state tun-

neling problems in a general manner and also suggests such a distance-time regime.²⁵

Sarai and DeVault studied the breakdown of the BO approximation by calculating the size of "nonadiabatic" matrix elements between donors and acceptors in a simple model.⁸ They evaluated matrix elements of the operator

$$H^{n,a} = \sum_k (-\hbar^2/2M_k) \langle \psi_L^e | \partial/\partial Y_k | \psi_R^e \rangle \partial/\partial Y_k, \quad (38)$$

where k sums over the normal modes of the molecule.²⁶ This is the larger of the two nonadiabatic operators. They compared the matrix elements of this operator with the electronic tunneling matrix elements. The nonadiabatic matrix elements are much smaller than the electronic tunneling matrix elements. One should not misinterpret this result to mean that the BO approximation is adequate. This technique does not probe the error in the functional forms of the BO wave functions.

If one had to rank the danger of the BO and FC approximations when applied to a Golden Rule formulation of electron transfer theory one should put the BO approximation at the top of the list because of its incorrect functional form at large electronic distance. Within the BO framework the FC approximation improves with transfer distance based on the work of Lee and DePristo. But ironically, as one approximation improves the other fails.

The probability of simultaneously finding an electron at $|x|$ and the donor nuclei in the (ion) vibrational state n illustrates the nature of the true wave functions. Figure 1 shows the dependence of this distribution on electronic position. An understanding of the quantitative importance of such shifts with distance—absent in elementary theories—must come from a model in which the choice of parameters can be more directly related to experiments. Although more complete models will be dealt with elsewhere,⁵ we draw five conclusions from this model study:

(1) BO wave functions are *not* necessarily reliable eigenstates to use should *ab initio* quantum chemical methods ever become practical for *long distance* electron transport calculations.²⁷

(2) At *different* distances the dependence of rate on donor-acceptor energy difference may not be identical.

(3) *Competition* between the ability of a molecule to have a favorable nuclear overlap factor (FC factor in conventional theory) and a favorable tunneling matrix element may distort the predicted dependence of rate on donor-acceptor energy difference. The sensitivity of the rate to these effects will be determined by the position of the donor and acceptor redox levels in the "band gap".¹⁹

(4) Nonexponential decay of rate with distance may occur.

(5) The energy of the optical charge transfer band should decrease at very large donor-acceptor distance if the spectral functions for electron removal (or insertion) are distance dependent.¹⁸

ACKNOWLEDGMENT

This research was supported in part by NSF Grant No. DMR-8107494.

APPENDIX: APPROXIMATION OF g_n

A Poisson distributed variable x has the probability distribution

$$P_n^2(x) = \exp(-x)x^n/n!, \quad (\text{A1})$$

where P_n is the probability amplitude. By substituting $n+1$ or $n-1$ for n in this formula and separating the P_n part we find

$$P_{n+1} = P_n \sqrt{x/(n+1)}, \quad (\text{A2})$$

$$P_{n-1} = P_n \sqrt{n/x}. \quad (\text{A3})$$

Multiplying both sides of Eq. (A3) by $\sqrt{n/(n+1)}$ and adding the corresponding sides with Eq. (A2) we find

$$P_{n+1} = -\sqrt{n/(n+1)}P_{n-1} + (\sqrt{x} + n/\sqrt{x})P_n(1/\sqrt{n+1}). \quad (\text{A4})$$

Equation (15) in atomic units ($\hbar = m_e = 1$) is

$$g_{n+1} = -[1/(\lambda \sqrt{n+1})](\kappa_n - \mu)g_n - \sqrt{n/(n+1)}g_{n-1},$$

$$\kappa_n = \sqrt{2[-E^{\text{Total}} + (n+1/2)\hbar\omega]}. \quad (\text{A5})$$

For the ground state

$$\kappa_n \approx \sqrt{\mu^2 + 2n\hbar\omega + 2\mu^2\lambda^2/\hbar\omega}, \quad (\text{A6})$$

where E^{Total} was approximated by Eq. (29). Consider the coefficient of g_n (F):

$$F = -(1/\lambda)[1/\sqrt{(n+1)}](\sqrt{\mu^2 + 2n\hbar\omega + 2\mu^2\lambda^2/\hbar\omega} - \mu). \quad (\text{A7})$$

Compared to the "electronic" energy (μ^2), $n\hbar\omega$ and $\mu^2\lambda^2/\hbar\omega$ are small. Expanding the radical to first order about $2n\hbar\omega + 2\mu^2\lambda^2/\hbar\omega$:

$$F \approx (-1/\sqrt{n+1})[n\hbar\omega/(\mu\lambda) + \mu\lambda/\hbar\omega]. \quad (\text{A8})$$

Thus, if $\sqrt{x} = \mu\lambda/\hbar\omega$, Eq. (A5) becomes

$$g_{n+1} = -(1/\sqrt{n+1})g_n(\sqrt{x} + n/\sqrt{x}) - \sqrt{n/(n+1)}g_{n-1}. \quad (\text{A9})$$

The sign of λ is arbitrary. Any sign causes an energy stabilization of $\lambda^2\mu^2/\hbar\omega$ so we may also write

$$g_{n+1} = (1/\sqrt{n+1})g_n(\sqrt{x} + n/\sqrt{x}) - \sqrt{n/(n+1)}g_{n-1}. \quad (\text{A10})$$

This is exactly Eq. (A4) with $x = (\mu\lambda/\hbar\omega)^2 = E_c/\hbar\omega$, where

E_c is the coupling energy. This is also the form that x takes in the simple Franck-Condon factor [Eq. (A1)] for transitions from the $n = 0$ unshifted vibrational state to the n' shifted state.¹⁶ There is, therefore, a direct correspondence (to first order) between the mixing constants of the ground state coupled wave function and the Poisson factors.

¹Tunneling in Biological Systems, edited by B. Chance, D. C. DeVault, H. Frauenfelder, R. A. Marcus, J. R. Schrieffer, and N. Sutin (Academic, New York, 1979).

²R. A. Marcus, in *Oxidases and Related Redox Systems*, edited by T. E. King, H. S. Mason, and M. Morrison (Pergamon, New York, 1982), p. 3.

³D. DeVault, *Q. Rev. Biophys.* **18**, 311 (1980).

⁴(a) J. J. Hopfield, in *Oxidases and Related Redox Systems*, edited by T. E. King, H. S. Mason, and M. Morrison (Pergamon, New York, 1982), p. 35.

⁵(b) For an interesting nonbiological example of relevance see, J. V. Beitz and J. R. Miller, *J. Chem. Phys.* **71**, 4579 (1979).

⁶D. N. Beratan and J. J. Hopfield (in preparation).

⁷J. Jortner, *Biochim. Biophys. Acta* **594**, 193 (1980).

⁸J. J. Hopfield, in *Tunneling in Biological Systems*, edited by B. Chance, D. C. DeVault, H. Frauenfelder, R. A. Marcus, J. R. Schrieffer, and N. Sutin (Academic, New York, 1979), p. 431.

⁹D. DeVault and A. Sarai, *Biophys. J.* **41**, 324 (abstract) (1983).

¹⁰P. Day, *Int. Rev. Phys. Chem.* **1**, 149 (1981).

¹¹C.-Y. Lee and A. E. DePristo, *J. Am. Chem. Soc.* **105**, 6775 (1983).

¹²W. Kolos and L. Wolniewicz, *Rev. Mod. Phys.* **35**, 473 (1963).

¹³M. A. Ratner and A. Madhukar, *Chem. Phys.* **30**, 201 (1978); J. Lindberg and M. A. Ratner, *J. Am. Chem. Soc.* **103**, 3265 (1981).

¹⁴R. Friesner and R. Silbey, *J. Chem. Phys.* **74**, 1166 (1981); **75**, 3925 (1981).

¹⁵Coupling to "intermolecular modes" is also of some interest; J. N. Onuchic (private communication).

¹⁶A. A. Frost, *J. Chem. Phys.* **25**, 1150 (1956).

¹⁷P. Siders and R. A. Marcus, *J. Am. Chem. Soc.* **103**, 741 (1981).

¹⁸There is a \sqrt{E} dependence in the decay constant. The exact form of this energy dependence is model dependent.

¹⁹M. Redi and J. J. Hopfield, *J. Chem. Phys.* **72**, 6651 (1980).

²⁰D. N. Beratan and J. J. Hopfield, *J. Am. Chem. Soc.* **106**, 1584 (1984).

²¹P. Siders, Thesis, California Institute of Technology, 1983.

²²P. Siders, R. J. Cave, and R. A. Marcus, *J. Chem. Phys.* (in press).

²³M. Bixon and J. Jortner, *Faraday Discuss. Chem. Soc.* **74**, 17 (1982).

²⁴L. N. Grigorov and D. S. Chernavskii, *Biophysics* **17**, 202 (1972).

²⁵J. J. Hopfield, *Proc. Natl. Acad. Sci. U.S.A.* **71**, 3640 (1974).

²⁶J. P. Sethna, *Phys. Rev. B* **24**, 698 (1981).

²⁷(a) C. J. Ballhausen, *Molecular Electronic Structures of Transition Metal Complexes* (McGraw-Hill, New York, 1979), p. 8. (b) M. Born and K. Huang, *Dynamical Theory of Crystal Lattices* (Oxford, New York, 1956), see the Appendices.

²⁸M. D. Newton, *Int. J. Quantum Chem. Quantum Chem. Symp.* **14**, 363 (1980).

We have shown that at particularly large transfer distances changes in the distance and ΔG dependence of the electron transfer rate may occur. The parameters used in the previous paper were chosen roughly to correspond to the experimental data of Miller, Beitz and Huddleston [4]. Quantitative predictions and interpretations of experiment come more readily from a more "molecular" model. The preliminary results from such a model are presented in the next section.

IV.C. Correctly Coupled Wave Functions in Bridged Systems

Abstract

The probability of finding a *bound* electron far from the nuclei which bind it is correlated with the motion of the nuclei. This coupling is improperly treated in the Born-Oppenheimer/Franck-Condon approach to the electron transfer problem [1]. Electron propagation through a model molecular linker is studied without decoupling electronic and nuclear motion. The correctly coupled donor wave function correlates the equilibrium internuclear geometry of a bond (or normal mode) with the electronic position. Non-exponential dependence of the rate on distance and deviations from the "inverted" dependence of rate on exothermicity may occur. Radiolysis initiated electron transfers in glasses show unusual ΔG and distance dependences. These reactions are candidates for quantitative analysis with this method.

Introduction

The calculation of electron transfer rates between reactants at a given distance is rather involved and many assumptions are invariably made [2]. Some approximations can be tested theoretically. One fundamental approximation, that the nuclear and electronic motion is separable, has not been adequately investigated. In fact, it has been suggested that the Born-Oppenheimer approximation may be inappropriate when calculating rates of long distance electron transfer reactions [3]. In a previous paper the analytically correct form of the long distance wave function "tail" was presented and contrasted to the Born-Oppenheimer result. The classical, semi-classical, and quantum mechanical electron transfer theories were developed assuming separability of nuclear and electronic motion [2]. This section extends the study of wave functions with analytically correct

long distance behavior to more relevant models with accessible parameters. A qualitatively different dependence of the rate on exothermicity and distance is found when the donor and acceptor energies are in critical ranges. This unusual behavior may appear in some recent experiments [4,5,6]. In particular, some results of Miller, Beitz, and Huddleston [4] may be explained with the model.

The aim of this chapter is to show that the previous correctly coupled vibronic model wave function may be extended using methods developed to study bridge mediated electron transfer. The model includes bridging groups in an explicit way and can be compared more directly with experiments. The parameters are available from the experiments: ΔE (the exothermicity), $\hbar\omega$ (the energy of the mode coupled to the transfer), λ (the reorganization energy), and β (the exchange interaction discussed in Chapter II). No new constants are necessary.

Theoretical Section

The "golden rule" for transitions between initial state (i) and final state (f) gives

$$k = (2\pi/\hbar) \sum_{i,f} | \langle i | H' | f \rangle |^2 \rho_f(E_i) B_i. \quad (IV.2)$$

k is the unimolecular electron transfer rate between the donor and acceptor at a single fixed geometry and distance. B_i is the thermal distribution of initial states. ρ_f is the density of acceptor states. The Hamiltonians for the donor, acceptor and bridge are adapted from Refs. 1, 7, and 8. As before, donor and acceptor are treated as small polarons. A single effective orbital is placed on each of these traps [7]. A periodic one orbital per bridging group Hamiltonian is

used for the intervening medium.

$$H_L = \hbar\omega_L(b_L^\dagger b_L + 1/2) + \lambda_L(b_L^\dagger + b_L)a_L^\dagger a_L + \alpha_L a_L^\dagger a_L \quad (IV.3)$$

$$H_R = \hbar\omega_R(b_R^\dagger b_R + 1/2) + \lambda_R(b_R^\dagger + b_R)a_R^\dagger a_R + \alpha_R a_R^\dagger a_R \quad (IV.4)$$

$$H_{bridge} = \alpha \sum_i a_i^\dagger a_i + (\beta/2) \sum_i (a_{i+1}^\dagger a_i + a_{i-1}^\dagger a_i) \quad (IV.5)$$

The a's are fermion operators and the b's are boson operators. All bridge orbitals are identical and interact only with nearest neighbors. i sums over a large number of sites which continue (in one dimension) to the left and right of both traps. The unperturbed bridging states span the energy range from 2β to -2β . The small polaron electron trapping sites are adjacent to sites 0 and N of the chain. The interactions between the trapping "molecules" and the bridge are described by the Hamiltonians:

$$H'_L = \beta_L(a_L^\dagger a_0 + a_0^\dagger a_L) \quad (IV.6)$$

$$H'_R = \beta_R(a_R^\dagger a_N + a_N^\dagger a_R). \quad (IV.7)$$

The vibronic interaction is turned on to the extent that the electron occupies the donor or acceptor molecular orbital. The Hamiltonians for the initial and final states are

$$H_{init} = H_L + H_R + H'_L + H_{bridge} \quad (IV.8)$$

and

$$H_{final} = H_L + H_R + H'_R + H_{bridge}. \quad (IV.9)$$

Fig. IV.1 shows the arrangement of groups and the interactions. The exact initial (donor) wave function is $\phi_R \Psi_L$ where

$$\Psi_L = \sum_i g_i \chi_i^{el}(x) \Phi_i^L(y_L). \quad (IV.10)$$



Figure IV.1. Arrangement of the donor, acceptor, and bridging orbitals.

g_i is a mixing constant, $\chi_i(x)$ is a function of the electronic position, $\Phi_i^L(y_L)$ is a function of donor nuclear coordinate, and $\phi_R(y_R)$ is the acceptor initial vibrational state. Each set of functions in Eq. IV.10 is complete, although the electronic functions are not orthogonal [1]. The basis functions are to be determined.

Two Schrödinger equations must now be solved in order to calculate a rate:

$$(H_{init} - H_R)\Psi_L = H_D\Psi_L = E_D\Psi_L \quad (IV.11)$$

and

$$(H_{final} - H_L)\Psi_R = H_A\Psi_R = E_A\Psi_R. \quad (IV.12)$$

Ψ_L and Ψ_R are correctly coupled donor or acceptor wave functions. ϕ_L and ϕ_R are the vibrational wave functions corresponding to the site without the transferable electron and are considered independently because the variables are separable. In each case there is nearly unit probability of finding the electron on the polaron site (L or R) and small but non-zero probability of finding it on the bridge. The probability of finding it on the other trap is zero since only H'_L (or H'_R) is included in the Hamiltonian for the localized state. It is convenient to write the donor Hamiltonian in terms of delocalized Bloch states rather than localized (Wannier) orbitals [8]. Defining

$$A_k = \frac{1}{\sqrt{N}} \sum_n e^{ikna} a_n \quad (IV.13)$$

$$a_n = \frac{1}{\sqrt{N}} \sum_k e^{-ikna} A_k \quad (IV.14)$$

the initial Hamiltonian is rewritten as

$$H_D = H_L + \sum_k [e_k A_k^\dagger A_k + V_L(k) a_L^\dagger A_k + V_L^*(k) A_k^\dagger a_L] \quad (IV.15)$$

where

$$V_L(k) = \frac{\beta_L}{\sqrt{N}} e^{-ikN_0 a}. \quad (IV.16)$$

This transformation is equivalent to changing the basis functions on the chain from the atomic orbitals to the delocalized Bloch wave functions. Capital A's denote operators for delocalized orbitals and lower case a's denote operators for local orbitals. N_0 is the number of the bridge orbital with which the *donor* interacts and was set equal to zero. Assuming cyclic boundary conditions on the chain the eigenvalues of H^{bridge} are

$$e_k = \alpha + 2\beta \cos\left(\frac{2\pi k}{P}\right) \quad (IV.17)$$

where there is a total of P orbitals in the bridge. α establishes an energy reference point in the center of the band of bridge states and is set equal to zero. The nuclear wave function basis set can be chosen as harmonic oscillator eigenstates [1]. Multiplying the Schrödinger equation for the initial state by $\Phi_j^*(y_L) \Upsilon_k^{Bloch*}(\vec{x})$ and integrating over the nuclear and electronic coordinates one finds the donor electronic states

$$\chi_i = u_{trap}^{(i)} \Upsilon_L(\vec{x}) + \sum_k u_k^{(i)} \Upsilon_k^{Bloch}(\vec{x}). \quad (IV.18)$$

$\Upsilon_L(\vec{x})$ is the unperturbed donor orbital, and $\Upsilon_k^{Bloch}(\vec{x})$ are the delocalized chain orbitals. \vec{x} is the electronic coordinate and i corresponds to a particular vibrational state in Eq. IV.10. Multiplication of the donor state Schrödinger equation by $\Phi_m^*(y_L)$ and integration over the nuclear coordinate gives

$$\begin{aligned} & \lambda_L a_L^\dagger a_L (g_{m-1} \sqrt{m} \chi_{m-1} + g_{m+1} \sqrt{m+1} \chi_{m+1}) \\ & + g_m \alpha_L a_L^\dagger a_L \chi_m + g_m \sum_k \left[e_k A_k^\dagger A_k + V_L(k) a_L^\dagger A_k + V_L^*(k) A_k^\dagger a_L \right] \chi_m \end{aligned}$$

$$= g_m \chi_m [E^{total} - (m + 1/2)\hbar\omega]. \quad (IV.19)$$

This equation when multiplied by $\Upsilon_k^*(\vec{x})$ and integrated over the electronic coordinate gives the ratio between mixing constants

$$\frac{u_{trap}^{(m)}}{u_k^{(m)}} = \frac{(E_m - e_k)}{V_L^*(k)} \quad (IV.20)$$

where $E_m = E_D^{total} - (m + 1/2)\hbar\omega$. Multiplying Eq. IV.19 by Υ_L^* , integrating over the electronic coordinate, using Eq. IV.20, and the defining $h_j = g_j u_{trap}^{(j)}$ gives the recursion relation

$$h_j [\alpha_L - \frac{\beta_L^2}{N} \sum_k \frac{1}{e_k - E_j} - E_j] + \lambda_L (h_{j+1} \sqrt{j+1} + h_{j-1} \sqrt{j}) = 0. \quad (IV.21)$$

The initial wave function (not normalized) is

$$\Psi_L(x, y_L) = \sum_m h_m [\Upsilon_L(\vec{x}) + \sum_k (\frac{V_L^*(k) \Upsilon_k^{Bloch}(\vec{x})}{E_m - e_k})] \Phi_m^{nuc}. \quad (IV.22)$$

Passing to the long chain limit the sum on k in Eq. IV.21 becomes

$$\frac{-\beta_L^2}{\sqrt{E_j^2 - 4\beta^2}}. \quad (IV.23)$$

Using the Wannier (localized) basis the wave function in the long chain limit is

$$\Psi_L(x, y_L) = \sum_m \left\{ h_m \Phi_m^{nuc} [\Upsilon_L(\vec{x}) + \frac{\beta_L}{\sqrt{E_m^2 - 4\beta^2}} \sum_n \epsilon_m^n \theta_n(\vec{x} - n\vec{a})] \right\}. \quad (IV.24)$$

$\theta_n(\vec{x} - n\vec{a})$ is the localized orbital at the n^{th} bridge site and

$$\epsilon_m = \frac{E_m}{2\beta} \pm \sqrt{(\frac{E_m}{2\beta})^2 - 1}; \quad |\epsilon| < 1. \quad (IV.25)$$

The wave function decays by the factor ϵ_m per linker unit and the decay depends explicitly upon m , the number of vibrations left in the donor “bond.” This form for the electronic decay is analogous to that found by McConnell [9] or Davydov [8] except that the wave function amplitude far from the donor is coupled to the vibrational state of the donor. For small ϵ_m , $\epsilon_m \simeq \beta/E_m$. For given m the electronic amplitude propagating along the chain decreases by the factor ϵ_m every repeating unit. This result is qualitatively similar to the result obtained with the coupled isolated Dirac delta function potential well. The wave function decay length here has a logarithmic rather than square root dependence on E_m . This is the expected difference for electron propagation through a periodic (spatially varying) potential [7].

Fig. IV.2 shows the $E_m - \epsilon_m$ relationship for several values of β . The wave function and recursion relation are the analogues of Eqs. 15 and 16 of Ref. 1. To the extent that the electron density on the donor is approximately unity in the initial state and $|\beta_L| \ll \sqrt{E_j^2 - 4\beta^2}$ the h_j ’s are Poisson-distributed in the ground state coupled wave function [1]. The normalization constant for the wave function is approximately $1/\sqrt{(\sum_m h_m^2)}$. Using the appropriate parameters for the acceptor, the coupled final state may also be found.

The Perturbing Hamiltonian

The initial and final states correspond to a well-localized electron slightly delocalized onto a very long chain of orbitals. The part of the total Hamiltonian which was neglected in writing the initial state Hamiltonian and which allows electron transfer is

$$H' = \beta_R (a_N^\dagger a_R + a_R^\dagger a_N). \quad (IV.26)$$

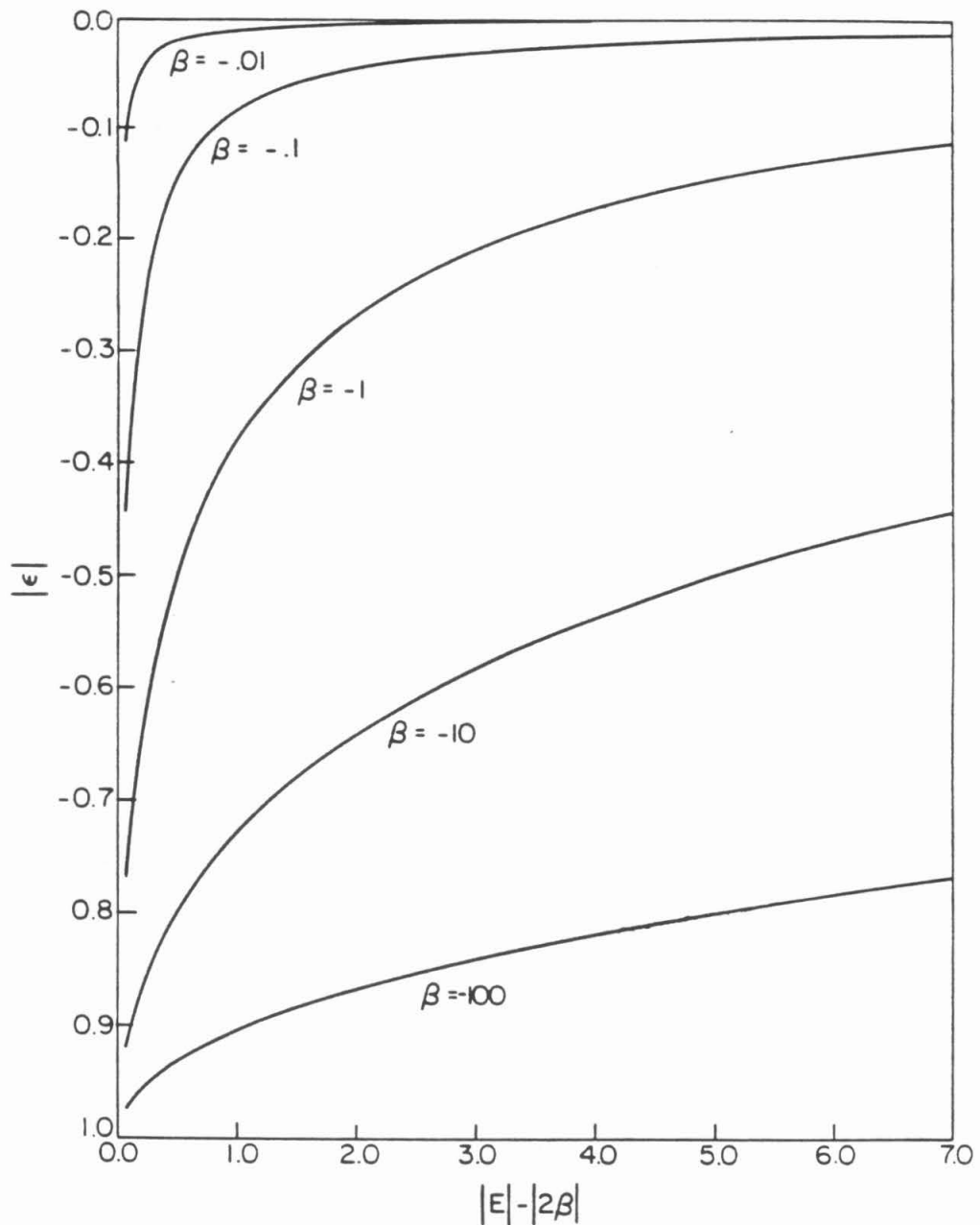


Figure IV.2. Dependence of ϵ on E as a function of distance from the band edge (at $\pm 2\beta$).

There is no electronic amplitude on the acceptor in the initial state. The final state decays from the acceptor orbital as ϵ_m^{N-n} where n is the bridge orbital number and N is the total number of bridging units between the donor and acceptor. In general, the electronic energy (α_L), polaron coupling energy ($\lambda^2/\hbar\omega$), and vibrational energy ($\hbar\omega$) need not be identical for the donor and acceptor. Because the acceptor-chain interaction is small, most of the final state amplitude is on the acceptor. Therefore, the operator $\beta_R a_R^\dagger a_N$ dominates the H' matrix element in Eq. 1.

Low Temperature Limit

Some unusual effects are predicted with this model and can be demonstrated by considering the low temperature limit of the rate. This temperature limit is also of experimental interest. At low temperature only the ground initial state is populated and the mixing constants h_j^2 are approximately Poisson-distributed in $\gamma = E_{reorg}/\hbar\omega = (\lambda_L/\hbar\omega)^2$. The acceptor oscillator is also initially in its ground vibrational state. Considering only terms which introduce rate changes with distance and exothermicity

$$k \propto \sum_f | \langle \Psi_i | H' | \Psi_f \rangle |^2 \quad (IV.27)$$

$$\begin{aligned} \Psi_i &= \Psi_L(x, y_L) \phi_{ground}^{nuc}(y_R) \\ \Psi_{f_j} &= \phi_j^{nuc}(y_L) \Psi_R^{M-j}(x, y_R) \\ \langle \Psi_i | H' | \Psi_f \rangle &\propto \sum_j |b_j \epsilon_j^N \left(\frac{e^{-\gamma/2} \gamma^{j/2}}{j!^{1/2}} \right) \left(\frac{e^{-\gamma/2} \gamma^{(M-j)/2}}{(M-j)!^{1/2}} \right)|^2 \end{aligned} \quad (IV.28)$$

$$\ln k = M \ln \gamma + \ln \sum_{j=0}^M \left[\frac{b_j^2 \epsilon_j^{2N}}{j! (M-j)!} \right] + const.(\beta_L, \beta_R, \gamma, \beta, \rho) \quad (IV.29)$$

where

$$b_j = 1/\sqrt{E_j^2 - 4\beta^2}.$$

ϵ_j is defined in Eq. IV.25. For convenience the case of $\lambda_L = \lambda_R$ and $\hbar\omega_L = \hbar\omega_R$ was studied. $N + 1$ is the number of units of the chain between donor and acceptor, $M = \Delta E/\hbar\omega$, and j is the number of vibrational quanta left on the donor after transfer. In the Born-Oppenheimer/Franck-Condon treatment a single ϵ enters the sum. The Franck-Condon-like term in the sum is a maximum for a single value of ΔE but ϵ_j is modulated by the vibrational coupling. In the Born-Oppenheimer/Franck-Condon treatments this ϵ *independent* sum gives the energy gap law dependence of rate on ΔE . However, in Eq. IV.29 the sum couples the distance and energetic dependence of the rate. One can anticipate long distance transfers where N is so large that ϵ_j^{2N} is negligible except for a limited number of j 's. Although the Franck-Condon-like term may be unfavorable at that value of j , competition between the factors may yield a qualitatively different $\ln k$ - ΔE relations at different transfer distances.

Previous studies of bridge mediated electron transport suggested that electron propagation along the bridge depends critically on the relative energies of the bridge and trap orbitals [7,8,9]. The donor energy may be close to the linker HOMO (hole transfer) or LUMO (electron transfer) energy of the unperturbed bridge. In either case there is a strong dependence of ϵ_j on the energy difference between the trap orbitals and the energetically closest bridging orbitals. Alternatively, the traps may be in the center of the HOMO-LUMO gap. In this case ϵ_j is a slowly varying function of the trap energies (see Fig. IV.2, large $|E_j| - 2|\beta|$). In the former case large qualitative changes from the Born-Oppenheimer/Franck-Condon results occur in the $\Delta G - \ln k$ relation at a fixed transfer distance.

However, the energies of typical biological and other organometallic redox centers apparently lie in the region near the band where ϵ is quite sensitive to E . $\ln k$ can also have a non-exponential distance dependence due to the sum of exponential terms in the rate expression.

The variation in experimentally accessible coupling energies, vibrational frequencies, and donor-acceptor energy positions is quite large although the actual number of experiments studying electron transfer over both a range of distances and ΔG 's is quite limited. Many common electron transport active metal ions are energetically close to common hydrocarbon HOMO's. This suggests "hole" transport as the dominant charge mediation mechanism. The redox potentials of many organic species [4,5] also suggest that this mechanism may dominate. In the current model only one orbital was placed on each linker site. This means only one "band" of electronic states exists for the isolated linker.

As a concrete example consider electron transfer through saturated n-alkane [e.g., see Ref. 10]. The mixing of the orbital on a redox site with bridging states depends on $|E| - 2|\beta|$, the energy of the trap relative to the band edge (Fig.IV.2). Fig. IV.3 compares the energy dependence of ϵ in this one orbital model with the energy dependence of ϵ in a more complete model for n-alkane (Ref. 8, Figs. 4b, 5b). β in the one orbital per site model was chosen so that the curves coincide at the minimum ϵ for the alkane. Inclusion of only one band in this model makes it impossible to precisely model n-alkane chains both near and far from the band of bridge states. Qualitatively, however, the representation is quite adequate. The curve is fit with $\beta = -1.6\text{eV}$. $\hbar\omega$ and λ are taken from the radiolysis experiments [4].

The sum in Eq. IV.28 includes contributions of decay constants between

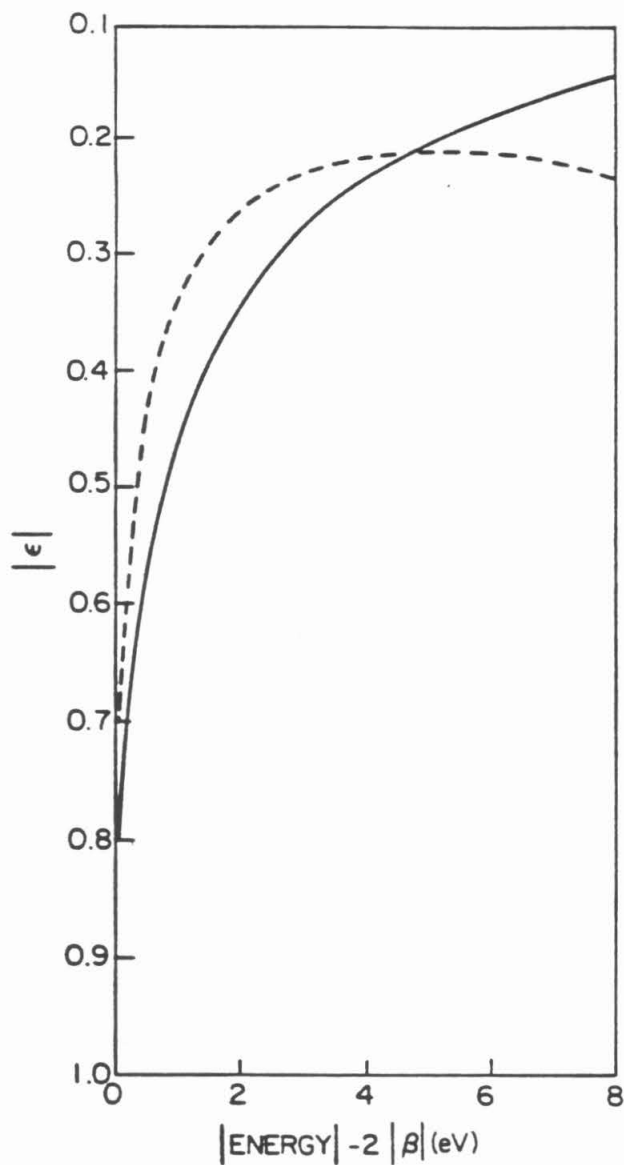


Figure IV.3. Dashed line: dependence of ϵ on E for n-alkane (Fig. 5b, Ref. 7).
 Solid line: one orbital per site model with $\beta = -1.6 \text{ eV}$ chosen to coincide with the alkane model at the band center.

$\epsilon(E^{donor})$ and $\epsilon(E^{acceptor})$. Fig. IV.4 shows the $\ln k$ dependence on N for different ΔE 's when the traps are near the band. Calculations for different ΔE 's correspond to moving the acceptor energy closer to the band at fixed donor energy. Fig. IV.5 shows similar calculations when the traps are further from the band. At short distance the ϵ_j^{2N} term does not cause any single element in the sum of Eq. IV.29 to dominate so the decay of rate with distance is not purely exponential. However, as the transfer distance becomes very large only terms in the sum with largest $|\epsilon_j|$ contribute to the rate and the decay again becomes exponential with distance. Far from the band edge, ϵ varies slowly with j and the rate decays exponentially with distance in all distance ranges.

The other qualitatively unusual behavior of the rate arises from the intrinsic coupling of the electronic decay (ϵ_j) with the energetic dependence of the rate, $e^{-2\gamma\gamma\Delta E/\hbar\omega}/[j!(\Delta E/\hbar\omega - j)!]$. In the old theory, since ϵ is j independent the change of rate with ΔE is determined solely by this nuclear overlap term. In the correctly coupled solution the smallness of ϵ_j^{2N} for particular values of j may strongly skew the $k-\Delta E$ relation from the distance independent, inverted form predicted by the standard classical, semiclassical, and quantum formulations of non-adiabatic electron transfer theory. The strong dependence of ϵ_j on E near the band edge makes transfers between donors and acceptors in this energetic region especially sensitive to non-Born-Oppenheimer effects. Calculations of the dependence of rate on ΔE are shown in Figs. IV.6a and IV.6b for donors and acceptors in different energetic regions and at different transfer distances. The shapes and locations of the peaks of the curves are distance and band donor energy dependent.

Examples of redox centers at fixed distance bound to hydrocarbon linkers

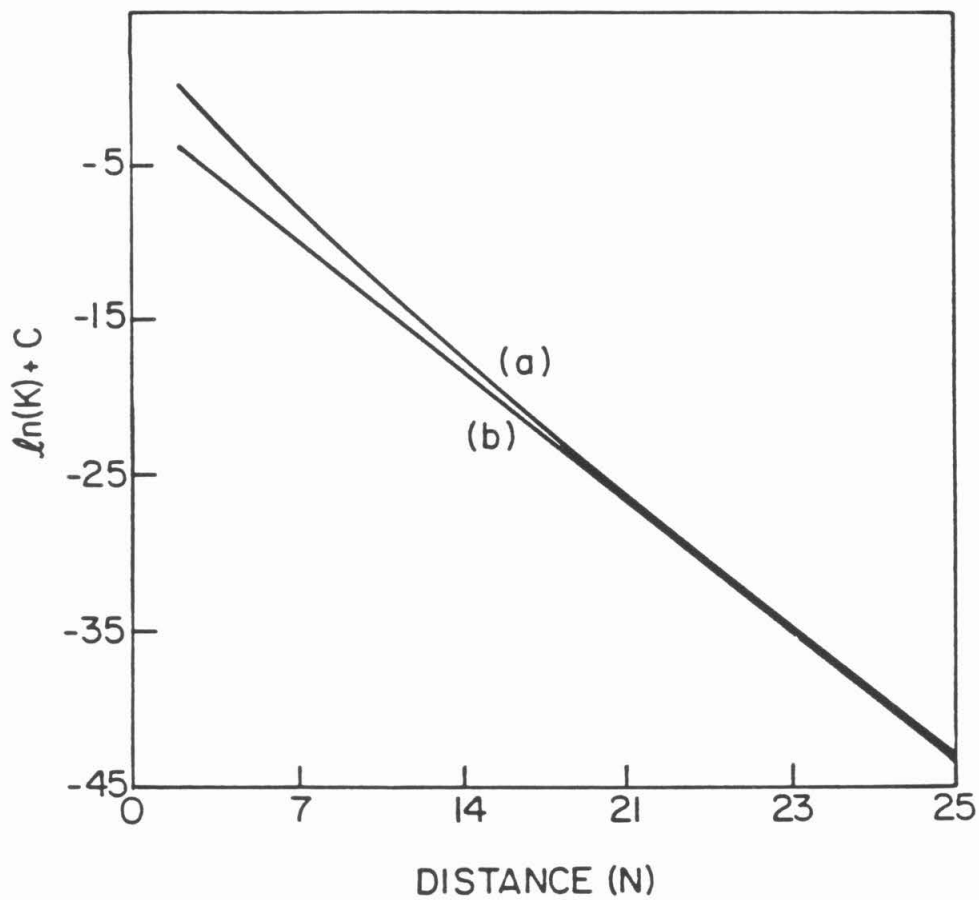


Figure IV.4. $\ln k - N$ plot for $\beta = -1.6\text{eV}$, $\hbar\omega = .2\text{eV}$, $\gamma = E^{reorg}/\hbar\omega = 4$,

$\Delta E = 8 \hbar\omega$. $E_D(E_A)$ = distance of donor (acceptor) from band.

(a) $E_D = 2.1$, $E_A = .5$

(b) $E_D = E_A = .5$

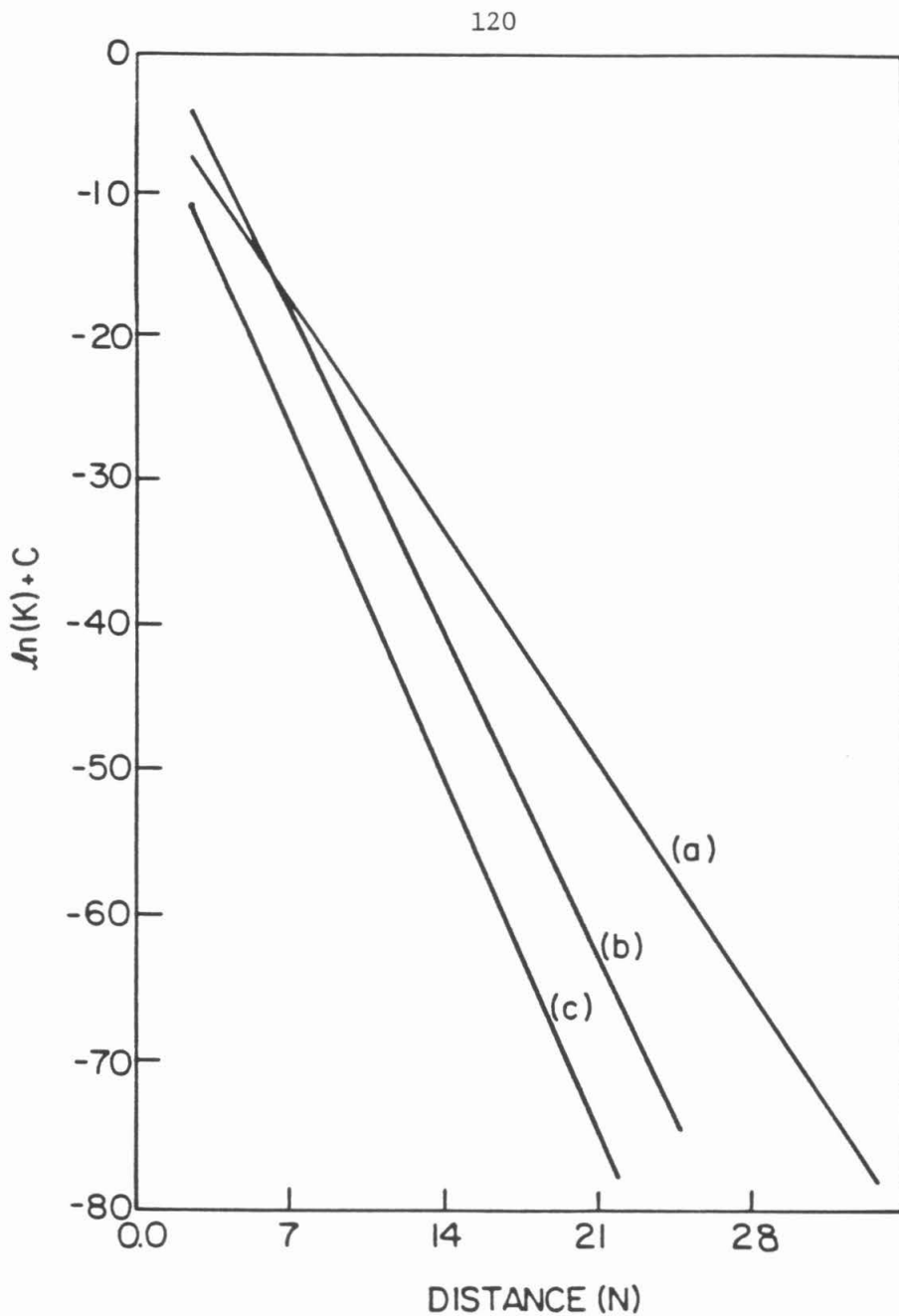


Figure IV.5. As in Fig. IV.4 with $\beta = -1.6eV$, $\hbar\omega = .2eV$, $\gamma = 4$

- (a) $E_D = E_A = 2.1eV$
- (b) $E_D = 5.6$, $E_A = 4.0$
- (c) $E_D = E_A = 5.6$

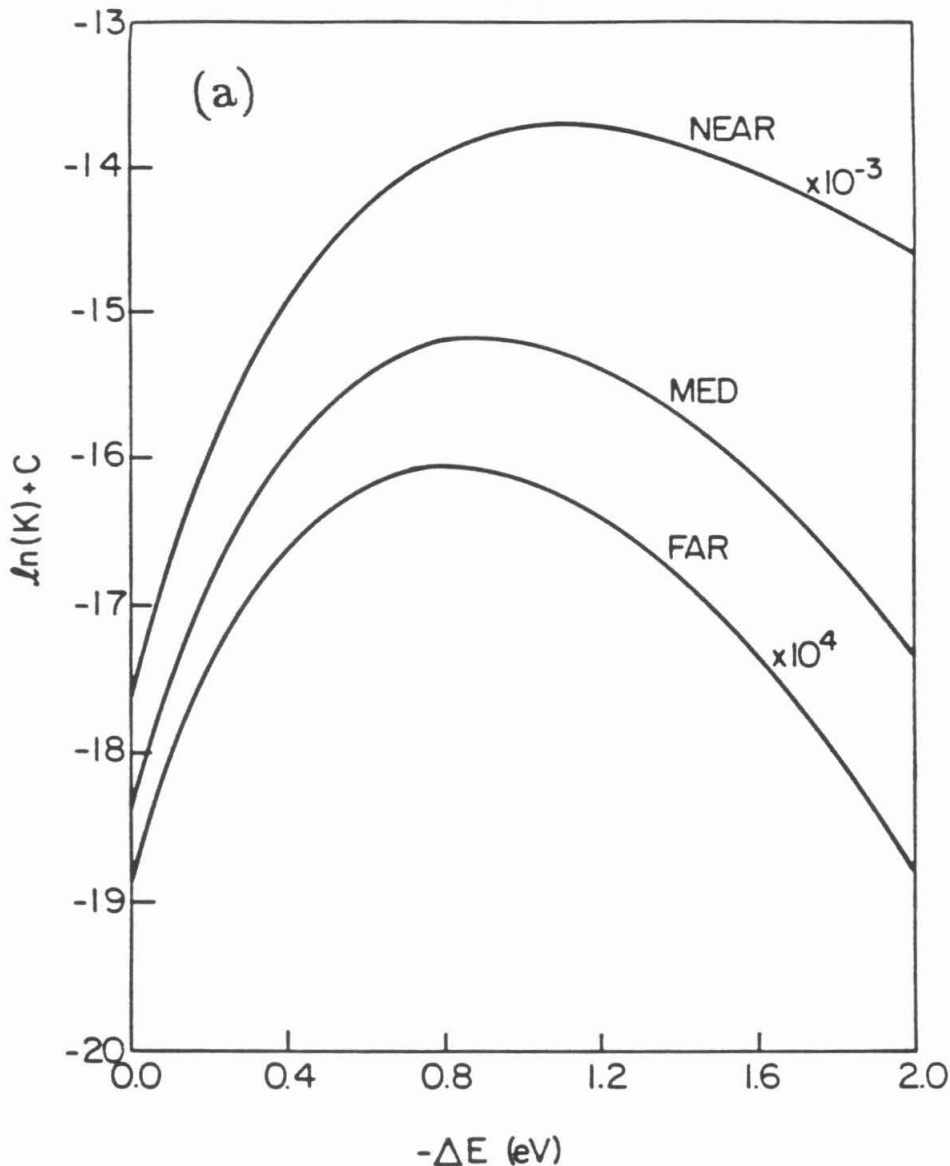


Figure IV.6a. The $\ln k - \Delta E$ dependence is shown for donor and acceptor connected by 5 bridging atoms when:

- (1) $E_D = 7\text{eV}$ ("far")
- (2) $E_D = 4\text{eV}$ ("med")
- (3) $E_D = 2.3\text{eV}$ ("near")

and $\beta = -1.6$, $\hbar\omega = .2$, $\gamma = 2$. E_A is varied by moving it closer to the band.

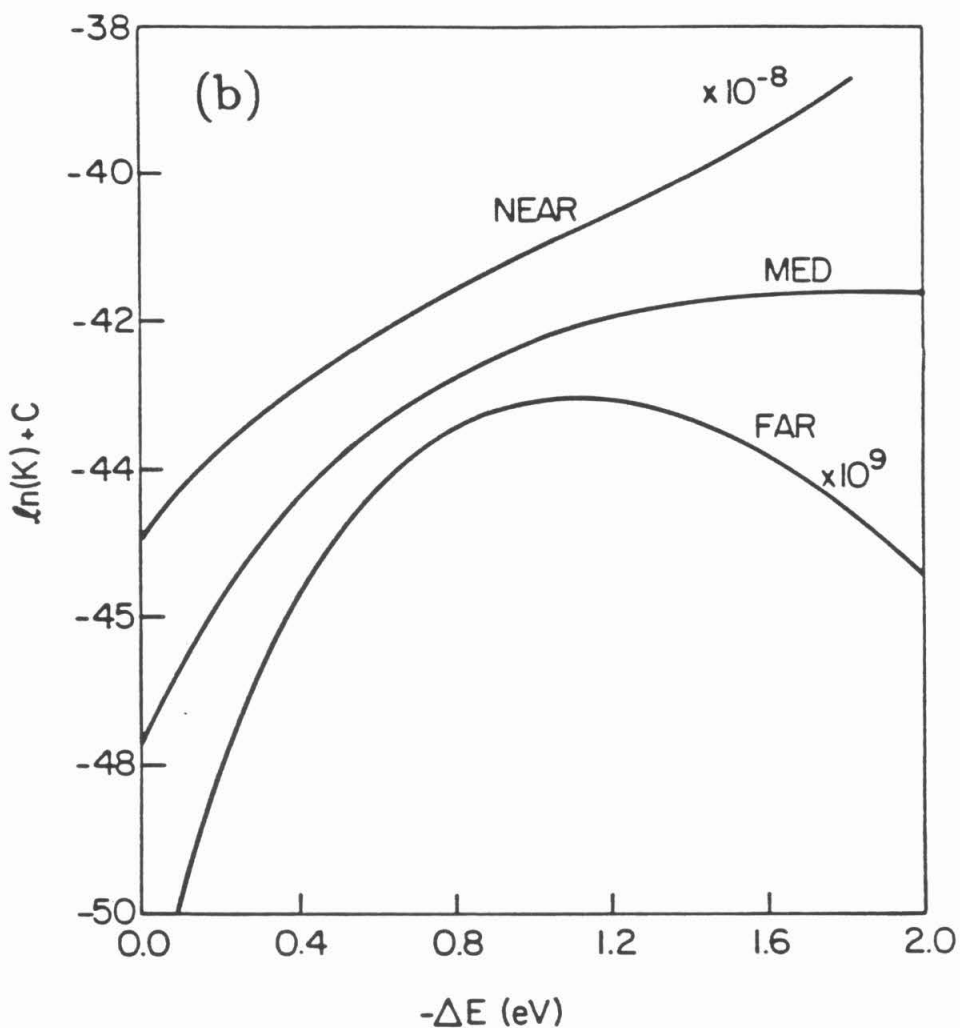


Figure IV.6b As in Fig IV.6a for a 15 atom separation between donor and acceptor.

actually span a range of energies. Ruthenium pentaamine modified alkane trap states may be only a few eV from the valence band. Electronic traps bound to modified steroids lie considerably higher in energy, perhaps 4-5 eV above the valence band [10]. Since hole transport appears to be the dominant process in most cases, increasing the reaction exothermicity by *lowering* the acceptor state energy should increase the rate considerably more than by raising the donor electronic energy an equal amount (especially at long distance).

Connections with experiment

The pulse radiolysis studies [4] measure the distance and ΔG dependence of long distance electron transfer reactions between randomly distributed organic species frozen in organic glasses. This technique allows study of the distance dependence of the rate. The results of these studies are in conflict with the standard electron transfer theories in two respects:

- (a) For small $-\Delta G$ the reactions are considerably slower than expected and behave as if the distance decay of the tunneling matrix element is different from other reactions at the same distance with different $-\Delta G$.
- (b) The maximum of the experimental rate vs. $-\Delta G$ curve moves to larger $-\Delta G$ for transfers over longer distances (Fig. IV.7).

The latter effect was explained with an untested time dependent solvent relaxation model (it can be tested by performing lower temperature experiments). That model adds a new completely independent parameter to the analysis. The non-Born-Oppenheimer/Franck-Condon calculations *predict* both of these effects (Figs IV.5 and 6). Future work will attempt to quantify this link.

Other experiments where less is known about the reorganization energies and coupled frequencies include studies by Guarr, McGuire, and McLendon [5]

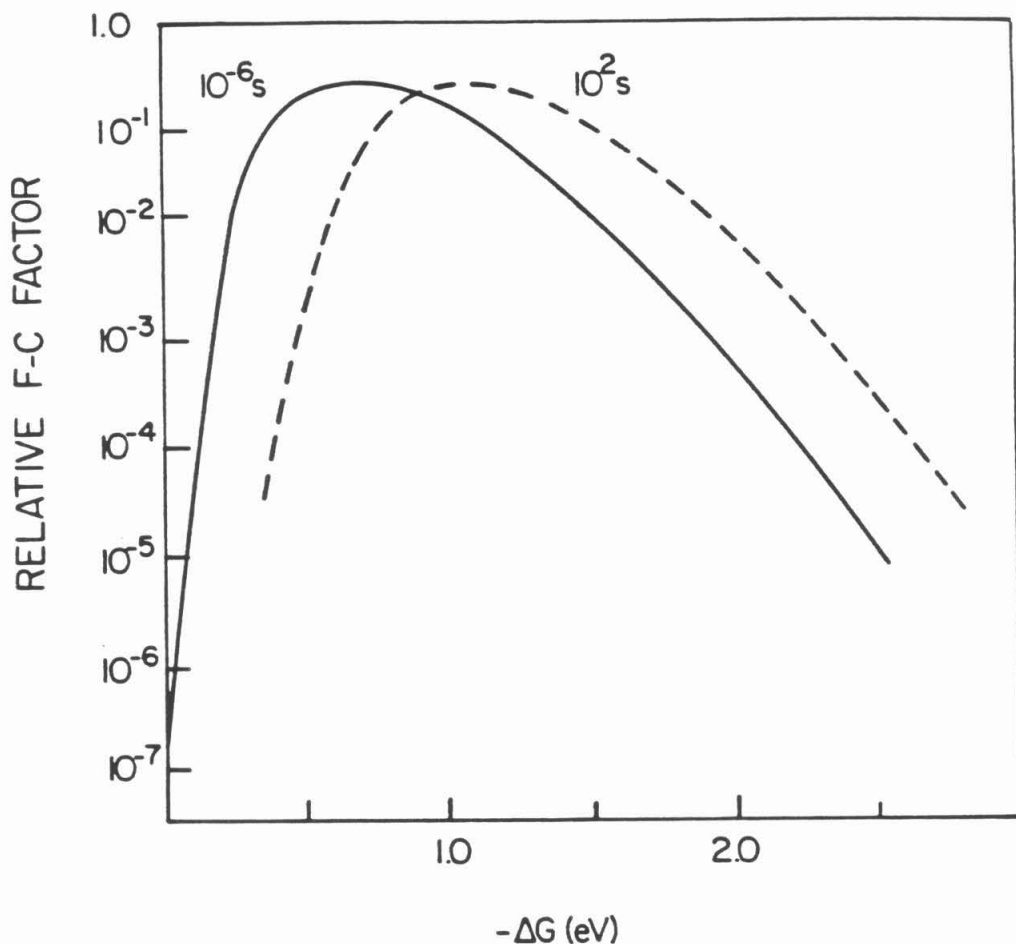


Figure IV.7 The dependence of the apparent Franck-Condon factor on ΔG for transfers occurring at 10^{-6} and 10^2 seconds after radiolysis shown. At 10^{-6} sec. transfer occurs over about 15-20 Å and over 30-40 Å at 10^2 sec. for typical acceptors. The shift in the peak of this curve may be explained by a time dependent solvent stabilization of the charge on the donor *or* by a breakdown of the Born-Oppenheimer approximation (see Fig. IV.6).

and Dutton, Gunner, Prince, Woodbury, and Parson [6].

IV.D. References – Chapter IV

1. D.N. Beratan and J.J. Hopfield, *J. Chem. Phys.* **81**, 5753(1984).
2. R.A. Marcus, in *Oxidases and Related Redox Systems*, edited by T.E. King, H.S. Mason, and M. Morrison (Pergamon, New York, 1982), p. 3.
- 3a. D. DeVault and A. Sarai, *Biophys. J.* **41**, 322(abstract) (1983).
- 3b. P. Day, *Int. Rev. Phys. Chem.* **1**, 149(1981).
- 3c. J.J. Hopfield in *Tunneling in Biological Systems*, edited by B. Chance, D.C. DeVault, H. Frauenfelder, R.A. Marcus, J.R. Schrieffer, and N. Sutin (Academic, New York, 1979), p. 431.
- 3d. K. Freed, private communication, 1985.
- 3e. A number of articles by Ivanov and Kozhushner in the 1982 and 1983 issues of *Khim. Fiz.* apparently address similar questions. At the time of writing, translations were not yet available.
4. J.R. Miller, J.V. Beitz, and K.R. Huddleston, *J. Am. Chem. Soc.* **106**, 5057 (1984).
- 5a. T. Guarr, M.E. McGuire, and G. McLendon, manuscript.
- 5b. T. Guarr, Ph.D. Thesis, The University of Rochester, 1983.
- 6a. P.L. Dutton, M.R. Gunner, and R.C. Prince, in *Trends in Photobiology*, 1982, edited by C. Helene, M. Chasier, T. Monteray-Garstier, and I.G. Lausiat, pp 561-570.
- 6b. M.R. Gunner, N. Woodbury, W.W. Parson, and P.L. Dutton, *Electron Transfer in Reaction Centers with Various Quinones Functioning as Q_A* , Abstract at Conference on Protein Structure: Molecular and Electronic Reactivity, Philadelphia, PA, April 15-17, 1985 (University City Science Center).

7. D.N. Beratan and J.J. Hopfield, *J. Am. Chem. Soc.* **106**, 1584(1984).
8. A. S. Davydov, *Phys. Stat. Sol. (b)* **90**, 457(1978)
9. H. M. McConnell, *J. Chem. Phys.* **35**, 508(1961).
10. L.T. Calcaterra, G.L. Closs, and J.R. Miller, *J. Am. Chem. Soc.* **105**, 670 (1983).